Graphic design: Communication Division, UiB / Print: Skipnes Kommunikasjon AS

ISBN: 978-82-308-3851-8

uib.no

2018 Cryostratigraphy and sedimentology of high-Arctic fjord-valleys • Graham Lewis Gilbert

Cryostratigraphy and sedimentology of high-Arctic fjord-valleys

Graham Lewis Gilbert

Thesis for the Degree of Philosophiae Doctor (PhD)
University of Bergen, Norway
2018

UNIVERSITY OF BERGEN

Cryostratigraphy and sedimentology of high-Arctic fjord-valleys

Graham Lewis Gilbert

Thesis for the Degree of Philosophiae Doctor (PhD)
at the University of Bergen

2018

Date of defence: 17.01.2018

Year: 2018

Title: Cryostratigraphy and sedimentology of high-Arctic fjord-valleys

Name: Graham Lewis Gilbert

Print: Skipnes Kommunikasjon / University of Bergen

CONTENTS

PAPERS:

I* **Gilbert GL, Kanevskiy M, Murton JB.** 2016.
Recent advances (2008–2015) in the study of ground ice and cryostratigraphy. *Permafrost and Periglacial Processes* **27**: 377–389. DOI: 10.1002/ppp.1912

II **Gilbert GL, Christiansen HH, Neumann U**. 2015.
Coring of unconsolidated permafrost deposits: methodological successes and challenges. In Proceedings GeoQuébec 2015 – 68th Canadian Geotechnical Conference and 7th Canadian Permafrost Conference, 20–23 September 2015, Québec, Canada. Paper 6 pp.

III **Gilbert GL, Cable S, Thiel C, Christiansen HH, Elberling B.** 2017.
Cryostratigraphy, sedimentology, and the late Quaternary evolution of the Zackenberg River delta, northeast Greenland. *The Cryosphere* **11**: 1265–1282. DOI: 10.5194/tc-11-1265-2017

IV **Gilbert GL, O'Neill HB, Nemec W, Thiel C, Christiansen HH, Buylaert JP.**
Late Quaternary sedimentation and permafrost development in a Svalbard fjord-valley, Norwegian high Arctic. *Sedimentology* (MS in review).

ABSTRACT

Fjord-valleys, as sediment-filled palaeofjords, are characteristic of formerly glaciated mountainous coastal areas. High-Arctic fjord-valleys commonly host permafrost, but are poorly accessible and hence have drawn relatively little research. The research presented in this thesis combines the methods of cryostratigraphy, clastic sedimentology, sequence stratigraphy, geomorphology and geochronology to investigate the sedimentary infilling, permafrost formation and late Quaternary landscape development in two classical high-Arctic fjord-valleys: the Zackenberg in northeast Greenland (74°30'N, 20°30'W) and the Adventdalen in central Svalbard (78°12'N, 15°49'E). The study involves analysis of a unique set of drilling cores from boreholes 20 m to 60 m deep. Novel research aspects include introduction of the concept of cryofacies and an analysis of the relationship between cryofacies and lithofacies. The existing model for fjord-valley sequence stratigraphy is improved, and the geomorphic response of these landscapes to permafrost degradation is considered in connection with the impending global climate change.

Both Svalbard and northeast Greenland were glaciated during the late Weichselian, with fast-flowing ice streams draining the local ice sheets through valleys, fjords and shelf troughs and removing sediment from previous glacial and interglacial periods. The fjord-valley infilling commenced at this stage with the deposition of basal lodgement till. The sediment supply decreased and fjord accommodation dramatically increased during deglaciation, when mainly muddy glaciomarine deposits accumulated in front of rapidly-retreating tidewater glaciers. The fjord-head shoreline was established and sediment supply reached its maximum once the glacier became land-based, whereby a Gilbert-type delta began to prograde along the fjord axis. The sediment yield declined in the Holocene, as glacial and paraglacial supply was exhausted, and the delta advance became driven mainly by river incision due to glacioisostatic land uplift and relative sea-level fall.

Epigenetic permafrost grew downwards in the fjord-valley deposits reaching subaerial exposure, whereas syngenetic permafrost grew upwards in raised fluvial terraces and their aggrading aeolian cover. The syngenetic permafrost and uppermost part of epigenetic permafrost are ice-rich, with cryofacies formed by segregation and segregative intrusion. The underlying epigenetic permafrost is ice-poor, with a cryofacies assemblage formed by ice segregation without moisture source replenishment. The potential geomorphic landscape change due to permafrost degradation is limited to the ice-rich upper part of permafrost. Given the common glacial and sea-level history of Svalbard and northeast Greenland, this investigation may serve as a reference analogue for other fjord-valleys in these regions.

ACKNOWLEDGEMENTS

This PhD study was carried out at the Arctic Geology Department, University Centre in Svalbard (UNIS) and at the Department of Earth Science, University of Bergen (UiB), with the funding from a four-year UNIS scholarship of which one year was funded by the Nordic Centre of Excellence, project DEFROST (*Impacts of a changing cryosphere – depicting ecosystem-climate feedbacks from permafrost, snow and ice*).

The technical part of research was partially funded by:

- the UNIS CO_2 Laboratory, which was funded by Gassnova, ConocoPhilips, Statoil, Statkraft, Store Norske Spitsbergen Kulkompani, LNS, Lundin Norway and Baker Hughes,
- the EU JPI research project (NRC project no. 244906) *"More than methane: quantifying melt-driven biogas production and nutrient export from Eurasian Arctic lowland permafrost (LowPerm),*
- the PAGE21 project *"Changing permafrost in the Arctic and its Global Effects in the 21st Century"* – grant agreement number 292700 under the EU seventh framework programme,
- the Svalbard Science Forum (RiS ID: 10103).

The supervision of Prof. Hanne H. Christiansen (UNIS) and Prof. Wojciech Nemec (UiB) is gratefully acknowledged. I thank Hanne for her support during the design, conduction and completion of this project, comments on the manuscripts in this thesis, providing me with access to many unique research and educational opportunities and for agreeing to let me freely develop this project. I also sincerely thank Wojtek for his inspiring supervision, contributing to my knowledge of sedimentology and for assistance in improving the manuscript of Paper IV and this thesis.

Completing this thesis would have been difficult without the support of several individuals. I thank Julian Murton and Mikhail Kanevskiy for helping me to develop my understanding of cryostratigraphy during the preparation of Paper I in this thesis. Ulli Neumann has been an indispensable member of all drilling operations and I have been fortunate to learn from him. Brendan O'Neill was a great resource of knowledge and inspiration during the final year of my PhD studies. Sincere thanks to Chris Burn for providing me with a comprehensive introduction to permafrost science as an undergraduate student and teaching me the traditions of field research in the western Canadian Arctic. I am grateful to my colleagues and friends at UNIS for their role in creating an exceptional research and learning environment in the high North. In particular, I thank Lis Allaart, Tor Kristian Berg, Sara Cohen, Mari Eiken, Wesley Farnsworth, Sten-Andreas Grundvåg, Holt Hancock, Jordan Mertes, Erik Myrum Næss, Sarah Strand, Sarah Thompson and others for their support and comradery in Svalbard.

Last, but not least, I wish to thank my parents, brothers and my life-partner Åse Manengen for their continuing love, support, patience and encouragement.

DISSERTATION STRUCTURE

This dissertation is organized into two main sections. *Section I* summarizes the author's case studies by providing their brief scientific background, a regional introduction to the study areas and an outline of the investigation aims. The research papers included in the dissertation are then summarized and a synthesis of their main results is presented, followed by broad research conclusions and an outline of perspective for future investigations. *Section II* consists of the four papers that constitute the main body of the dissertation. **Paper I** reviews recent advances in the study of ground ice and sedimentary cryostratigraphy. **Paper II** presents and discusses the drilling methods used in the author's investigation to retrieve frozen sediment cores. **Paper III** is a reconstruction of the late Quaternary landscape development and aggradational history of permafrost in the Zackenberg River delta, northeast Greenland. **Paper IV** is a sedimentological study of fjord-head delta progradation and the development of cryofacies in the Adventdalen fjord-valley, central Svalbard.

INTRODUCTION

Fjord-valleys (Corner, 2005), as sediment-filled palaeofjords, are characteristic of formerly glaciated mountainous coastal areas. High-Arctic, fjord-valleys commonly host permafrost, but are poorly accessible and hence have drawn relatively little research. The research presented in this dissertation pertains to the late Quaternary sedimentation history and ground-ice development conditions of two classical high-Arctic fjord-valleys: the Zackenberg in northeast Greenland (74°30'N, 20°30'W, Fig. 1) and the Adventdalen in central Svalbard (78°12'N, 15°49'E, Fig. 1). Novel research aspects include introduction of the concept of cryofacies and an analysis of the relationship between cryofacies and lithofacies in a fjord-valley stratigraphic profile. Little of such research, initiated by Gilbert (2014), has thus far been conducted. Furthermore, the existing sequence-stratigraphic model for fjord-valley glaciation–deglaciation cycle (Corner, 2006) is modified and improved on the basis of the Svalbard case study.

It has long been pointed out by researchers that the geomorphic response of high-Arctic landscapes to the impending global climate warming is expected to bear the greatest impact from permafrost degradation and hence depends strongly on the amount and vertical distribution ground ice (e.g. Mackay, 1970; Burn, 1998; Rowland *et al.*, 2010; Kokelj *et al.*, 2017). The present case studies address this issue of the landscape geomorphic sensitivity to permafrost degradation on the basis of the observed vertical pattern of ground-ice development in fjord-valleys, which are the main areas of thick Quaternary sediment accumulation and water flow in high-Arctic regions. The evidence provided by the present studies has important implications for the construction of permafrost thermal degradation models (cf. Riseborough *et al.*, 2008; Westermann *et al.*, 2015) and for the planning of infrastructure in the high Arctic (cf. Humlum *et al.*, 2003; Andersland & Ladanyi, 2004; Oswell, 2011).

Fjord-valleys

Fjords are incised bedrock valleys carved by glaciers and inundated by the sea (Holtedahl, 1967). Fjord landscapes are characteristic of mountainous coastal areas formerly glaciated by Quaternary Ice Sheets (Syvitski *et al.*, 1986; Kessler *et al.*, 2008). These depocentres are scoured by ice flow and accumulate subglacial deposits during glacial periods and are filled by fjord-head deltas during deglaciation and in post-glacial time. Such sediment-filled

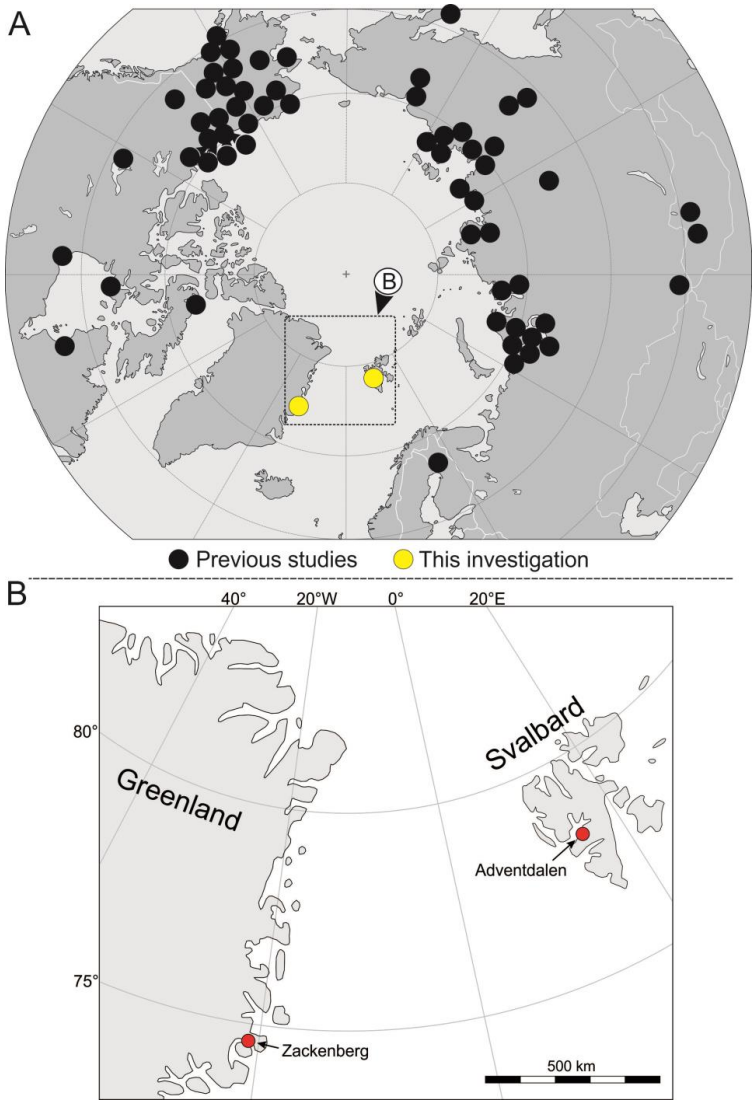

Fig. 1. (A) Location of recent (2008-2016) field studies of ground ice and cryostratigraphy (black dots) and the field sites in this thesis (yellow dots). Modified from Gilbert et al. (2016). (B) Field sites in this thesis.

palaeofjords are termed fjord-valleys (Corner, 2005). Most of the Quaternary fjords in their upper reaches have been filled in with sediment to the sea level in the Holocene.

The existing concept of the infilling of fjords has drawn a far-going analogy to the common incised valleys in non-glaciated terrains. The main controls are postulated to be the sediment supply, the fjord accommodation space and the glacio-isostatic sea-level change (Hansen, 2004; Eilertsen *et al.*, 2006; Eilertsen *et al.*, 2011); and the maximum of sedimentation is thought to occur at the phase of relative sea-level fall and forced regression (Corner, 2006; Marchand *et al.*, 2013). However, the infilling pattern of fjord-valleys differs considerably from that of common incised valleys (Dalrymple *et al.*, 1994; Dalrymple *et al.*, 2006; Gobo *et al.*, 2012), because the advance−retreat dynamics and ultimate demise of ice streams and the paraglacial 'wave' of sediment yield come further into play as specific important controls. This issue is addressed herein by **Paper III** and **Paper IV**, with a modified concept of fjord-valley infilling suggested in terms of the systems tracts and sequence stratigraphy of a glaciation−deglaciation cycle.

Permafrost and cryostratigraphy

Permafrost is ground that remains at or below 0 °C for two or more consecutive years, and permafrost-hosting fjord-valleys are a characteristic feature of high-Arctic terrains. There have been several case studies of fjord-valleys in Canada (Syvitski, 1993; Marchand *et al.*, 2013), Norway (Corner, 2006; Eilertsen *et al.*, 2006; Eilertsen *et al.*, 2011) and Greenland (Hansen, 2004; Storms *et al.*, 2012; Gilbert *et al.*, 2017), but few studies have thus far addressed the issue of permafrost development and its relationship to fjord-fill sedimentary deposits (Gilbert, 2014; Gilbert *et al.*, 2016).

The term ground ice refers collectively to the ice mass formed and buried beneath the ground surface (Mackay, 1972). Ground ice may be preserved indefinitely in permafrost regions, forming a valuable palaeoenvironmental record of the thermal history and cryostratigraphy of the local permafrost development in unconsolidated sediments (Murton, 2013; Gilbert, 2014; Gilbert *et al.*, 2016). Where permafrost degradation occurs, the thaw of ice-rich permafrost – with an ice volume greater than the host-sediment pore volume − causes ground subsidence and thermokarst (Mackay, 1970; Burn, 1998; Kokelj & Jorgenson, 2013; Murton, 2013; Kokelj *et al.*, 2017).

Permafrost is generally classified according to the timing of its formation relative to the deposition time of the host sediment (Murton & French, 1994; French & Shur, 2010). Syngenetic permafrost grows upwards concurrently with the vertical accretion of the host

sediment, whereas epigenetic permafrost expands downwards in the older sedimentary deposits as they become successively elevated above the sea level or as local climate or landscape changes induce permafrost formation. The distinction of these modes of permafrost development is a main subject of cryostratigraphy (e.g. Murton & French, 1994; Gilbert, 2014; Gilbert *et al.*, 2016). The principles and recent advances of cryostratigraphy are reviewed and discussed in **Paper I**, and a novel concept of cryofacies is introduced in **Paper IV** as a useful method for cryostratigraphic analysis.

Previous cryostratigraphic studies (Mackay, 1970, 1972, 1983; Murton & French, 1994; French & Shur, 2010; Kanevskiy *et al.*, 2011; Wetterich *et al.*, 2011; Vasil'chuk *et al.*, 2012; Kokelj & Jorgenson, 2013; Murton, 2013; Murton *et al.*, 2015; Gilbert *et al.*, 2016; Couture & Pollard, 2017; Kokelj *et al.*, 2017) have mainly focused on the ice-rich syngenetic permafrost. Little has thus far been known about the deeper, ice-poor epigenetic permafrost and about the relationship between cryofacies – or the genetic styles of ground-ice formation – and the hosting sedimentary lithofacies. These issues are addressed herein by **Paper III** and **Paper IV** on the basis of a unique database of drilling cores.

Study areas

The selected study areas of the Zackenberg fjord-valley in northeast Greenland and Adventdalen fjord-valley in central Svalbard (Fig. 1) are in the continuous permafrost region of the high Arctic and have a common history of the last glaciation−deglaciation cycle, relative sea-level change and permafrost development (Funder *et al.*, 1994; Brown *et al.*, 1997; Mangerud *et al.*, 1998; Christiansen *et al.*, 2002; Forman *et al.*, 2004; Lønne & Nemec, 2004; Lønne, 2005; Bennike *et al.*, 2008; Ingólfsson & Landvik, 2013). Regional details of the two study areas are given in **Paper III** and **Paper IV**, respectively.

These study areas exemplify the sedimentary infilling and permafrost development history of high-Arctic fjords where the post-Weichselian deglaciation shoreline was established. The warm-based tidewater ice streams in these fjords removed much of the sedimentary record from previous glacial−interglacial cycles (Elverhøi *et al.*, 1995), with a limited formation or preservation of permafrost due to the frictional heat at the base of a sliding glacier and the entrapment of geothermal heat under the ice mass (Humlum, 2005). The development of permafrost below the Holocene marine limit was thus most likely related to the post-glacial fall of relative sea level and the fjord-fill isostatic elevation above the sea level (Gilbert, 2014; Gilbert *et al.*, 2017).

Few previous studies of ground ice and cryostratigraphy have been conducted in high-Arctic fjord-valleys (Gilbert *et al.*, 2016). Fjord-valleys are numerous in the high-relief permafrost landscapes of Greenland, eastern Arctic Canada, western Arctic Russia and Svalbard. The cases at Zackenberg and Adventdalen may then serve as potential analogues for other high-Arctic fjord-valleys with a similar palaeogeographic history of the last glaciation−deglaciation cycle.

Research objectives

The principal objective of the research conducted for this dissertation was to investigate the sedimentary characteristics and pattern of ground-ice development in two classical, high-relief fjord-valleys in the high Arctic by using the integrated methods of cryostratigraphy, clastic sedimentology, sequence stratigraphy, geomorphology and geochronology. The specific objectives of the dissertation are:

- to review recent literature and identify knowledge gaps and under-studied geographic regions within the topic of this investigation;
- to summarize the use of innovative drilling techniques for the retrieval of high-quality sediment cores in remote high-Arctic terrain and permafrost landscapes;
- to provide detailed sedimentary facies analysis of a classical high-Arctic fjord-valley and its sequence stratigraphy – with implications for the existing conceptual model;
- to analyse the vertical distribution of ground ice in a fjord-valley in terms of cryofacies and establish their genetic relationship to the host sedimentary facies;
- to reconstruct the late Quaternary palaeogeographic development in the study areas and determine the timing and processes of permafrost growth in fjord-valley deposits; and
- to assess the potential for geomorphic change resulting from permafrost degradation in high-Arctic fjord-valleys due to the impending climate warming.

ARTICLE SUMMARIES

Paper I

Recent advances (2008−2015) in the study of ground ice and cryostratigraphy

Gilbert, G.L., Kanevskiy, M., Murton, J.B.

2016 – *Permafrost and Periglacial Processes*, 27: 377-389. DOI: 10.1002/ppp.1912

This paper reviews contributions to the study of ground ice and cryostratigraphy published between 2008 and 2015. Key earlier papers are included to provide context. The paper was published as a part of the *Transactions of the International Permafrost Association (IPA)*, in a volume consisting of review papers and designed to reveal an international perspective on the progress in permafrost research (Burn, 2013).

Cryostratigraphy, the study of layering within permafrost based on the description of ice, concerns the distribution of ground ice in soil, sediment, or bedrock (Murton, 2013). Ground ice formation within sediment produces cryostructures (cryofacies in this thesis) which can be used to elucidate the thermal history and origin of the substrate. Recent advances are discussed in relation to four cryostratigraphic themes: (1) permafrost aggradation, (2) renewed aggradation of permafrost following degradation, (3) massive ground ice, and (4) the evaluation of ground ice content.

The development of cryofacies relates to three main factors: (1) the physical properties of soil, sediment or bedrock, (2) moisture availability, and (3) the mode of permafrost formation. Nine cryofacies are commonly described in recent literature. Three modes of permafrost formation are identified – epigenetic, syngenetic, and quasi-syngenetic – and patterns in the vertical distribution of cryofacies associated with each mode are recognized. Epigenetic permafrost tends to be ice poor with ground ice concentrated in the top few meters. In epigenetic permafrost, the distance between ground-ice bodies generally increases with depth, as the overall ice content decreases. In contrast, syngenetic permafrost forms within aggrading sedimentary sequences during deposition, mainly as segregated ice near the top of permafrost (Mackay, 1972). Syngenetic permafrost successions are typically characterized by rhythmic layering of layered and lenticular cryofacies and overall high ice content. Permafrost which aggrades due to thinning of the active layer is termed quasi-syngenetic. This is typically due to the development of a surface organic layer or climate deterioration. In quasi-syngenetic permafrost successions, the ground ice distribution and characteristics resemble syngenetic permafrost.

Quantifying the amount and distribution of ground ice is required to predict the geomorphic response of permafrost landscapes in the future. Moisture content is best determined in the laboratory and recent investigations rely on three methods to assess ice content. Gravimetric moisture content is typically expressed as the ratio of the mass of water or ice in a sample to the mass of the dry sample. Volumetric ice content (VIC) is the ratio of the volume of ice to the volume of the whole sample. VIC can be estimated from photographs of permafrost samples (Kanevskiy *et al.*, 2013) or by using computed tomography (CT) scanning. Lastly, excess ice content is the volume of ice in excess of the pore volume in an unfrozen state.

For the purposes of this thesis, a key outcome of this paper was identifying that few recent studies had investigated permafrost materials and ground ice in high-relief fjord landscapes. **Paper III** and **Paper IV** are structured to fill this research gap by adding knowledge regarding the distribution of ground ice and cryofacies present within fjord-valley fills in permafrost environments.

Paper II

Coring of unconsolidated permafrost deposits: methodological successes and challenges

Gilbert, G.L., Christiansen, H.H., Neumann, U.

2015 – *Proceedings from GeoQuébc 2015 – 68th Canadian Geotechnical Conference and 7th Canadian Conference on Permafrost.* Paper 6 pp.

This conference paper summarizes three scales of drilling methods used in recovering frozen sediment cores from permafrost environments. These methods vary in terms of maximum drill depth, operational cost and ease of transport. A qualitative assessment of these methods and the retrieved cores based on recent field investigations in Svalbard and northeast Greenland is provided.

The smallest drill consists of a STIHL BT 121 power head and a smooth core barrel with diamond cutting teeth. Extensions can be added to the core barrel, enabling drilling down to ca. 5 m depth. Though this setup is limited by its maximum drilling depth it is a reliable and effective method for retrieving cores from the near surface in ice-rich fine-grained sediment and organic material. Next, the UNIS permafrost drill rig is described as intermediate in size. It was manufactured by Kurth Bohr- und Brunnenausrüstungen GmbH and consists of a hydraulic engine, two air compressors, a drill head and a drill boom. The rig has a total packed weight of ca. 1600 kg and is designed to fit on two snowmobile sledges for winter transport. The maximum drilling depth is 50 m. This system was used to retrieve the four ca. 20 m long cores analysed in **Paper III** and **Paper IV**. Unlike the STIHL drill, the UNIS permafrost drill rig benefits from interchangeable drill bits, which allow for core retrieval in a variety of substrates. Finally, an industrial drill rig equipped with a Boart Longyear HQ-3 wireline triple core barrel was used to retrieve a 60 m core through ice-bonded sediments analysed in **Paper IV**.

All methods perform well in ice-rich material and fine-grained sediments. This observation is consistent with those reported using other types of drills in permafrost areas (e.g. Dickinson *et al.*, 1999; Calmels *et al.*, 2005). The effectiveness of coring in these deposits is attributed to the presence of ice and the sediment grain size. Ice, acting as cement between individual grains and organic material, prevents core fragmentation during drill operation. Fine-grained sediments are additionally less susceptible to mechanical disintegration than coarser deposits. At present, both the STIHL drill and the UNIS permafrost drill rig are ineffective when coring in coarser material. This is attributed to the

amount of energy generated while cutting through rock fragments which effectively melts the ice contained in the core resulting in the retrieval of disturbed samples. In contrast, cores were retrieved using the industrial drill rig in all grain sizes.

In areas without appreciable exposures of Quaternary sediments, drilling is the only method available to retrieve samples of the substrate. Furthermore, access to undisturbed, frozen samples is required to characterize ground ice content and analyse sedimentary stratigraphy and cryostratigraphy in perennially frozen sediments. Adequate drilling technologies and core-processing techniques are vital to the success of cryostratigraphic studies such as those presented in **Paper III** and **Paper IV**.

Paper III

Cryostratigraphy, sedimentology, and the late Quaternary evolution of the Zackenberg River delta, northeast Greenland

Gilbert, G.L., Cable, S., Thiel, C., Christiansen, H.H., Elberling, B.

2017 – *The Cryosphere*, 11: 1265–1282. DOI: 10.5194/tc-11-1265-2017

This paper focuses on the sedimentary development and aggradational history of permafrost in the Zackenberg River delta, NE Greenland, (74°30'N, 20°30'W, Fig. 1B). The study combines sedimentological, sequence stratigraphic, geomorphological and cryostratigraphic techniques together with optically stimulated luminescence (OSL) dating. The objectives are to: (1) describe sedimentary facies in sections and ice-bonded sediment cores, (2) relate ground ice formation in permafrost to sediment properties and depositional environments, and (3) to combine observations to reconstruct landscape change since the LGM.

Nine sedimentary facies, arranged into four facies associations (FA I–IV), are identified. Facies associations each represent distinct depositional environments or subenvironments of the delta system. FA I is interpreted as a subglacial till, deposited during the LGM (ca. 22 ka). FA II is polygenetic and was deposited in a fjord-basin during and following deglaciation. The vertical transition in the component facies of FA II records an approaching delta front. FA III consists of inclined planar beds deposited on a delta slope. FA IV records fluvial activity associated with a deltaic distributary plain or braided-river system. In addition, three cryofacies are identified – pore, layered, and suspended. Cryofacies are identified based on the bulk macroscopic characteristics of ground ice and form due to spatial and temporal variations in sediment grain size, moisture availability, and the mode of permafrost aggradation. The vertical distribution of ground ice indicates that permafrost in the Zackenberg Delta terraces is primarily epigenetic. The OSL results suggest the Zackenberg region was deglaciated ca. 13–11 ka.

Four distinct sequence stratigraphic systems tracts are recognized. These relate to major changes in sediment supply and relative-sea level. During the late Weichselian glaciation a subglacial till (FA I) was deposited. This stage is recognized as the forced-regressive glacial systems tract (GRST) in **Paper IV**. Accommodation space plays a crucial role during the GRST where it reaches a minimum in the subglacial environment. The deglacial transgressive systems tract (DTST) formed during the aerial deglaciation of the Zackenberg area. The deglacial highstand systems tract (DHST) is marked by the rapid progradation of a glaciofluvial fjord-head delta and concurrent deposition of glaciomarine sediments on the

fjord floor. The bulk of the relict delta terraces formed during this stage. Lastly, the postglacial forced-regressive systems tract (PRST) formed after aerial deglaciation and is characterized by fluvial delta progradation, fluvial incision and terracing during relative sea-level fall. Epigenetic permafrost formation commenced after the subaerial exposure of the delta plain during relative-sea level fall, incision and abandonment of relict fluvial surfaces. Variations in cryofacies and ground ice content between cores suggest that lateral variations in sediment characteristics, unresolvable at the core scale, result in spatial differences in ice content in epigenetic permafrost.

Paper IV

Late Quaternary sedimentation and permafrost development in a Svalbard fjord-valley, Norwegian high Arctic

Gilbert, G.L., O'Neill, H.B., Nemec, W., Thiel, C., Christiansen, H.H., Buylaert, J.P.

Sedimentology (MS in review).

This paper combines methods from clastic sedimentology, cryostratigraphy, geochronology, sequence stratigraphy and geomorphology to reveal the late Quaternary history of Adventdalen, a classic fjord-valley located in central Svalbard (78°12'N, 15°49'E, Fig. 1B). The objectives are to: (1) provide a sedimentological analysis of the fjord-valley deposits and their sequence stratigraphy; (2) recognize cryofacies and establish their genetic relationship to sedimentary facies; and (3) determine the timing and mode of permafrost aggradation in fjord-valley deposits.

The unique data set consists of three drilling cores, 20 m to 60 m deep, logged bed-by-bed with observations on lithofacies, cryofacies, bioturbation and macrofossils. Excess ice content and gravimetric moisture content were determined in ca. 400 samples. The techniques of OSL and radiocarbon AMS ^{14}C dating were used to determine the depositional ages of sediment (n=38) and of fossil plant and shell remains (n=6), respectively.

Twelve lithofacies are identified and arranged into 7 facies associations (FA I–VII). Facies associations represent different depositional environments of the fjord-valley sedimentary succession and are listed in stratigraphic order. FA I is a fjord-floor blanket of well-compacted diamictic deposits formed as a lodgement till of the late Weichselian ice stream. FA II was deposited in a glaciomarine environment during the glacier's rapid retreat by calving, with sediment derived from melt-out suspension and shed by icebergs, coastal ice-foot and fjord-side slope collapses. The overlying facies associations FA III to FA VI recorded the Holocene advance of a fjord-head Gilbert-type delta with a valley-wide distributary braidplain in Adventdalen. As the post-glacial isostatic rebound enforced a relative-sea level fall, the fluvial system incised itself by a few metres – leaving raised valley-flank terraces on which the aeolian deposits of FA VII have accumulated. In general, the scenario presented for Adventdalen is in agreement with other studies of post-glacial infilling in fjord-valleys (e.g. Syvitski & Shaw, 1995; Hansen, 2004; Corner, 2006; Gilbert, 2014).

Nine cryofacies are identified and arranged into two cryofacies associations (CFA I and CFA II). CFA I is a syngenetic permafrost zone, formed by the upwards growth of

permafrost. These deposits contain excess ice and cryofacies formed by ice segregation. CFA II is epigenetic permafrost, formed during downwards permafrost growth. The top of CFA II is ice rich and contains a suite of cryofacies formed by segregation and segregative intrusion. The deeper CFA II is ice poor and contains cryofacies formed by segregation processes. The vertical distribution of cryofacies indicates that permafrost formation commenced with the subaerial exposure and transition to FA VII.

This study suggests that sediment from previous interglacial periods is flushed from fjord-valleys by ice during glaciation. Infilling commences with the deposition of a subglacial lodgement till, during the GRST, and proceeds during the upfjord retreat of the occupying glacier thru the DTST. The bulk of the infilling occurs during due to the progradation of the fjord-head delta system. The rate of sediment supply is highest during the DHST as the glacial and paraglacial sediment outputs reach their effective maximum. The sediment supply rate declines during the PRST when sediment is primarily supplied by the reworking of deposits by fluvial incision spurred by relative sea-level fall. Permafrost begins to grow downwards beneath stable terraces boarding the active fluvial system. As a result permafrost is predominantly epigenetic. Syngenetic permafrost develops in areas where sediment accumulated on terrace surfaces following emergence.

SYNTHESIS

This section is a synthesis of the various aspects of fjord-valleys analysed in **Papers I, III** and **IV**, investigated using the drilling methods presented in **Paper II**, including sedimentary lithostratigraphy and cryostratigraphy. Although local differences in the interplay of sediment supply, glacioisostatic rebound and basin configuration resulted in some differences in the sedimentary facies and cryofacies between the Zackenberg and Adventdalen fjord-valleys, there are also many similarities and a generalized model for landscape evolution can be formulated. This synthesis focuses on two main aspects of fjord-valleys: (1) sedimentary infilling and sequence stratigraphy and (2) permafrost development and cryostratigraphy.

Fjord-valley infilling and sequence stratigraphy

The case studies presented in **Papers III** and **IV** have recognized sequential stages of fjord infilling associated with a glaciation−deglaciation cycle, supporting the conceptual notions derived from previous studies of other fjord-valleys (e.g. Syvitski & Shaw, 1995; Hansen, 2004; Corner, 2006; Marchand *et al.*, 2013).

The fjord infilling commences during glaciation, when a basal lodgement till is deposited beneath the fjord-occupying ice stream (Fig. 2A) and a grounding-line moraine forms at the glacier terminus so long as the ice flow persists (cf. Nemec *et al.*, 1999; Lønne *et al.*, 2001). The retreat of tidewater glacier is relatively rapid, by bulk foundering and calving, and hence the marine sediment deposition during deglaciation is chiefly by suspension fallout, ice rafting and fjord-side collapses (Fig. 2B; Lønne & Nemec, 2011), rather than by a systematic retrogradational stacking in front of a gradually retreating glacier – as envisaged by some authors (Hansen, 2004; Corner, 2006). A sea-level highstand follows the glacier retreat and a fjord-head shoreline is established once the glacier terminus becomes land-based (Syvitski & Shaw, 1995). Sediment supply reaches its effective maximum in the proglacial conditions of this stage, when a fjord-head Gilbert-type delta begins to prograde rapidly down the fjord (Fig. 2C; cf. Eilertsen *et al.*, 2006). High rates of early post-glacial delta progradation are recognized in the Zackenberg and Adventdalen fjord-valleys. The OSL dates in Zackenberg (**Paper III**) indicate that the alluvial terraces near the Holocene marine limit formed within a short period during deglaciation. The dating results in Adventdalen (**Paper IV**) indicate that the fjord-head delta prograded at a rate of ca. 4.4 m yr^{-1} prior to 9.2 ka and at a much lower

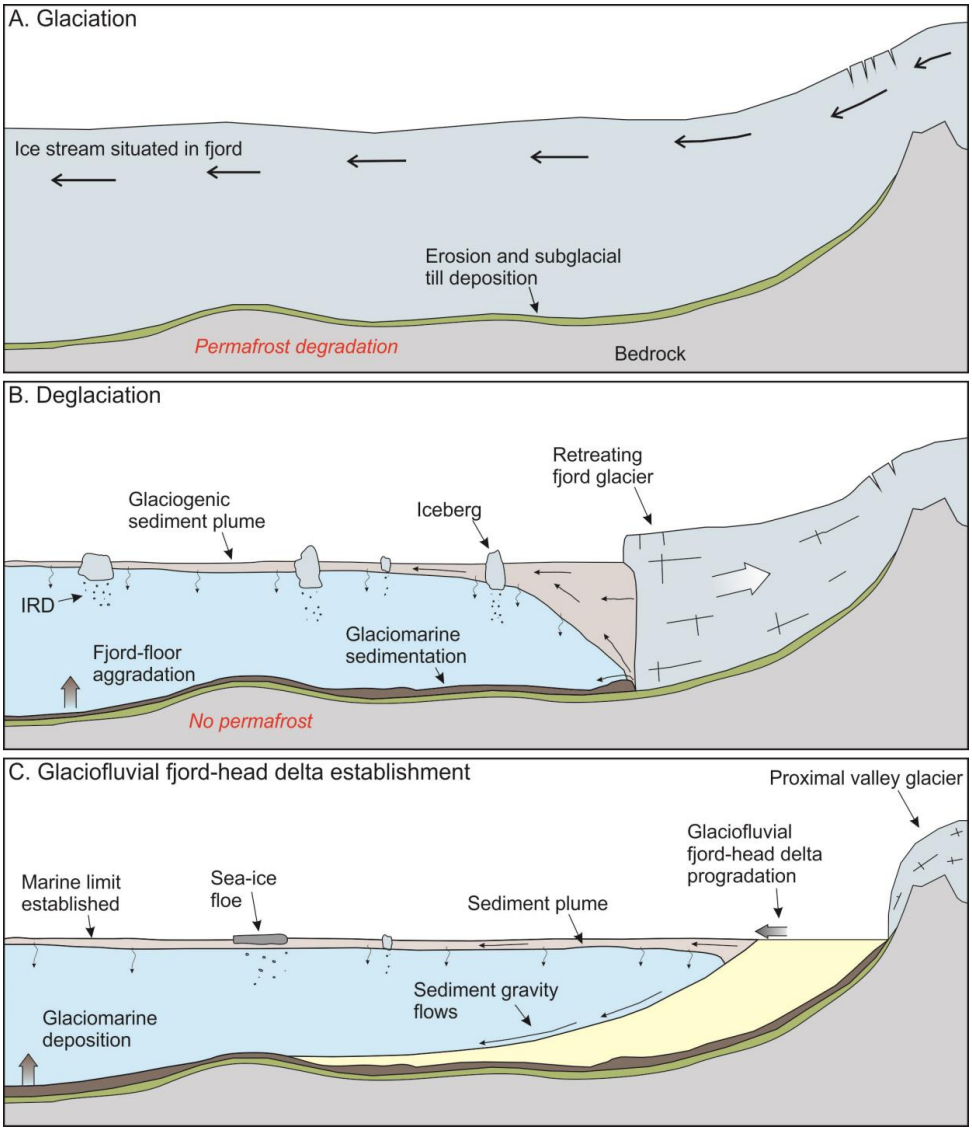
A. Glaciation
Ice stream situated in fjord
Erosion and subglacial till deposition
Permafrost degradation
Bedrock
B. Deglaciation
Retreating fjord glacier
Glaciogenic sediment plume
Iceberg
IRD
Glaciomarine sedimentation
Fjord-floor aggradation
No permafrost
C. Glaciofluvial fjord-head delta establishment
Proximal valley glacier
Glaciofluvial fjord-head delta progradation
Marine limit established
Sea-ice floe
Sediment plume
Sediment gravity flows
Glaciomarine deposition

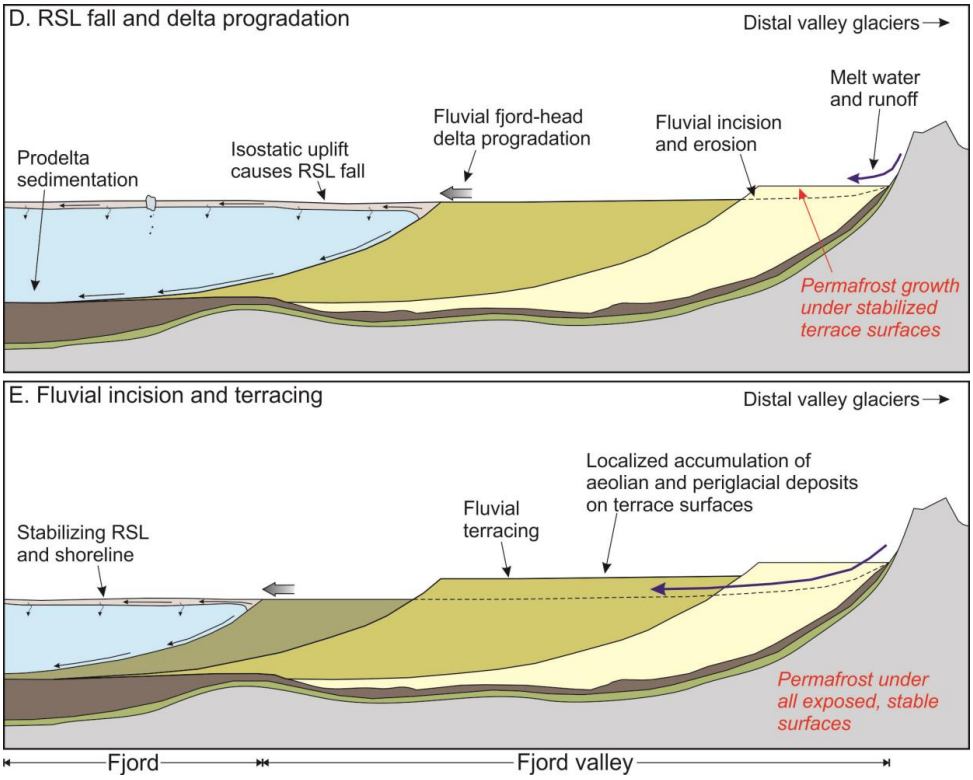

Fig. 2. Illustration summarizing fjord-valley infilling, emergence and terracing during: (A) forced-regressive glacial systems tract; (B) deglacial transgressive systems tract; (C) deglacial highstand systems tract; (D) the early stages of the postglacial force-regressive systems tract (PRST); and (E) the later stages of the PRST and PLST. Stages based on Corner (2006), Paper 3 and Paper 4.

rate of 0.9 m yr^{-1} in the later Holocene. The sediment supply to the fjord-head delta was initially by the glacial meltwater runoff and paraglacial sediment yield, and subsequently by the fluvial reworking of glacial, alluvial and delta-plain deposits due to glacioisostatic sea-level fall. As the glacier decayed and retreated, sediment input by paraglacial processes waned (Fig. 2D; cf. Church & Ryder, 1972; Ballantyne, 2002a, b). The fjord-filling delta, sheltered from storm waves by a high-relief fjord, continues to prograde at a low rate due to seasonal meltwater runoff, although the relative sea level has largely stabilized (Fig. 2E).

This scenario of fjord-valley sedimentation can also be viewed in terms of sequence stratigraphy. The sequence stratigraphic model arising from the present case studies (**Papers III** and **IV**) is a modification of the three-tract model postulated by Corner (2006), encompassing the record of an entire glaciation-deglaciation cycle. Four basic systems tracts are distinguished: (1) a *forced-regressive glacial systems tract* (GRST) comprising subglacial till and a coeval terminal moraine (formed at unknown distant locations outside the fjords in the present cases); (2) a *deglacial transgressive systems tract* (DTST) formed during the retreat of tidewater fjord glacier; (3) a *deglacial highstand systems tract* (DHST) formed during the onshore retreat of valley glacier and progradation of an early fjord-head delta at the marine limit; and (4) a *postglacial forced-regressive systems tract* (PRST) formed after a significant decline of meltwater and sediment discharges, during and after the glacioisostatic sea-level fall (Fig. 2). Two more systems tracts are suggested in the following discussion below.

At stage GRST, the sediment supply by warm-base ice stream is high, but the accommodation space is at a minimum in the subglacial environment and at a maximum at the glacier terminus. The coeval *glacial lowstand systems tract* (GLST), absent in the studied fjord reaches, would be represented by the grounding-line terminal moraine or shelf-edge submarine outwash apron formed at a distant seaward location (cf. Lønne *et al.*, 2001; Lønne & Nemec, 2011). The base of the GRST is a surface of subglacial erosion, truncating older fjord-fill deposits or reaching bedrock (as in the case of Adventdalen, **Paper IV**). The upper boundary, termed the *deglaciation flooding surface* by Hansen (2004), is the transition to proglacial marine deposits (DTST). Tidewater glaciers retreat rapidly, by bulk foundering and calving (Benn *et al.*, 2007; Lønne & Nemec, 2011). The deposition of sediment at stage DTST is thus by the fallout of 'background' muddy suspension and a random shedding of coarse debris by ice rafting and fjord-side collapses (Lønne *et al.*, 2001; Lønne & Nemec, 2011), rather than by a systematic retrogradational stacking in front of a gradually retreating

glacier (Corner, 2006). The fjord accommodation reaches its maximum in DTST, but the supply of sediment is low and declining due to the rapid glacier retreat (cf. Lønne *et al.*, 2001; Lønne & Nemec, 2011). The upper boundary of DTST is the *maximum flooding surfac*e (Hansen, 2004; Corner, 2006), dating the establishment of the fjord-head deltaic shoreline and marked by a distinct increase in turbiditic sand supply to the fjord floor. This boundary is time-transgressive in the down-fjord direction, reflecting the prodelta advance. The fjord accommodation is up to the marine limit and the sediment supply reaches its maximum at stage DHST, when the meltwater runoff is high and the paraglacial 'wave' of sediment yield comes into play (cf. Eilertsen *et al.*, 2011). Corner (2006) defined conceptually the upper boundary of DHST as a transition from glacial to non-glacial sediment supply, but without offering any sedimentological criteria for its recognition. As a practical criterion, the present case studies suggest the evidence of a recognizable decrease in sediment supply with the glacier demise, reflected in the decreased rate of fjord-head delta progradation. The catchment sediment yield at stage PRST is already low, as the glacial source vanished and also the paraglacial 'wave' declines, whereby the delta progradation is driven chiefly by fluvial incision due to the glacioisostatic sea-level fall. The key record of this forced regression are raised alluvial terraces (Eilertsen *et al.*, 2006), well-evidenced in both the Zackenberg (**Paper III**) and the Adventdalen fjord-valley (**Paper IV**).

As the glacioisostatic land uplift declines and the relative sea level stabilizes, the PRST turns into a *postglacial lowstand systems tract* (PLST), which means normal, purely progradational regression. The modern Zackenberg and Adventdalen fjord-valleys show an incipient transition to the normal-regressive PLST.

Permafrost growth and cryostratigraphy

Permafrost in fjord-valleys begins to form within the delta-plain raised alluvial terraces, which are the first morphogenic areas to emerge above the sea level (Gilbert, 2014). Permafrost formation in submarine environment prior to emergence is unlikely due to the warm boundary conditions at the sediment/water interface (Fig. 2A−C; Nilsen *et al.*, 2008). The permafrost in Zackenberg and Adventdalen fjord-valleys (**Papers III** and **IV**) is, therefore, predominantly epigenetic – grown downwards within the emerging raised terraces (Fig. 2D−E). Syngenetic permafrost overlies epigenetic permafrost and grows upwards in the aggrading niveo-fluvial (**Paper III**) or aeolian (**Paper IV**) deposits. The exact timing of permafrost aggradation depends upon the local pattern of emergence (relative sea-level fall) and the dynamics of the fluvial system (channel shifting) – which determine the areal extent

and preservation of terraces (Corner, 2006). In general, the formation of permafrost in fjord-valleys is diachronous, following closely the advance of the fjord-filling delta and hence younger in down-valley direction.

The cryofacies and ice-richness of syngenetic permafrost record the growth of ground ice in aggrading sedimentary deposits by ice-segregation processes within the top zone of permafrost (Mackay, 1972; Cheng, 1983). The top part of the underlying epigenetic permafrost also tends to be ice-rich, due to the segregation of ice at the early stages of permafrost formation (**Paper IV**). In sedimentary successions containing permeable gravel aquifers, thick ice bodies tend to develop by segregative ice intrusion (Mackay & Dallimore, 1992; Lauriol *et al.*, 2010). Otherwise, the epigenetic permafrost is characteristically ice-poor and its cryofacies reflect ice segregation with downward permafrost expansion. The moisture available for epigenetic ice formation segregation is thought to be limited to the moisture content of the host sediment, with no external moisture supply (French & Shur, 2010). An exception from this rule is noted in the Zackenberg case (**Paper III**), where excess ice occurs in sand and gravel lithofacies deposited at the DTST stage. This observation highlights the importance of ground sediment properties and moisture conditions for the development of permafrost and its cryofacies (**Paper I**).

Excess ice appears to be concentrated in syngenetic permafrost and the top few metres of epigenetic permafrost (**Paper IV**). This observation has important implications for the modelling of permafrost degradation in the context of impending climatic warming, as it indicates that the geomorphic effects of active-layer deepening and permafrost decay in fjord-valleys will be limited to this ice-rich zone and depend on its local thickness. Ground subsidence due to the degradation of ice-poor epigenetic permafrost will likely be minimal and limited to the volume loss by sheer sediment compaction (**Paper IV**).

CONCLUSIONS

- Previous studies of permafrost have focused mainly on ground ice and cryostratigraphy in fine-grained deposits of aeolian, fluvial or lacustrine origin in landscapes of low relief. Few studies have thus far investigated ground-ice development in the high-relief Arctic landscapes of northeastern Greenland and Svalbard, from where come the present research contributions.
- The unique database for **Papers III** and **IV** included drill cores, 20 m to 60 m in depth, retrieved by innovative drilling techniques designed for the coring of ice-bonded sediments and reviewed in **Paper II**.
- The stratigraphic history of sedimentation and permafrost development in two classical high-Arctic fjord-valleys, the Zackenberg in northeast Greenland and the Adventdalen in central Svalbard, has been reconstructed by using the combined methods of clastic sedimentology, sequence stratigraphy, cryostratigraphy, geomorphology and geochronology. These areas were stripped of sedimentary cover during the Last Glacial Maximum, when a basal lodgement till covered the bedrock floor of an ice-occupied fjord. Mud-dominated glaciomarine sedimentation occurred in the fjord when the tidewater glacier retreated rapidly by calving. A fjord-head Gilbert-type delta prograded into the fjord once its post-glacial shoreline was established. The delta advance was affected by glacioisostatic sea-level fall, when fluvial incision resulted in raised delta-plain terraces – commonly hosting aeolian sedimentation.
- In sequence-stratigraphic interpretation, the fjord-floor till were deposited during the forced-regressive glacial systems tract (GRST). The distant location of coeval grounding-line terminal moraine (GLST) is unknown. Glaciomarine deposits above the deglacial flooding surface represent the deglacial transgressive systems tract (DTST). The fjord-fill deltaic succession comprises the deglacial highstand (DHST) and postglacial forced-regressive systems tract (PRST), with a transition to normal-regressive lowstand systems tract (PLST) marked by relative sea-level stabilization.
- Most of the permafrost in high-Arctic fjord-valleys is epigenetic and ice-poor, formed in sediments gradually emerged above the falling relative sea level. Syngenetic permafrost formed within the raised delta-plain terraces hosting aeolian sedimentation. Excess ground ice occurs in the syngenetic permafrost and the top few metres of the underlying epigenetic permafrost – and this ice-rich zone and its local thickness effectively define the geomorphic sensitivity of fjord-valleys to regional permafrost degradation.

- The high Arctic has a common history of the late Quaternary glaciation−deglaciation cycle and sea-level change, and the case studies from central Svalbard and northeast Greenland may then serve as a tentative sedimentological and geocryological reference model for similar other fjord-valleys in the region.

PERSPECTIVE

The studies presented in this dissertation, by combining methods of clastic sedimentology and cryostratigraphy, have given major new insights into the sedimentary infilling and ground-ice development in high-Arctic fjord-valleys. Potential attractive avenues for related future research are as follows:

- Relatively little cryostratigraphic research has thus far been conducted in high-relief Arctic landscapes. While further studies of fjord-valleys will likely bring new advances at the interface of geocryology and sedimentology, other Arctic depositional systems – such as the arrays of raised beach terraces, valley-side alluvial fans and rock glaciers − should also be investigated. In particular, a systematic investigation of the relationship between ground ice and sediment characteristics in mountain-slope colluvium would help to answer questions surrounding the role of permafrost in slope-wasting processes and to assess the response of colluvial aprons to permafrost degradation due to climatic change.
- Recent advances have rendered the drilling technology well-suited for coring ice-bonded sediments, providing material of sufficient quality for cryological and sedimentological analysis. However, the drilling results are unsatisfactory when it comes to the coring of ice-bonded gravels, because the greater frictional heat generated by drilling through gravel melts the ice cement. Coarse-grained deposits are widespread in high-relief fjord landscapes and are significant repositories of permafrost. Improved drilling techniques should be developed for retrieving ice-bonded cores from such highly heterolithic substrates. A suggestion is to adapt the existing drills by using cold water as the primary drilling fluid.
- The present case studies have demonstrated that the Arctic permafrost comprises a wide range of cryofacies. More laboratory experimental research is now urgently needed to improve the existing limited knowledge of the formative processes of particular cryofacies, also in relation to the host sediment characteristics. The laboratory studies should include such crucial aspects as the response of particular cryofacies to permafrost degradation and the post-degradation fingerprints of ice in the host sedimentary deposit. Such studies may potentially help recognize traces of ancient permafrost in the sedimentary record and hence open the gates for palaeo-cryology.

LITERATURE

Andersland, O.B. and Ladanyi, B. (2004) *Frozen ground engineering*. John Wiley & Sons, New Jersey, 363 pp.

Ballantyne, C.K. (2002a) A general model of paraglacial landscape response. *Holocene*, **12**, 371–376.

Ballantyne, C.K. (2002b) Paraglacial geomorphology. *Quat. Sci. Rev.*, **21**, 1935–2017.

Benn, D.I., Warren, C.R. and Mottram, R.H. (2007) Calving processes and the dynamics of calving glaciers. *Earth-Sci. Rev.*, **82**, 143–179.

Bennike, O., Sorensen, M., Fredskild, B., Jacobsen, B.H., Bocher, J., Amsinck, S.L., Jeppesen, E., Andreasen, C., Christiansen, H.H. and Humlum, O. (2008) Late quaternary environmental and cultural changes in the Wollaston Forland region, Northeast Greenland. *Adv Ecol Res*, **40**, 45–79.

Brown, J., Ferrians Jr, O., Heginbottom, J. and Melnikov, E. (1997) *Circum-Arctic map of permafrost and ground-ice conditions*. US Geological Survey Reston, VA.

Burn, C.R. (1998) The response (1958–1997) of permafrost and near-surface ground temperatures to forest fire, Takhini River valley, southern Yukon Territory. *Can. J. Earth Sci.*, **35**, 184–199.

Burn, C.R. (2013) Transactions of the International Permafrost Association. *Permafr. Periglac. Process.*, **24**, 96–98.

Calmels, F., Gagnon, O. and Allard, M. (2005) A portable earth-drill system for permafrost studies. *Permafr. Periglac. Process.*, **16**, 311–315.

Cheng, G. (1983) The mechanism of repeated-segregation for the formation of thick layered ground ice. *Cold Reg. Sci. Technol.*, **8**, 57–66.

Christiansen, H.H., Bennike, O., Bocher, J., Elberling, B., Humlum, O. and Jakobsen, B.H. (2002) Holocene environmental reconstruction from deltaic deposits in northeast Greenland. *J Quaternary Sci*, **17**, 145–160.

Church, M. and Ryder, J.M. (1972) Paraglacial sedimentation: A consideration of fluvial processes conditioned by glaciation. *Geol. Soc. Am. Bull.*, **83**, 3059–3072.

Corner, G.D. (2005) Atlantic coast and fjords. In: *The Physical Geography of Fennoscandia, 5* (Ed M. Seppälä), 203–228. Oxford University Press, Oxford.

Corner, G.D. (2006) A transgressive-regressive model of fjord-valley fill: stratigraphy, facies and depositional controls. In: *Incised Valleys in Time and Space* (Eds R.W. Dalrymple, D.A. Leckie and R.W. Tillman). *SEPM Spec. Publ.*, **85**. 161–178.

Couture, N.J. and Pollard, W.H. (2017) A Model for Quantifying Ground-Ice Volume, Yukon Coast, Western Arctic Canada. *Permafr. Periglac. Process.*, **28**, 534–542.

Dalrymple, R.W., Boyd, R. and Zaitlin, B.A. (Eds) (1994) *Incised-Valley Systems: Origin and Sedimentary Sequences*. *SEPM Spec. Publ.*, **51**, 391 pp.

Dalrymple, R.W., Leckie, D.A. and Tillman, R.W. (Eds) (2006) *Incised Valleys in Time and Space*. *SEPM Spec. Publ.*, **85**, 343 pp.

Dickinson, W., Cooper, P., Webster, B. and Ashby, J. (1999) A portable drilling rig for coring permafrosted sediments. *J. Sed. Res.*, **69**, 518–521.

Eilertsen, R.S., Corner, G.D., Aasheim, O., Andreassen, K., Kristoffersen, Y. and Ystborg, H. (2006) Valley-fill stratigraphy and evolution of the Målselv fjord valley, northern Norway. In: *Incised-Valleys in Time and Space* (Eds R.W. Dalrymple, D. Leekie and R. Tilman), ***SEPM Spec. Publ.*, 85**, 179–195.

Eilertsen, R.S., Corner, G.D., Aasheim, O. and Hansen, L. (2011) Facies characteristics and architecture related to palaeodepth of Holocene fjord–delta sediments. *Sedimentology*, **58**, 1784–1809.

Elverhøi, A., Svendsen, J.I., Solheim, A., Andersen, E.S., Milliman, J., Mangerud, J. and Hooke, R.L. (1995) Late Quaternary sediment yield from the high Arctic Svalbard area. *J. Geol.*, **103**, 1–17.

Forman, S.L., Lubinski, D.J., Ingólfsson, Ó., Zeeberg, J.J., Snyder, J.A., Siegert, M.J. and Matishov, G.G. (2004) A review of postglacial emergence on Svalbard, Franz Josef Land and Novaya Zemlya, northern Eurasia. *Quat. Sci. Rev.*, **23**, 1391–1434.

French, H. and Shur, Y. (2010) The principles of cryostratigraphy. *Earth-Sci. Rev.*, **101**, 190–206.

Funder, S., Hjort, C. and Landvik, J.Y. (1994) The Last Glacial Cycles in East Greenland, an Overview. *Boreas*, **23**, 283–293.

Gilbert, G.L. (2014) *Sedimentology and Geocryology of an Arctic Fjord-Head Delta (Adventdalen, Svalbard)*. MSc thesis, University of Oslo, Oslo, 124 pp.

Gilbert, G.L., Cable, S., Thiel, C., Christiansen, H.H. and Elberling, B. (2017) Cryostratigraphy, sedimentology, and the late Quaternary evolution of the Zackenberg River delta, northeast Greenland. *Cryosphere*, **11**, 1265–1282.

Gilbert, G.L., Kanevskiy, M. and Murton, J.B. (2016) Recent advances (2008–2015) in the study of ground ice and cryostratigraphy. *Permafr. Periglac. Process.*, **27**, 377–389.

Gobo, K., Ghinassi, M. and Nemec, W. (2012) The architecture of incised valley-fill as a record of the relative sea-level change and sediment supply, Abstract, SEQS Meeting *At*

the Edge of the Sea: Sediments, Geomorphology, Tectonics and Stratigraphy in Quaternary Studies, Sassari, Sardinia.

Hansen, L. (2004) Deltaic infill of a deglaciated Arctic fjord, East Greenland: Sedimentary facies and sequence stratigraphy. *J. Sed. Res.*, **74**, 422–437.

Holtedahl, H. (1967) Notes on the Formation of Fjords and Fjord-Valleys. *Geogr. Ann.*, **49**, 188-203.

Humlum, O. (2005) Holocene permafrost aggradation in Svalbard. In: *Cryospheric Systems: Glaciers and Permafrost* (Eds C. Harris and J.B. Murton), 119–129. The Geological Society of London, London, United Kingdom.

Humlum, O., Instanes, A. and Sollid, J.L. (2003) Permafrost in Svalbard: a review of research history, climatic background and engineering challenges. *Polar Res.*, **22**, 191–215.

Ingólfsson, Ó. and Landvik, J.Y. (2013) The Svalbard–Barents Sea ice-sheet: Historical, current and future perspectives. *Quat. Sci. Rev.*, **64**, 33–60.

Kanevskiy, M., Shur, Y., Fortier, D., Jorgenson, T. and Stephani, E. (2011) Cryostratigraphy of late Pleistocene syngenetic permafrost (yedoma) in northern Alaska, Itkillik River exposure. *Quatern. Res.*, **75**, 584–596.

Kanevskiy, M., Shur, Y., Krzewinski, T. and Dillon, M. (2013) Structure and properties of ice-rich permafrost near Anchorage, Alaska. *Cold Reg. Sci. Technol.*, **93**, 1–11.

Kessler, M.A., Anderson, R.S. and Briner, J.P. (2008) Fjord insertion into continental margins driven by topographic steering of ice. *Nat. Geosci.*, **1**, 365.

Kokelj, S.V. and Jorgenson, M.T. (2013) Advances in Thermokarst Research. *Permafr. Periglac. Process.*, **24**, 108–119.

Kokelj, S.V., Lantz, T.C., Tunnicliffe, J., Segal, R. and Lacelle, D. (2017) Climate-driven thaw of permafrost preserved glacial landscapes, northwestern Canada. *Geology*, **45**, 371–374.

Lauriol, B., Lacelle, D., St-Jean, M., Clark, I.D. and Zazula, G.D. (2010) Late Quaternary paleoenvironments and growth of intrusive ice in eastern Beringia (Eagle River valley, northern Yukon, Canada). *Can. J. Earth Sci.*, **47**, 941–955.

Lønne, I. (2005) Faint traces of high Arctic glaciations: an early Holocene ice-front fluctuation in Bolterdalen, Svalbard. *Boreas*, **34**, 308–323.

Lønne, I. and Nemec, W. (2004) High-arctic fan delta recording deglaciation and environment disequilibrium. *Sedimentology*, **51**, 553–589.

Lønne, I. and Nemec, W. (2011) The kinematics of ancient tidewater ice margins: criteria for recognition from grounding-line moraines. In: *Ice-Marginal and Periglacial Processes and Sediments: Ancient and Modern* (Eds I.P. Martini, H.M. French and A. Pérez-Alberti), *Geol. Soc. London Spec. Publ.*, **354**, 57–75.

Lønne, I., Nemec, W., Blikra, L.H. and Lauritsen, T. (2001) Sedimentary architecture and dynamic stratigraphy of a marine ice-contact system. *J. Sed. Res.*, **71**, 922–943.

Mackay, J.R. (1970) Disturbances to the tundra and forest tundra environment of the western Arctic. *Can. Geotech. J.*, **7**, 420–432.

Mackay, J.R. (1972) The world of underground ice. *Ann. Assoc. Am. Geogr.*, **62**, 1–22.

Mackay, J.R. (1983) Downward water movement into frozen ground, western Arctic coast, Canada. *Can. J. Earth Sci.*, **20**, 120–134.

Mackay, J.R. and Dallimore, S.R. (1992) Massive ice of the Tuktoyaktuk area, western Arctic coast, Canada. *Can. J. Earth Sci.*, **29**, 1235–1249.

Mangerud, J., Dokken, T., Hebbeln, D., Heggen, B., Ingólfsson, Ó., Landvik, J.Y., Mejdahl, V., Svendsen, J.I. and Vorren, T.O. (1998) Fluctuations of the Svalbard-Barents Sea Ice Sheet during the last 150 000 years. *Quat. Sci. Rev.*, **17**, 11–42.

Marchand, J.-P., Buffin-Bélanger, T., Hétu, B. and St-Onge, G. (2013) Stratigraphy and infill history of the glacially eroded Matane River Valley, eastern Quebec, Canada. *Can. J. Earth Sci.*, **51**, 105–124.

Murton, J.B. (2013) Ground ice and cryostratigraphy. In: *Treatise on Geomorphology: Glacial and Periglacial Geomorphology* (Eds R. Giardino and J. Harbor), **8**, 173–201. Academic Press, San Diego.

Murton, J.B. and French, H.M. (1994) Cryostructures in permafrost, Tuktoyaktuk coastlands, western arctic Canada. *Can. J. Earth Sci.*, **31**, 737–747.

Murton, J.B., Goslar, T., Edwards, M.E., Bateman, M.D., Danilov, P.P., Savvinov, G.N., Gubin, S.V., Ghaleb, B., Haile, J., Kanevskiy, M., Lozhkin, A.V., Lupachev, A.V., Murton, D.K., Shur, Y., Tikhonov, A., Vasil'chuk, A.C., Vasil'chuk, Y.K. and Wolfe, S.A. (2015) Palaeoenvironmental Interpretation of Yedoma Silt (Ice Complex) Deposition as Cold-Climate Loess, Duvanny Yar, Northeast Siberia. *Permafr. Periglac. Process.*, **26**, 208–288.

Nemec, W., Lønne, I. and Blikra, L.H. (1999) The Kregnes moraine in Gauldalen, west-central Norway: anatomy of a Younger Dryas proglacial delta in a palaeofjord basin. *Boreas*, **28**, 454–476.

Nilsen, F., Cottier, F., Skogseth, R. and Mattsson, S. (2008) Fjord–shelf exchanges controlled by ice and brine production: The interannual variation of Atlantic Water in Isfjorden, Svalbard. *Continental Shelf Research*, **28**, 1838–1853.

Oswell, J.M. (2011) Pipelines in permafrost: geotechnical issues and lessons 12010 R.M. Hardy Address, 63rd Canadian Geotechnical Conference. *Can. Geotech. J.*, **48**, 1412–1431.

Riseborough, D., Shiklomanov, N., Etzelmüller, B., Gruber, S. and Marchenko, S. (2008) Recent advances in permafrost modelling. *Permafr. Periglac. Process.*, **19**, 137–156.

Rowland, J.C., Jones, C.E., Altmann, G., Bryan, R., Crosby, B.T., Hinzman, L.D., Kane, D.L., Lawrence, D.M., Mancino, A., Marsh, P., McNamara, J.P., Romanvosky, V.E., Toniolo, H., Travis, B.J., Trochim, E., Wilson, C.J. and Geernaert, G.L. (2010) Arctic Landscapes in Transition: Responses to Thawing Permafrost. *EOS Trans. Am. Geophys. Union*, **91**, 229–230.

Storms, J.E.A., de Winter, I.L., Overeem, I., Drijkoningen, G.G. and Lykke-Andersen, H. (2012) The Holocene sedimentary history of the Kangerlussuaq fjord-valley fill, West Greenland. *Quat. Sci. Rev.*, **35**, 29–50.

Syvitski, J.P.M. (1993) Glaciomarine environments in Canada: an overview. *Can. J. Earth Sci.*, **30**, 354–371.

Syvitski, J.P.M., Burrell, D.C. and Skei, J.M. (1986) *Fjords: Processes and Products*. Springer, New York, 377 pp.

Syvitski, J.P.M. and Shaw, J. (1995) Sedimentology and Geomorphology of Fjords. *Dev. Sedimentol.*, **53**, 113–178.

Vasil'chuk, Y.K., Vasil'chuk, A.C. and Budantseva, N.A. (2012) Isotopic and palynological compositions of a massive ice in the Mordyyakha River, Central Yamal Peninsula. *Doklady Earth Sciences*, **446**, 1105–1109.

Westermann, S., Elberling, B., Højlund Pedersen, S., Stendel, M., Hansen, B.U. and Liston, G.E. (2015) Future permafrost conditions along environmental gradients in Zackenberg, Greenland. *Cryosphere*, **9**, 719–735.

Wetterich, S., Rudaya, N., Tumskoy, V., Andreev, A.A., Opel, T., Schirrmeister, L. and Meyer, H. (2011) Last Glacial Maximum records in permafrost of the East Siberian Arctic. *Quat. Sci. Rev.*, **30**, 3139–3151.

SCIENTIFIC PAPERS

Paper I

PERMAFROST AND PERIGLACIAL PROCESSES
Permafrost and Periglac. Process. **27**: 377–389 (2016)
Published online 8 August 2016 in Wiley Online Library
(wileyonlinelibrary.com) DOI: 10.1002/ppp.1912

Recent Advances (2008–2015) in the Study of Ground Ice and Cryostratigraphy

Graham L. Gilbert,[1,2]* *Mikhail Kanevskiy*[3] *and Julian B. Murton*[4]

[1] Department of Arctic Geology, The University Centre in Svalbard, Longyearbyen, Norway
[2] Department of Earth Science, The University of Bergen, Bergen, Norway
[3] Institute of Northern Engineering, University of Alaska Fairbanks, Fairbanks, AK, USA
[4] Permafrost Laboratory, Department of Geography, University of Sussex, Brighton, UK

ABSTRACT

Cryostratigraphy involves the description, interpretation and correlation of ground-ice structures (cryostructures) and their relationship to the host deposits. Recent advances in the study of ground ice and cryostratigraphy concern permafrost aggradation and degradation, massive-ice formation and evaluation of ground-ice content. Field studies have increased our knowledge of cryostructures and massive ground ice in epigenetic and syngenetic permafrost. Epigenetic permafrost deposits are relatively ice-poor and composed primarily of pore-filled cryostructures, apart from an ice-enriched upper section and intermediate layer. Syngenetic permafrost deposits are commonly identified from cryostructures indicative of an aggrading permafrost table and are characterised by a high ice content, ice-rich cryofacies and nested wedge ice. Degradation of ice-rich permafrost can be marked by thaw unconformities, truncated buried ice wedges, ice-wedge pseudomorphs and organic-rich 'forest beds'. Studies of massive ground ice have focused on wedge ice, thermokarst-cave ice, intrusive ice and buried ice. Significant advances have been made in methods for differentiating between tabular massive-ice bodies of glacier and intrasedimental origin. Recent studies have utilised palynology, isotope geochemistry and hydrochemistry, in addition to sedimentary and cryostratigraphic analyses. The application of remote sensing techniques and laboratory methods such as computed tomography scanning has improved estimations of the ice content of frozen sediments. Copyright © 2016 John Wiley & Sons, Ltd.

KEY WORDS: cryostratigraphy; ground ice; permafrost; cryostructures

INTRODUCTION

Cryostratigraphy concerns the distribution and organisation of ground ice in soil, sediment or bedrock. It can be defined as 'the study of layering within permafrost; based on the description and interpretation of ice, sediment and rock, cryostratigraphy identifies and correlates stratigraphic units – usually layers – of permafrost' (Murton, 2013, p. 174). The value of cryostratigraphy stems from the fact that ground ice within sediment produces structures whose identification can elucidate the thermal history and origin of the substrate, because ground-ice formation, morphology and preservation are influenced by various climatic, geologic and environmental factors (Katasonov, 2009; French and Shur, 2010; Popov, 2013; Murton, 2013). Ground ice may be preserved indefinitely in permafrost environments, providing an enduring palaeoenvironmental archive. The principles of cryostratigraphy and general problems related to ground-ice studies have been recently discussed in English (French and Shur, 2010; Y.K. Vasil'chuk, 2012; Murton, 2013) and in Russian (Rogov, 2009; Badu, 2010; Shpolyanskaya, 2015).

Ice-rich permafrost is commonly associated with frost-susceptible sediment and occurs where moisture is sufficient for ground-ice formation or where ice is buried (Murton, 2013). Conditions conducive to extensive ground-ice formation have existed for much of the Quaternary Period in Arctic and Subarctic lowlands underlain by fine-grained sediments. Hence, the geographical distribution of recent cryostratigraphic studies has focused mainly on northern and central Siberia, Alaska and western Arctic Canada (Figure 1).

This review identifies recent advances in the understanding of ground ice and cryostratigraphy of present-day permafrost regions based on literature published between 2008 and 2015. We focus on four cryostratigraphic themes:

* Correspondence to: *Graham L. Gilbert*, Department of Arctic Geology, The University Centre in Svalbard, Longyearbyen, Norway.
E-mail: Graham.Gilbert@unis.no

Received 21 January 2016
Revised 5 May 2016
Accepted 17 June 2016

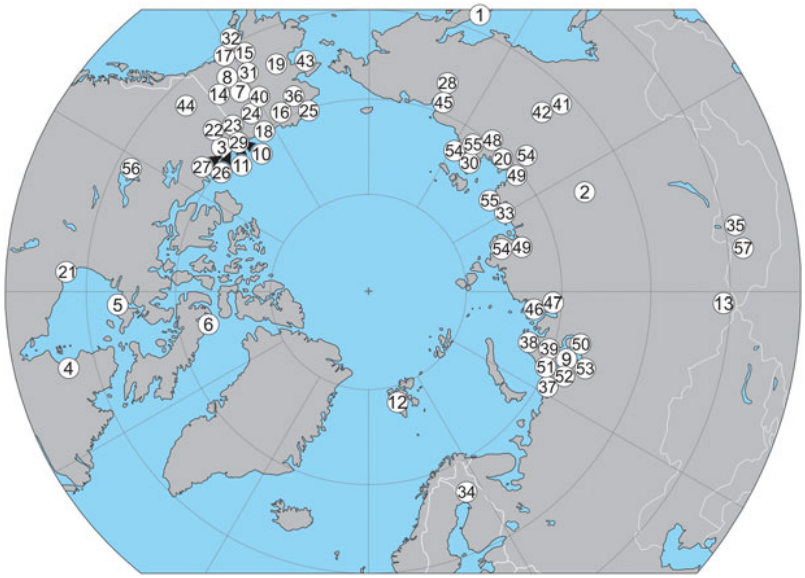

Figure 1 Approximate locations of field investigations included in this review. Regional studies and investigations which predate 2008 are not included. (1) Abramov *et al.* (2008); (2) Alexeev *et al.* (2016); (3) Bode *et al.* (2008); (4) Calmels *et al.* (2008); (5) Calmels *et al.* (2012); (6) Coulombe *et al.* (2015); (7) Douglas *et al.* (2011); (8) Fortier *et al.* (2012); (9) Fotiev (2014); (10) Fritz *et al.* (2011); (11) Fritz *et al.* (2012); (12) Härtel *et al.* (2012); (13) Iwahana *et al.* (2012); (14) Kanevskiy *et al.* (2008); (15) Kanevskiy *et al.* (2011); (16) Kanevskiy *et al.* (2012); (17) Kanevskiy *et al.* (2013a); (18) Kanevskiy *et al.* (2013b); (19) Kanevskiy *et al.* (2014); (20) Katasonov (2009); (21) Kuhry (2008); (22) D. Lacelle *et al.* (2009); (23) Lauriol *et al.* (2010); (24) Meyer *et al.* (2008); (25) Meyer *et al.* (2010); (26) Morse and Burn (2013); (27) Murton (2009); (28) Murton *et al.* (2015); (29) O'Neill and Burn (2012); (30) Opel *et al.* (2011); (31) Osterkamp *et al.* (2009); (32) Riddle and Rooney (2012); (33) Schirrmeister *et al.* (2011); (34) Seppälä (2011); (35) Sharkuu *et al.* (2012); (36) Shur *et al.* (2012); (37) Slagoda *et al.* (2010); (38) Slagoda *et al.* (2012a); (39) Slagoda *et al.* (2012b); (40) Sliger *et al.* (2015); (41) Spektor *et al.* (2011); (42) Spektor *et al.* (2008); (43) Stephani *et al.* (2012); (44) Stephani *et al.* (2014); (45) Strauss *et al.* (2012); (46) Streletskaya and Vasilev (2012); (47) Streletskaya *et al.* (2011); (48) Tumskoy (2012); (49) Ulrich *et al.* (2014); (50) Y. K. Vasil'chuk *et al.* (2014); (51) Y. K. Vasil'chuk *et al.* (2009); (52) Y. K. Vasil'chuk *et al.* (2011); (53) Y. K. Vasil'chuk *et al.* (2012); (54) Wetterich *et al.* (2011); (55) Wetterich *et al.* (2014); (56) Wolfe *et al.* (2014); and (57) Yoshikawa *et al.* (2013).

(1) permafrost aggradation; (2) renewed aggradation of permafrost following degradation; (3) massive ground ice; and (4) evaluation of ground-ice content. The dating of permafrost and the cryostratigraphy of past permafrost regions (e.g. northwest Europe) are beyond the scope of this review.

PERMAFROST AGGRADATION

Cryostratigraphic reconstructions of permafrost aggradation tend to focus on ground-ice development in unconsolidated sediments and classify permafrost in terms of its time of formation relative to the deposition of the host material. *Epigenetic permafrost* aggrades after the host material has formed, sometimes with a time lag of thousands or millions of years (French and Shur, 2010). *Syngenetic permafrost* aggrades at a rate proportional to the sedimentation rate at the ground surface, and characterises cold-climate landscapes influenced by relatively continuous deposition by fluvial, colluvial, lacustrine or aeolian processes. *Quasi-syngenetic permafrost* forms the top layer of permafrost (ice-rich intermediate layer) by upwards freezing as a result of the gradual thinning of the active layer over time – usually due to the development of surface vegetation (Shur, 1988). Many permafrost bodies consist of epigenetic, syngenetic and/or quasi-syngenetic components and so are *polygenetic*. The distinction between them is made by systematically analysing the spatial distribution of cryostructures and the nature of ground ice.

Cryostructures, or patterns formed by ice inclusions in frozen ground, are defined as structures that reflect the amount and distribution of pore and segregated ice within frozen sediment (French and Shur, 2010). Individual cryostructures are identified based on the shape, distribution and proportions of ice, sediment or rock within frozen ground (Murton, 2013). Nine cryostructures are commonly described in recent literature (Figure 2). *Pore* cryostructure develops where porewater freezes *in situ* in the interstices between mineral grains, forming an ice cement; the pore cryostructure may be visible to the naked eye in sands and gravels or non-visible in silts or clays (Figure 2A). *Organic-matrix* cryostructure forms where ice fills void spaces in organic material (e.g. peat or organic-rich soil) (Figure 2B). *Crustal* cryostructure occurs where ice segregation creates an ice crust around an object such as a rock

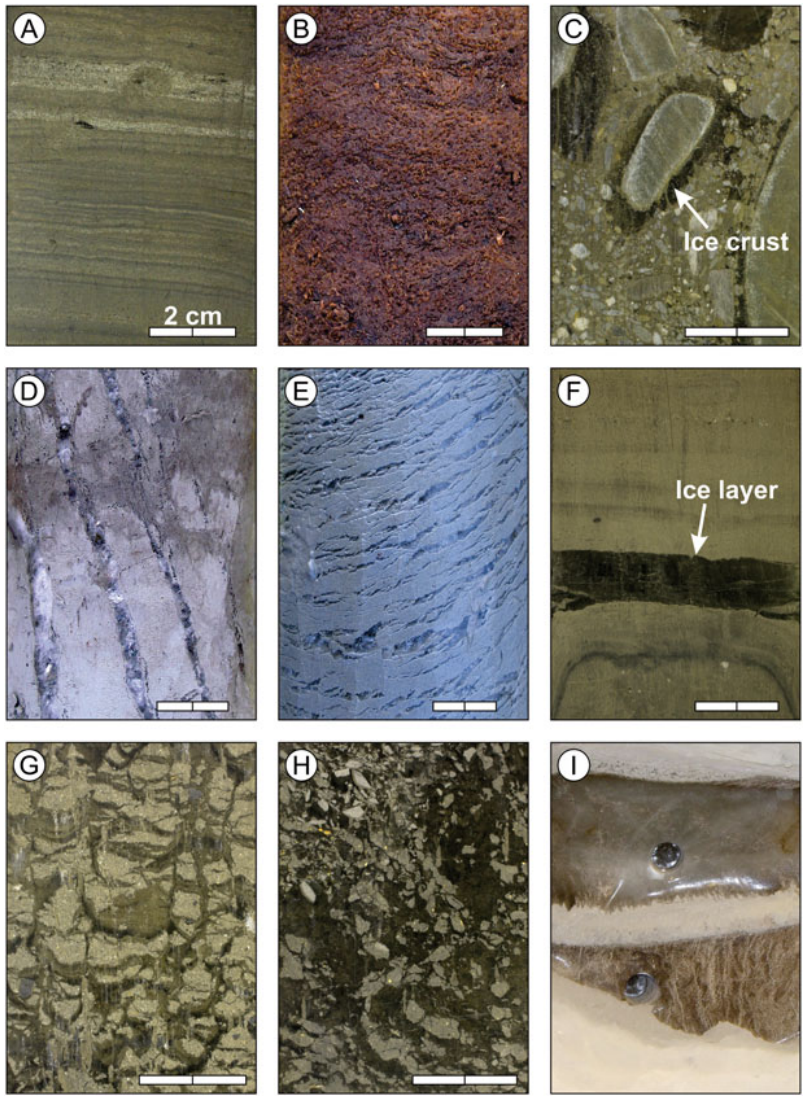

Figure 2 Simplified classification of cryostructures in unconsolidated sediments based on a classification presented by Murton (2013), which is modified from previous classifications. All photographs are oriented vertically such that the long axis of the image is perpendicular to the ground surface. (A) Pore cryostructure – note the absence of visible ice. (B) Organic-matrix cryostructure – ice present in the void space but not visible. (C) Crustal cryostructure. (D) Vein cryostructure. (E) Lenticular cryostructure. (F) Layered cryostructure. (G) Reticulate cryostructure. (H) Ataxitic cryostructure. (I) Solid cryostructure – thermokarst-cave (pool) ice overlying a vertically foliated ice wedge. Two drill holes several centimetres in diameter are visible in the ice.

clast or wood fragment in frost-susceptible material (Figure 2C). *Vein* cryostructure denotes ice veins that are inclined to vertical in orientation (Figure 2D). *Lenticular* cryostructure denotes lens-shaped ice bodies, often horizontal to subhorizontal, formed by ice segregation in frost-susceptible material (Figure 2E). *Layered* (or bedded) cryostructure comprises horizontal to dipping ice layers formed by ice segregation or injection of pressurised water (Figure 2F). *Reticulate* cryostructure represents a three-dimensional (3D) network of vertical ice veins and

horizontal ice lenses that separate clayey or silty sediment blocks (Figure 2G). *Ataxitic* (suspended) cryostructure develops where sediment grains or aggregates are suspended in ice; in many cases, it forms in the intermediate layer at the top of permafrost (Figure 2H). *Solid* cryostructure occurs where bodies of ice exceed 10 cm in thickness (Figure 2I). These cryostructures are useful for logging of permafrost sequences, but in reality some cryostructures are transitional, composite or hierarchical in nature (Murton, 2013).

The development of cryostructures relates to three main factors: (1) the physical properties of soil, sediment or bedrock; (2) moisture availability; and (3) the mode of permafrost formation (epigenetic, syngenetic or quasi-syngenetic). A key property is the grain size distribution (particularly the proportion of silt) and packing of grains, which influence the frost susceptibility of the host sediment (i.e. the degree to which the soil favours the formation of segregated ice). Frost susceptibility in soils depends primarily on the continuous network of unfrozen water films in the frozen fringe. Moister sites promote the formation of ice-rich cryostructures compared to drier ones (Murton, 2013; Stephani *et al*., 2014).

Distinguishing cryostructures is scale-dependent and may be difficult when working with cores. The small diameter of cores (mostly between 5 cm and 10 cm) means that lateral continuity of ground-ice bodies in many cases cannot be established. For instance, it may not be possible to distinguish between lenticular and layered cryostructures at the core scale. Natural sections or trial pits best reveal cryostructures.

Epigenetic Permafrost

When the ground surface begins to experience cold subaerial conditions, epigenetic permafrost aggrades downward. Under such conditions, ground ice and permafrost decrease in age with depth.

Outside of areas with buried ice, epigenetic permafrost tends to be ice-poor, with wedge and segregated ice concentrated mostly in the top few metres. However, ice-rich epigenetic permafrost (including massive-ice bodies of segregated or intrusive origin) may form at any depth where the freezing front encounters a significant source of groundwater. The distance between visible ice lenses generally increases with depth, whereas the overall ice content decreases. The ice-rich top, in many cases, may be explained by the formation of the ice-rich intermediate layer, which results from a gradual decrease in active-layer thickness (mostly due to the accumulation of organic matter) and is characterised by an ataxitic (suspended) cryostructure (French and Shur, 2010). Formation of the intermediate layer is considered 'quasi-syngenetic' because permafrost aggrades upward without any sedimentation on the ground surface (Shur *et al*., 2011).

Cryostructures of ataxitic, lenticular and layered type are common in the intermediate layer (Osterkamp *et al*., 2009; Calmels *et al*., 2012). The type of cryostructure in this layer depends strongly on the rate of upward permafrost aggradation. Prolonged stability of the permafrost table favours layered cryostructures (so-called 'ice belts', discussed below), whereas slow aggradation of the permafrost table favours ataxitic cryostructures (Calmels *et al*., 2012), as illustrated from till deposits in Yukon, Canada (Stephani *et al*., 2014).

Where the groundwater supply is limited, epigenetic freezing forms a pore cryostructure with very low ice content (Stephani *et al*., 2014), whose presence in frost-susceptible material is a hallmark of epigenetic permafrost. Reticulate cryostructures also indicate epigenetic permafrost, and are believed to develop by desiccation and shrinkage during sediment freezing while moisture migrates towards an advancing freezing front (French and Shur, 2010).

Ice-rich epigenetic permafrost commonly forms in sediments where groundwater is abundant. Layered and reticulate cryostructures characterise epigenetically frozen lacustrine silts in the lowlands of west-central Alaska, with the volume of visible segregated ice varying from 10 to 50 per cent, and ice lenses up to 10 cm thick (Kanevskiy *et al*., 2014). Similar cryostructures have been described in Nunavik, Canada (Calmels and Allard, 2008). Ice-rich epigenetic permafrost was also detected near Anchorage, close to the southern boundary of permafrost in Alaska (Riddle and Rooney, 2012). In the 10 m thick section of glaciolacustrine deposits (silty clay with numerous layers of segregated ice up to 70 cm thick) there, the average volume of visible ice exceeded 40 per cent (Kanevskiy *et al*., 2013a).

In the discontinuous permafrost zone, epigenetic permafrost often starts to form with the development of palsas or lithalsas, which may eventually transform into permafrost plateaus elevated above the initial ground surface by the accumulation of segregated ice. Palsas and lithalsas have been recently studied in Fennoscandia (Seppälä, 2011), the Altai and Sayan regions of Russia (Iwahana *et al*., 2012; Y. K. Vasil'chuk *et al*., 2015), the Northwest Territories (e.g. Wolfe *et al*., 2014) and northern Quebec, Canada (Kuhry, 2008; Calmels and Allard, 2008; Calmels *et al*., 2008), the Himalayas (Wünnemann *et al*., 2008) and Mongolia (Sharkuu *et al*., 2012).

Ice-rich syngenetic permafrost sometimes degrades, drains and subsequently re-establishes as epigenetic permafrost. Thawed and refrozen soils typically undergo a reduction in ice content when compared with their former state. However, in many cases, ice-rich quasi-syngenetic permafrost forms on top of such refrozen soils, usually due to the development of surface vegetation and formation of an organic-rich surface horizon (Stephani *et al*., 2014; Kanevskiy *et al*., 2014).

Bedrock hosts epigenetic permafrost in many areas, especially alpine settings and areas eroded by Pleistocene glaciers, for example, the Canadian Shield. Classification of cryostructures in bedrock adopted from the Russian

permafrost literature (translated by Mel'nikov and Spesivtsev, 2000) is presented by French and Shur (2010). Pore and layered cryostructures in basalt lava have recently been described from Kamchatka (Abramov *et al*., 2008) and intrusive ice layers and lenses in limestones, dolomites, marls and kimberlites from central Yakutia (Alexeev *et al*., 2016).

Syngenetic Permafrost

Ground ice in syngenetic permafrost forms within aggrading sedimentary sequences during or soon after deposition, mainly as segregated ice at the top of permafrost (also named *aggradational ice*; Mackay, 1972; Cheng, 1983) or as syngenetic wedge ice. Layered and lenticular cryostructures record the progressively aggrading ground surface, and are typical of syngenetic permafrost (French and Shur, 2010). Russian studies of the 1950–60s (Katasonov, 2009; Popov, 2013) revealed rhythmic structure of syngenetic permafrost, formed by relatively uniform layers with a predominantly lenticular cryostructure separated by '*ice belts*' (distinct icy layers several millimetres to several centimetres thick that indicate the position of the permafrost table during periods when it was relatively stable). Cryostructures between ice belts have been termed '*microcryostructures*' (Kanevskiy *et al*., 2011), formed mainly by thin (<1 mm) densely spaced ice lenses and include microlenticular, microbraided and microataxitic types.

Moisture availability, soil texture and sedimentation rate strongly control cryostructure distribution in syngenetic permafrost. Two cryofacies diagnostic of syngenetic permafrost have been distinguished in organic-rich silts, in Yukon, Canada (Stephani *et al*., 2014). Microlenticular cryostructures formed in near-surface permafrost during periods of relatively rapid surface aggradation (e.g. by deposition of windblown silt). Conversely, ataxitic and reticulate cryostructures with thick ice belts formed during periods of slower siliciclastic sedimentation that favoured the accumulation of peat and resulted in active-layer thinning and formation of the intermediate layer. Buried ice-rich intermediate layers with thick ice belts and predominantly ataxitic cryostructure are typical of thick sequences of syngenetic permafrost (Stephani *et al*., 2014; Kanevskiy *et al*., 2011).

Syngenetic permafrost of Holocene age tends to be thinner than that of Pleistocene age. Currently, syngenetic permafrost forms in mineral soils within floodplains of Arctic rivers (Shur and Jorgenson, 1998), deltas (Morse and Burn, 2013) and areas of loess accumulation (Härtel *et al*., 2012), and the reported thickness of modern syngenetic permafrost seldom exceeds 5 m. Cryostratigraphic studies of syngenetic permafrost, however, have focused mainly on Pleistocene '*yedoma*' (or 'Ice Complex'), which represents relic ice-rich syngenetic permafrost with large ice wedges that formed in Siberia and North America during the Late Pleistocene (Figure 3A; Schirrmeister *et al*., 2013; Murton *et al*., 2015). Continued supply of fine-grained sediment favoured yedoma development over tens of thousands of years, producing syngenetic permafrost sequences often several tens of metres thick that archive Late Pleistocene environmental history. General maps of yedoma distribution in Siberia were presented by Konishchev (2009, 2011) and Kanevskiy *et al*. (2011), with the latter authors including a preliminary map of yedoma distribution in Alaska. Detailed maps of Siberian yedoma (scale 1:1 000 000) have been developed by Grosse *et al*. (2013) from Russian Quaternary geological maps. Yedoma sections have been recently described from northern Yakutia (Schirrmeister *et al*., 2011; Tumskoy, 2012; Strauss *et al*., 2012; Wetterich *et al*., 2011, 2014), central Yakutia (Spektor *et al*., 2008), Taymyr (Streletskaya and Vasilev, 2012), northern Alaska (Kanevskiy *et al*., 2011), interior Alaska (Kanevskiy *et al*., 2008; Meyer *et al*., 2008), the Seward Peninsula (Shur *et al*., 2012; Stephani *et al*., 2012) and Yukon (Froese *et al*., 2009; Pumple *et al*., 2015; Sliger *et al*., 2015).

Ground ice is abundant and buried cryosols are present within many yedoma sequences. Ground ice observed at 14 locations along the coast of the Laptev and East Siberian seas was primarily wedge ice, 'net-like reticulated' cryostructures and ice bands (Schirrmeister *et al*., 2011). The ice wedges were identified as syngenetic on the basis of their large size and morphology. Ice bands (belts in the Russian literature) were interpreted to reflect stable surface conditions and active-layer thicknesses, leading to ice enrichment of the near-surface permafrost. Buried cryosols within the yedoma contained peat 'nests' and terrestrial plant leaves and woody debris. Schirrmeister *et al*. (2011) attributed these deposits to formation subaerially in polygonal terrain.

PERMAFROST DEGRADATION AND RE-AGGRADATION

The degradation of ice-rich permafrost (thermokarst) may produce distinctive features in the cryostratigraphic record that indicate the depth or mode of past thermokarst activity prior to re-aggradation of permafrost. This is well illustrated in two case studies from yedoma regions, which are particularly susceptible to thermokarst. The first identified cryostratigraphic evidence for shallow degradation of permafrost in non-glaciated Yukon and Alaska during the last interglaciation: (1) buried relic ice wedges whose tops were thaw truncated at the base of a palaeo-active layer; (2) ice-wedge pseudomorphs formed by complete melting of ice wedges; (3) wood-rich organic silt deposits ('forest beds') that represent forest vegetation reworked by thaw slumping or deposition in thermokarst ponds or depressions; and (4) lenticular and reticulate cryostructures interpreted as segregated ice at the top of permafrost and the bottom of the active layer (Reyes *et al*., 2010). This study inferred a depth of thaw on the order of metres during the last interglaciation, highlighting the resilience of ice-rich discontinuous permafrost over glacial-interglacial timescales. The second case

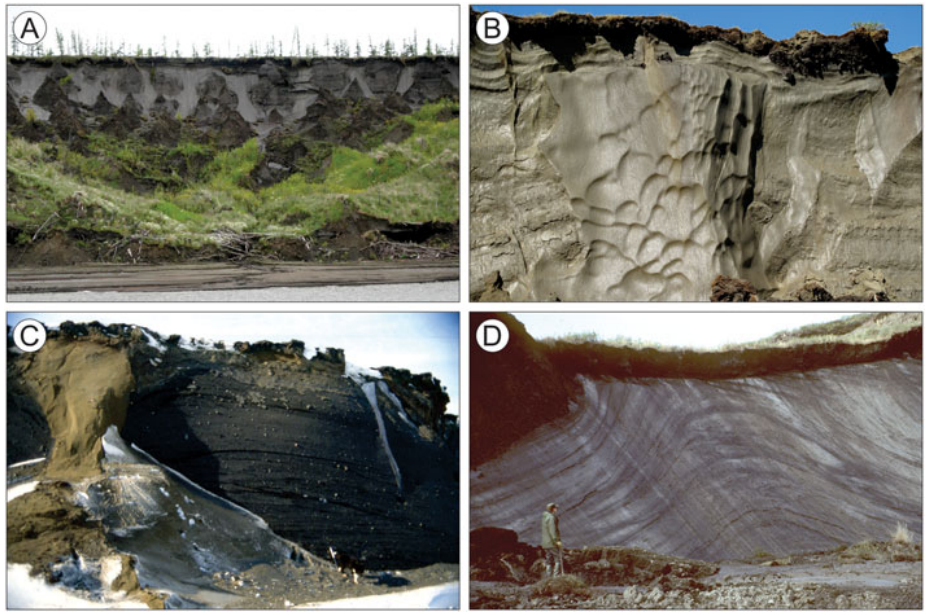

Figure 3 (A) Yedoma exposed in the headwall of a retrogressive thaw slump at Duvanny Yar, northeast Yakutia, Russia. Syngenetic ice wedges (lighter-coloured grey) enclose columns of silt (darker-coloured grey), some of which degrade to form conical thermokarst mounds (baydzherakhs). The top of the headwall is about 39 m above the level of the Kolyma River (in foreground). (B) Ice-rich *c.* 1 m thick intermediate layer with a thin active ice wedge on top of a large buried syngenetic ice wedge, 35 m high Itkillik River yedoma exposure, northern Alaska. (C) Buried basal ice from the Laurentide Ice Sheet, Mason Bay, Richards Island, Northwest Territories, Canada. Pebbles and cobbles protrude from the surface of massive ice, and folds occur within it. Sand wedge (left) and two ice wedges (right) penetrate massive ice. Dog and ice axe for scale (bottom centre). (D) Post-glacial intrasedimental massive ice at Peninsula Point, near Tuktoyaktuk, Northwest Territories, Canada. Anticline in banded massive ice underlies a small slump.

study used cryostratigraphic observations to evaluate the permafrost response to clearance of surface vegetation in discontinuous permafrost of the Klondike region, Yukon (Calmels *et al.*, 2012). There, a thaw unconformity at a depth of about 2 m was interpreted to mark the thaw depth following deforestation during the gold rush era, beginning about 1900 AD.

MASSIVE GROUND ICE

Massive ice is a comprehensive term applied to large bodies of ground ice with ice contents exceeding 250 per cent by weight (van Everdingen, 1998). Recent studies of massive ice have focused on four main genetic classes (wedge ice, thermokarst-cave (pool) ice, intrusive ice and buried ice) and on the origin of tabular massive-ice bodies.

Wedge Ice

Ice wedges are the most common type of massive ice, and syngenetic wedges are particularly valuable in cryostratigraphy because both the wedge ice and surrounding sediments contain palaeoenvironmental archives. Syngenetic ice wedges grow both vertically and horizontally, resulting often in a vertically nested chevron pattern (Mackay, 1990). Syngenetic ice wedges in the outer Mackenzie Delta, Canada, have been identified from 'shoulders' indicative of vertical growth stages and from the cross-sectional width of the wedges decreasing towards the top of permafrost (Figure 3B; Morse and Burn, 2013). The ice wedges developed below a slowly aggrading surface.

A conceptual model of syngenetic ice-wedge development invokes micro-, meso- and macrocycles (Y.K. Vasil'chuk, 2013). Microcycles affect ice wedges by changes in active-layer depth and rates of deposition of thin sediment layers over timescales of several years to hundreds of years. Mesocycles of ice-wedge growth result from changes in water level, where ice wedges are located close to or under shallow water bodies. Deposits overlying wedge ice consist of alternating layers of peat (formed during exposure) and siliciclastic sediment (deposited during submergence). Ice-wedge growth is reduced or suspended during submergence. Macrocycles result from major changes in sedimentary regimes over timescales of tens of thousands to hundreds of thousands of years.

Syngenetic ice wedges account for a significant proportion of the ground-ice record in lowland permafrost environments, especially in yedoma. Recent studies of the isotopic or trapped gas composition in wedge ice have reconstructed

palaeoclimate and investigated infilling processes (e.g. Meyer *et al*., 2010; Opel *et al*., 2011; Raffi and Stenni, 2011; Lachniet *et al*., 2012). For example, Streletskaya *et al*. (2011) identified a trend of warming palaeoclimate since the Late Weichselian from different generations of syngenetic ice wedges near the Kara Sea. St-Jean *et al*. (2011) showed that site-specific factors influence the infilling characteristics of wedge ice: in cold, dry settings, wedge ice shows evidence of snow densification, and in moister settings of freezing of liquid water.

Thermokarst-Cave Ice

Thermokarst-cave ice (or pool ice) forms by freezing of water trapped in underground cavities or channels (Murton, 2013), typically along degrading ice wedges (Figure 2I). Recent studies have described thermokarst-cave ice bodies underlain by silts with reticulate cryostructure in the CRREL permafrost tunnel, interior Alaska (Fortier *et al*., 2008; Kanevskiy *et al*., 2008; Douglas *et al*., 2011). Measurements performed along a 600 m long and 10 m high exposure at Barter Island (Alaskan Beaufort Sea coast) showed that numerous thermokarst-cave ice bodies occupied almost 2 per cent of the face of the coastal bluff (Kanevskiy *et al*., 2013b).

Intrusive Ice

Intrusive ice forms by freezing of water injected under pressure into freezing or frozen ground (Murton, 2013). Recent cryostratigraphic studies of intrusive ice have focused on stable isotope stratigraphy and the identification and development of tabular massive ice.

Stable isotope analysis has been applied to reconstruct the freezing processes and growth history of pingos. Two different isotopic patterns, indicative of open-system and semi-closed-system freezing, were observed in ice sections in an open-system (hydraulic) pingo in northwest Mongolia, indicating an oscillation between periods where the groundwater reservoir fed open-system ice lens development and those of flow interruption, forming a closed-system environment (Yoshikawa *et al*., 2013). Y. K. Vasil'chuk *et al*. (2014) distinguished between two periods of development in a closed-system (hydrostatic) pingo in northwest Siberia.

Massive bodies of intrusive ice may form following the drainage of palaeo-lake systems, or from the repeated injection of lake water into marine sediments following shoreline regression. In glaciolacustrine deposits of central Yukon, Lauriol *et al*. (2010) identified, using stable O and H isotopes and occluded gas composition, intrusive ice bodies (10 m wide and 3–4 m thick) that aggraded following the lowering of the water level in a palaeo-glacial lake. The glaciolacustrine sediments are underlain by permeable gravels and sands, which served as the water source during permafrost aggradation. The formation mechanism is therefore likely similar to growth conditions of hydrostatic pingos.

Buried Ice

Various types of ice bodies may be buried by soil or sediment. Recent literature on buried ice primarily concerns buried basal glacier ice (Murton, 2009; Fortier *et al*., 2012; Solomatin and Belova, 2012; Solomatin, 2013; Coulombe *et al*., 2015; Lacelle *et al*., 2015) and buried snow (Spektor *et al*., 2011). Investigations of cryostructures in basal ice from existing glaciers provide a basis for comparison with buried counterparts (e.g. Fortier *et al*., 2012).

Several stratigraphic characteristics aid in identifying buried glacier ice, including: (1) a discordant upper contact; (2) inclusions of glacial sediment (Figure 3C); and (3) dynamic metamorphic structures. A discordant upper contact is identified by the truncation of internal ice structures such as folds, stratification, and structural and textural heterogeneities (Solomatin and Belova, 2012). Such thaw or erosional unconformities develop due to either glaciofluvial erosion or the thaw front reaching the ice surface (Murton, 2013; Coulombe *et al*., 2015). Glaciotectonic deformation structures in ice-rich diamictons and ice structures similar to those in modern basal glacier ice may also serve as genetic indicators. Murton (2009) used an event stratigraphy related to the timing of glaciotectonic deformation to help distinguish between massive ice that was buried or at least glacially deformed from that which post-dated deformation and must be of intrasedimental origin. Though the stratigraphic context for massive ice may provide a good indication of the ice origin, it is not always conclusive, and interpretations may be strengthened by studies of ice crystallography, geochemistry and palynology.

Origin of Tabular Massive Ice

Most descriptions of tabular bodies of massive ice are from regions formerly occupied by Pleistocene glaciers or ice sheets. Such ice bodies commonly overlie coarse-grained (sand-rich) deposits, underlie fine-grained ones (muds) (Mackay and Dallimore, 1992) and contain sediment as individual particles or aggregates. Three models are generally employed to explain the origin of massive ice: (1) intrasedimental ice growth as segregated and/or intrusive ice; (2) burial of glacier ice; and (3) subglacial permafrost aggradation (Murton, 2013). Investigations commonly combine traditional stratigraphy and cryostratigraphy with other methods (ice crystallography, geochemistry and analysis of gas inclusions).

Recent studies of tabular massive ice have been conducted along the western Arctic coast of Canada (Murton, 2009; Fritz *et al*., 2011), central Yukon (Lauriol *et al*., 2010), the Alaskan Coastal Plain (Kanevskiy *et al*., 2013b), the Canadian Arctic islands (Coulombe *et al*., 2015) and northwest Siberia (Slagoda *et al*., 2010, 2012a, 2012b; Kritsuk, 2010; Leibman *et al*., 2011; Solomatin

and Belova, 2012; Fotiev, 2014, 2015; Y. K. Vasil'chuk *et al*., 2009, 2011, 2012, 2014; Vasiliev *et al*., 2015). Intrasedimental and buried ice have been distinguished on several lines of evidence. This includes the stratigraphic, sedimentological and geomorphological setting of the ice bodies; the upper and lower contacts between the ice and the surrounding sediments; internal characteristics of the ice body (e.g. bubble characteristics, suspended sediment and deformation structures; Figure 3D); and ice palynology, stable isotope geochemistry and hydrochemistry. However, in many cases, the origin of tabular massive ice is disputed. For example, Y. K. Vasil'chuk (2012, p. 496) stated that 'It should be particularly noted that presently not a single massive ice body identified in the plain areas of the permafrost regions of Russia can be definitely identified as buried glacier ice.' In contrast, Solomatin and Belova (2012, p. 430) wrote in the same proceedings that 'The materials, experimental data, and theoretical concepts collected at the present time lead to the clear conclusion that tabular massive ice represents a single and separate genetic type of ground ice: the buried remnants of glaciers that formed during deglaciation of the ancient glaciation areas.'

Interpreting the origin of massive ice is often challenging because the growth of segregated ice, intrusive ice and gradations between them can occur in both non-glacial and subglacial settings. Intrasedimental bodies of tabular massive ice frequently display characteristics similar to those of buried glacier ice (Coulombe *et al*., 2015). Recently, however, some valuable contributions have come from studies of ice palynology, isotope geochemistry and hydrochemistry. Studies in western Siberia have suggested that pollen and spores occur in most massive-ice bodies, and although redeposited pre-Quaternary palynomorphs of Cenozoic, Mesozoic and Palaeozoic age are common, the pollen of aquatic plants, horsetail spores, limnetic diatoms and green algae remains indicate a non-glacial genesis of the ice (A. C. Vasil'chuk and Y. K. Vasil'chuk, 2010, 2012). Vasiliev *et al*. (2015) reported extremely high concentrations of methane in tabular massive-ice bodies of the Yamal Peninsula, supporting the intrasedimental interpretation of tabular massive ice in this area.

Isotopic and hydrochemical analysis of massive ice is now commonly used to assist interpretation, with the values of and relations between $\delta^{18}O$, δD and d-excess providing insights into the processes of fractionation, sublimation and ionic segregation during freezing (D. Lacelle *et al*., 2011; Michel, 2011), including in Martian regolith (D. Lacelle *et al*., 2008). Such analyses often supplement field observations of the cryostratigraphy (Murton, 2009), and have permitted identification of buried perennial snowbank ice (D. Lacelle *et al*., 2009), intrusive ice (Lauriol *et al*., 2010) and aufeis (icing ice) (Lacelle and Vasil'chuk, 2013; Lacelle *et al*., 2013) and basal regelation glacier ice (Fritz *et al*., 2011, 2012).

A new classification of tabular massive ice, developed by Y. K. Vasil'chuk (2012), is based on three divisions. The first distinguishes between homogeneous and heterogeneous massive-ice bodies. *Homogeneous* massive-ice bodies have a similar genesis, composition and properties in all parts of a massive-ice complex. An example would be a single ice sill or body of massive segregated ice. *Heterogeneous* massive-ice bodies have a variable genesis, composition and properties across a massive-ice complex, and consist of two or more homogeneous ice bodies. Numerous examples occur on the Yamal Peninsula and adjacent regions of western Siberia (Y. K. Vasil'chuk *et al*., 2009, 2011, 2012, 2014). The second division distinguishes between *autochthonous* (intrasedimental) and *allochthonous* (buried) ice, and the third division classifies the massive ice according to its specific genetic process (e.g. injection, segregation, infiltration, burial). Overall, this classification provides a valuable framework for investigating massive ice, and emphasises its genetic diversity.

GROUND-ICE CONTENT

Quantifying the amount and distribution of ground ice is necessary in order to predict permafrost landscape change in the future. Ground-ice content has become an important input to landscape and ecosystem models and in estimating organic carbon pools in permafrost (Kuhry *et al*., 2013; Strauss *et al*., 2013; Ulrich *et al*., 2014). Cryostratigraphic observations provide valuable field data to help evaluate ground-ice content. Ground-ice content has recently been assessed using three distinct approaches: (1) landscape-scale estimation of wedge-ice volume (WIV) using remote sensing; (2) laboratory analysis of permafrost samples; and (3) fine-scale determination of ice volume by x-ray computed tomography (CT) scanning.

Y. K. Vasil'chuk (2009) reviewed different methods of WIV estimation (mainly based on ice-wedge geometry) developed by permafrost researchers since the 1960s. Several recent studies have estimated WIV in polygonal terrain using remotely sensed images (e.g. Bode *et al*., 2008; Morse and Burn, 2013; Skurikhin *et al*., 2013; Jorgenson *et al*., 2015). Ulrich *et al*. (2014) presented a method for calculating WIV in yedoma and Holocene thermokarst basin deposits, utilising 3D surface models generated from satellite images to identify ice-wedge polygon morphometry. Individual wedge volume is estimated using measurements obtained from field data. Some assumptions are employed when calculating WIV: epigenetic ice wedges are usually assumed to have the shape of isosceles triangles or trapezoids in cross-section (Kanevskiy *et al*., 2013b; Ulrich *et al*., 2014), and syngenetic ice wedges that of a rectangular-shaped frontal cut (Strauss *et al*., 2013). Ice-wedge size and morphology are commonly determined by field studies. Parameters determined from field measurements include the top and bottom width of individual wedges and the depth. Field data are used to parameterise 3D subsurface models and to upscale to the landscape scale.

The ice content of sediments containing pore, segregated or intrusive ice can be determined by laboratory analysis of permafrost samples. Gravimetric moisture content is commonly expressed on a dry basis (the ratio of the mass of ice in a sample to the mass of the dry sample). Phillips *et al*. (2015) compared dry- and wet-basis gravimetric moisture contents and concluded that the latter has some advantages when used for ice-rich mineral soils. Volumetric ice content (VIC) is the ratio of the volume of ice in a sample to the volume of the whole sample. Excess ice content is equal to the volume in excess of the pore volume in an unfrozen state, and estimations of excess ice content (e.g. O'Neill and Burn, 2012) correspond to thaw strain measurements commonly performed during geotechnical investigations (e.g. Kanevskiy *et al*., 2012). In ice-rich soils, excess ice content is similar to the volumetric content of visible ice. In ice-rich epigenetic permafrost, VIC can be estimated relatively easily by analysing photographs of frozen cores and exposures (Kanevskiy *et al*., 2013a, 2014). Total VIC of the upper layers of permafrost (which includes pore, segregated and massive ice) has been estimated based on a terrain-unit approach for the Beaufort Sea coastal area of Alaska (Kanevskiy *et al*., 2013b) and Yukon (Couture and Pollard, 2015).

CT scanning of frozen sediment cores provides a reasonable estimate of VIC and a non-destructive method of 3D imaging and analysing their internal structure (Calmels and Allard, 2008; Calmels *et al*., 2010, 2012; Lapalme *et al*., 2015). CT scans image features such as stratification, sediment properties, fractures, gas inclusions, ice distribution and density variations. The method utilises the density contrasts in the sample, allowing users to distinguish between gas, ice, organic and mineral components (Cnudde and Boone, 2013). Two limiting factors must be considered when determining VIC using image analysis of CT scans. Firstly, materials of similar densities are not easily differentiated. For example, organic-rich horizons (e.g. frozen, saturated peat) are similar in density to ice, which results in an overestimation of ice content unless the material can be correctly classified visually. Secondly, the spatial scan resolution (0.35 mm in the transverse direction and 0.5 mm in the longitudinal direction) limits the identification of pore ice in fine-grained sediment. Similarly, constituents (e.g. gas bubbles) that are smaller than the resolution size cannot be accounted for in volume calculations, which may lead to their underestimation, unless accounted for using calibration factors (Ducharme *et al*., 2015).

CONCLUSIONS AND PERSPECTIVES FOR FUTURE RESEARCH

Recent cryostratigraphic research in modern permafrost environments has focused on fine-grained deposits of aeolian, fluvial or lacustrine origin. As seen in Figure 1, however, relatively few cryostratigraphic studies have investigated permafrost in eastern Arctic Canada, Greenland and Scandinavia. Such landscapes include highly variable relief and depositional systems, where permafrost formation is closely tied to late Quaternary glacial and sea-level history. Evaluation of the cryostratigraphy of these environments may provide valuable insight into permafrost aggradation and ground-ice formation during the Holocene Epoch. Targeted studies in these locations may help to assess the nature of ground-ice formation in coarse-grained deposits, for example, in alluvial fans and colluvium.

Cryostructural classifications have been successfully applied to describe the occurrence and variability of ground ice in permafrost sediment sequences. To complement these largely descriptive and inferential studies, future research needs to investigate mechanistically the processes of cryostructure development. Freezing and thawing experiments under controlled field and laboratory conditions may allow hypothesis testing about cryostructure processes and boundary conditions, as well as quantification of rates of cryostructure formation.

The presence of ground ice has important consequences for landscape and infrastructure development as well as ecosystem and climate models. Recent studies into VIC have integrated a number of remotely sensed and indirect methods to assess ground-ice characteristics in permafrost. Future research needs to constrain the uncertainty in these estimations.

ACKNOWLEDGEMENTS

We would like to thank the two reviewers, D. Lacelle and one anonymous, and the Editor, C. R. Burn, for their constructive comments on the manuscript. M. Kanevskiy acknowledges the National Science Foundation (grants ARC 1023623 and ArcSEES 1233854) for financial support.

REFERENCES

Abramov A, Gruber S, Gilichinsky D. 2008. Mountain permafrost on active volcanoes: field data and statistical mapping, Klyuchevskaya volcano group, Kamchatka, Russia. *Permafrost and Periglacial Processes* **19**(3): 261–277. DOI:10.1002/ppp.622

Alexeev SV, Alexeeva LP, Kononov AM. 2016. Trace elements and rare earth elements in ground ice in kimberlites and sedimentary rocks of Western Yakutia. *Cold Regions Science and Technology* **123**: 140–148. DOI:10.1016/j.coldregions.2015.10.008

Badu YB. 2010. Cryolithology: Textbook. KDU: Moscow; 528 in Russian.

Bode JA, Moorman BJ, Stevens CW, Solomon SM. 2008. Estimation of ice wedge volume in the Big Lake Area, Mackenzie Delta, NWT, Canada. In Proceedings of the Ninth International Conference on Permafrost, Fairbanks, USA, 29 June–3 July 2008, Vol. **1**, Kane DL, Hinkel KM (eds). Institute for Northern Engineering, University of Alaska Fairbanks; 131–136.

Calmels F, Allard M. 2008. Segregated ice structures in various heaved permafrost landforms through CT scan. *Earth Surface Processes and Landforms* **33**: 209–225. DOI:10.1002/esp.1538

Calmels F, Allard M, Delisle G. 2008. Development and decay of a lithalsa in Northern Quebec: A geomorphological history. *Geomorphology* **97**: 287–299. DOI:10.1016/j.geomorph.2007.08.013

Calmels F, Clavano WE, Froese DG. 2010. Progress on x-ray computed tomography (CT) scanning in permafrost studies. In Proceedings Geo2010 Calgary–63rd Canadian Geotechnical Conference and 6th Canadian Permafrost Conference, 12–16 September 2010, Calgary, Canada; 1353–1358.

Calmels F, Froese DG, Clavano WR. 2012. Cryostratigraphic record of permafrost degradation and recovery following historic (1898-1992) surface disturbances in the Klondike region, central Yukon Territory. *Canadian Journal of Earth Sciences* **49**(8): 938–952. DOI:10.1139/e2012-023

Cheng G. 1983. The mechanism of repeated segregation for the formation of thick-layered ground ice. *Cold Regions Science and Technology* **8**: 57–66. DOI:10.1016/0165-232X(83)90017-4

Cnudde V, Boone MN. 2013. High-resolution x-ray computed tomography in geosciences: A review of the current technology and applications. *Earth-Science Reviews* **123**: 1–17. DOI:10.1016/j.earscirev.2013.04.003

Coulombe S, Fortier D, Shur Y, Kanevskiy M, Lacelle D. 2015. Cryofacies and cryostructures of massive ice found on Bylot Island, Nunavut. In Proceedings GeoQuébec 2015–68th Canadian Geotechnical Conference and 7th Canadian Permafrost Conference, 20–23 September 2015, Quebec, Canada.

Couture N, Pollard W. 2015. Ground ice determinations along the Yukon coast using a morphological model. In Proceedings GeoQuébec 2015–68th Canadian Geotechnical Conference and 7th Canadian Permafrost Conference, 20–23 September 2015, Quebec, Canada.

Douglas TA, Fortier D, Shur Y, Kanevskiy M, Guo L, Cai Y, Bray M. 2011. Biogeochemical and geocryological characteristics of wedge and thermokarst-cave ice in the CRREL permafrost tunnel, Alaska. *Permafrost and Periglacial Processes* **6**: 120–128. DOI:10.1002/ppp.709

Ducharme M-A, Allard M, Côté J, L'Hérault E. 2015. Measurements of permafrost thermal conductivity through CT-scan analysis. In Proceedings GeoQuébec 2015–68th Canadian Geotechnical Conference and 7th Canadian Permafrost Conference, 20–23 September 2015, Quebec, Canada.

Everdingen RO van. 1998revised May 2005. Multi-language Glossary of Permafrost and Related Ground-ice Terms. National Snow and Ice Data Center/World Data Center for Glaciology: Boulder, CO.

Fortier D, Kanevskiy M, Shur Y. 2008. Genesis of reticulate-chaotic cryostructure in permafrost. In Proceedings of the Ninth International Conference on Permafrost, June 29–July 3, 2008, Fairbanks, Alaska, Kane DL, Hinkel KM (eds), **1**. Institute of Northern Engineering, University of Alaska Fairbanks: Alaska; 451–456.

Fortier D, Kanevskiy M, Shur Y, Stephani E, Dillon M, Jorgenson T. 2012. Cryostructures of basal glacier ice as an object of permafrost study: observations from the Matanuska Glacier, Alaska. In Proceedings of the Tenth International Conference on Permafrost, June 25–29, 2012, Salekhard, Russia, Hinkel KM (ed), Vol. **1**. International contributions. The Northern Publisher: Salekhard, Russia; 107–112.

Fotiev SM. 2014. Massive ice beds, Marre-Sale Cape (western coast of the Yamal Peninsula). *Earth Cryosphere* **XVIII**(2): 34–46(in Russian).

Fotiev SM. 2015. Genesis and mechanism of formation of repeated-intrusive massive ice layers. *Earth Cryosphere* **XIX**(1): 27–36.

French H, Shur Y. 2010. The principles of cryostratigraphy. *Earth-Science Reviews* **101**: 190–206. DOI:10.1016/j.earscirev.2010.04.002

Fritz M, Wetterich S, Meyer H, Schirrmeister L, Lantuit H, Pollard WH. 2011. Origin and characteristics of massive ground ice on Herschel Island (western Canadian arctic) as revealed by stable water isotope and hydrochemical signatures. *Permafrost and Periglacial Processes* **22**(1): 26–38. DOI:10.1002/ppp.714

Fritz M, Wetterich S, Shirrmeister L, Meyer H, Lantuit H, Preusser F, Pollard WH. 2012. East Beringia and beyond: Late Wisconsinan and Holocene landscape dynamics along the Yukon Coastal Plain, Canada. *Palaeogeography, Palaeoclimatology, Palaeoecology* **319-320**: 28–45. DOI:10.1016/j.palaeo.2011.12.015

Froese DG, Zazula GD, Westgate JA, Preece SJ, Sanborn PT, Reyes AV, Pearce NJG. 2009. The Klondike goldfields and Pleistocene environments of Beringia. *GSA Today* **19**(8): 4–10. DOI:10.1130/GSATG54A.1

Grosse G, Robinson JE, Bryant R, Taylor MD, Harper W, DeMasi A, Kyker-Snowman E, Veremeeva A, Schirrmeister L, Harden J. 2013. Distribution of late Pleistocene ice-rich syngenetic permafrost of the Yedoma Suite in East and Central Siberia, Russia. USGS Geological Survey Open-File Report 2013-1078, 37pp.

Härtel S, Christiansen HH, Elberling B. 2012. Cryostratigraphy and ice content of the near-surface permafrost in lower Adventdalen, Svalbard. In Proceedings of the Tenth International Conference on Permafrost, June 25-29, 2012, Salekhard, Russia, Vol. **4** Extended abstracts. The Northern Publisher: Salekhard, Russia; 207–208.

Iwahana G, Fukui K, Mikhailov N, Ostanin O, Fujii Y. 2012. Structure of a Lithalsa in the Akkol Valley, Russian Altai Mountains. *Permafrost and Periglacial Processes* **23**(2): 107–118. DOI:10.1002/ppp.1734

Jorgenson T, Kanevskiy MZ, Shur Y, Moskalenko NG, Brown DRN, Wickland K, Striegl R, Koch J. 2015. Ground ice dynamics and ecological feedbacks control ice-wedge degradation and stabilization. *Journal of Geophysical Research: Earth Surface* **120**(11): 2280–2297. DOI:10.1002/2015JF003602

Kanevskiy M, Fortier D, Shur Y, Bray M, Jorgenson T. 2008. Detailed cryostratigraphic mapping of syngenetic permafrost in the Winze of the CRREL Permafrost Tunnel, Fox, Alaska. In *Proceedings of the Ninth International Conference on Permafrost, June 29 – July 3, 2008, Fairbanks, Alaska*, Kane DL, Hinkel KM (eds), Vol. **2**. Institute of Northern Engineering, University of Alaska Fairbanks; 889–894.

Kanevskiy M, Shur Y, Jorgenson MT, Stephani E. 2011. Cryostratigraphy of late Pleistocene syngenetic permafrost (yedoma) in northern Alaska, Itkillik River exposure. *Quaternary Research* **75**: 584–596. DOI:10.1016/j.yqres.2010.12.003

Kanevskiy M, Shur Y, Connor B, Dillon M, Stephani E, O'Donnell J. 2012. Study of the ice-rich syngenetic permafrost for road design (Interior Alaska). In Proceedings of the Tenth International Conference on Permafrost, June 25–29, 2012, Salekhard, Russia, Hinkel KM (ed), Vol. **1**. International contributions. The Northern Publisher: Salekhard, Russia; 191–196.

Kanevskiy M, Shur Y, Krzewinski T, Dillon M. 2013a. Structure and properties of ice-rich permafrost near Anchorage, Alaska. *Cold Regions Science and Technology* **93**: 1–11. DOI:10.1016/j.coldregions.2013.05.001

Kanevskiy M, Shur Y, Jorgenson MT, Ping C-L, Michaelson GJ, Fortier D, Stephani E, Dillon M, Tumskoy V. 2013b. Ground ice in the upper permafrost of the Beaufort Sea coast of Alaska. *Cold Regions Science and Technology* **85**: 56–70. DOI:10.1016/j.coldregions.2012.08.002

Kanevskiy M, Jorgenson MT, Shur Y, O'Donnell JA, Harden JW, Zhuang Q, Fortier D. 2014. Cryostratigraphy and permafrost evolution in the lacustrine lowlands of West-Central Alaska. *Permafrost and Periglacial Processes* **25**: 14–34. DOI:10.1002/ppp.1800

Katasonov EM. 2009. *Lithology of Frozen Quaternary Deposits* (*Cryolithology*) *of the*

Yana Coastal Plain (PhD thesis, Obruchev Permafrost Institute, 1954), Kaplina TN (ed). PNIIIS: Moscow; 176(in Russian).

Konishchev VN. 2009. Climate warming and permafrost. Moscow State University, Geography-Environment-Sustainability **1**: 4–19.

Konishchev VN. 2011. Permafrost response to climate warming. *Earth Cryosphere* **XV**(4): 13–16.

Kritsuk LN. 2010. Ground ice of West Siberia. Nauchniy Mir: Moscow; 352(in Russian).

Kuhry P. 2008. Palsa and peat plateau development in the Hudson Bay Lowlands, Canada: timing, pathways and causes. *Boreas* **37**(2): 316–327. DOI:10.1111/j.1502-3885.2007.00022.x

Kuhry P, Grosse G, Harden JW, Hughlius G, Koven CD, Ping C-L, Schirrmeister L, Tarnocai C. 2013. Characterization of the permafrost carbon pool. *Permafrost and Periglacial Processes* **24**: 146–155. DOI:10.1002/ppp.1782

Lacelle D, Fisher DA, Clark ID, Berinstain A. 2008. Distinguishing between vapor- and liquid-formed ground ice in the northern martian regolith and potential for biosignatures preserved in ice bodies. *Icarus* **197**: 458–469. DOI:10.1016/j.icarus.2008.05.017

Lacelle D, St-Jean M, Lauriol B, Clark ID, Lewkowicz A, Froese DG, Kuehn SC, Zazula. 2009. Burial and preservation of a 30,000 year old perennial snowbank in Red Creek valley, Ogilvie Mountains, central Yukon, Canada. *Quaternary Science Reviews* **28**: 3401–3413. DOI:10.1016/j.quascirev.2009.09.013

Lacelle D, Davila AF, Pollard WH, Andersen D, Heldmann J, Marinova M, McKay CP. 2011. Stability of massive ground ice bodies in University Valley, McMurdo Dry Valleys of Antarctica: Using stable O–H isotope as tracers of sublimation in hyperarid regions. *Earth and Planetary Science Letters* **301**: 403–411. DOI:10.1016/j.epsl.2010.11.028

Lacelle D, Lauriol B, Zazula G, Ghaleb B, Utting N, Clark ID. 2013. Timing of advance and basal conditions of the Laurentide Ice Sheet during the last glacial maximum in the Richardson Mountains, NWT. *Quaternary Research* **80**: 274–283. DOI:10.1016/j.yqres.2013.06.001

Lacelle D, Brooker A, Fraser RH, Kokelj SV. 2015. Distribution and growth of thaw slumps in the Richardson Mountains-Peel Plateau region, northwestern Canada. *Geomorphology* **235**: 40–51. DOI:10.1016/j.geomorph.2015.01.024

Lacelle DM, Vasil'chuk YK. 2013. Recent progress (2007-2012) in permafrost isotope geochemistry. *Permafrost and Periglacial Processes* **24**(2): 138–145. DOI:10.1002/ppp.1768

Lachniet MS, Lawson DE, Sloat AR. 2012. Revised ^{14}C dating of ice wedge growth in interior Alaska (USA) to MIS 2 reveals cold paleoclimate and carbon recycling in ancient permafrost terrain. *Quaternary Research* **78**: 217–225. DOI:10.1016/j.yqres.2012.05.007

Lapalme CM, Lacelle D, Davila AF, Pollard W, Fortier D, McKay CP. 2015. Cryostratigraphy of near-surface permafrost in University Valley, McMurdo Dry Valleys of Antarctica. In Proceedings GeoQuébec 2015–68 th Canadian Geotechnical Conference and 7th Canadian Permafrost Conference, 20–23 September 2015, Quebec, Canada.

Lauriol B, Lacelle D, St-Jean M, Clark ID, Zazula GD. 2010. Late Quaternary paleoenvironments and growth of intrusive ice in eastern Beringia (Eagle River valley, northern Yukon, Canada). *Canadian Journal of Earth Sciences* **47**: 941–955. DOI:10.1139/E10-012

Leibman MO, Kizyakov AI, Lein AY, Perednya DD, Savvichev AS, Vanshtein BG. 2011. Sulfur and carbon isotopes within atmospheric, surface and ground water, snow and ice as indicators of the origin of tabular ground ice in the Russian Arctic. *Permafrost and Periglacial Processes* **22**(1): 39–48. DOI:10.1002/ppp.716

Mackay JR. 1972. The world of underground ice. *Annals of the American Association of Geographers* **62**: 1–22. DOI:10.1111/j.1467-8306.1972.tb00839.x

Mackay JR. 1990. Some observations on the growth and deformation of epigenetic, syngenetic and anti-syngenetic ice wedges. *Permafrost and Periglacial Processes* **1**: 15–29. DOI:10.1002/ppp.3430010104

Mackay JR, Dallimore SR. 1992. Massive ice in the Tuktoyaktuk area, western Arctic coast, Canada. *Canadian Journal of Earth Sciences* **29**(6): 1235–1249. DOI:10.1139/e92-099

Mel'nikov VP, Spesivtsev VI. 2000. Cryogenic Formations in the Earth's Lithosphere. Siberian Publishing Center UIGGM, Siberian Branch, Russian Academy of Sciences: Novosibirsk.

Meyer H, Yoshikawa K, Schirrmeister L, Andreev A. 2008. The Vault Creek Tunnel (Fairbanks Region, Alaska) – A Late Quaternary Palaeoenvironmental Permafrost Record. In Proceedings of the Ninth International Conference on Permafrost, June 29–July 3, 2008, Fairbanks, Alaska, Kane DL, Hinkel KM (eds), Vol. **2**. Institute of Northern Engineering, University of Alaska Fairbanks: Alaska; 1191–1196.

Meyer H, Schirrmeister L, Andreev A, Wagner D, Hubberten HW, Yoshikawa K, Bobrov A, Wetterich S, Opel T, Kandiano E, Brown J. 2010. Lateglacial and Holocene isotopic and environmental history of northern coastal Alaska – results from a buried ice-wedge system at Barrow. *Quaternary Science Reviews* **29**: 3720–3735. DOI:10.1016/j.quascirev.2010.08.005

Michel FA. 2011. Isotope characterisation of ground ice in northern Canada. *Permafrost and Periglacial Processes* **22**: 3–12. DOI:10.1002/ppp.721

Morse PD, Burn CR. 2013. Field observations of syngenetic ice wedge polygons, outer Mackenzie Delta, western Arctic coast, Canada. *Journal of Geophysical Research: Earth Surface* **118**: 1320–1332. DOI:10.1002/jgrf.20086

Murton JB. 2009. Stratigraphy and palaeoenvironments of Richards Island and the eastern Beaufort Continental Shelf during the last glacial–interglacial cycle. *Permafrost and Periglacial Processes* **20**: 107–125. DOI:10.1002/ppp.647

Murton JB. 2013. Ground ice and cryostratigraphy. In Treatise on Geomorphology, Vol. 8, Glacial and Periglacial Geomorphology, Schoder JF, Giardino R, Harboor J (eds). Academic Press: San Diego; 173–201.

Murton JB, Goslar T, Edwards ME, Bateman MD, Danilov PP, Savvinov GN, Gubin SV, Ghaleb B, Haile J, Kanevskiy M, Lozhkin AV, Lupachev AV, Murton DK, Shur Y, Tikhonov A, Vasil'chuk AC, Vasil'chuk YK, Wolfe SA. 2015. Paleoenvironmental interpretation of yedoma silt (ice complex) deposition as cold-climate loess, Duvanny Yar, northeast Siberia. *Permafrost and Periglacial Processes* **26**: 208–288. DOI:10.1002/ppp.1843

O'Neill HB, Burn CR. 2012. Physical and temporal factors controlling the development of near-surface ground ice at Illisarvik, western Arctic coast, Canada. *Canadian Journal of Earth Sciences* **49**: 1096–1110. DOI:10.1139/E2012-043

Opel T, Dereviagin AY, Meyer H, Schirrmeister L, Wetterich S. 2011. Palaeoclimatic Information from Stable Water Isotopes of Holocene Ice Wedges on the Dmitrii Laptev Strait, Northeast Siberia, Russia. *Permafrost and Periglacial Processes* **22**(1): 84–100. DOI:10.1002/ppp.667

Osterkamp TE, Jorgenson MT, Schuur EAG, Shur YL, Kanevskiy MZ, Vogel JG, Tumskoy VE. 2009. Physical and ecological changes associated with warming permafrost and thermokarst in interior Alaska. *Permafrost and Periglacial Processes* **20**: 235–256. DOI:10.1002/ppp.656

Phillips M, Burn C, Wolfe S, Morse P, Gaanderse A, O'Neill B, Shugar D, Gruber S. 2015. Improving water content description of ice-rich permafrost soils. In Proceedings GeoQuébec 2015–68 th Canadian Geotechnical Conference and 7th Canadian Permafrost Conference, 20–23 September 2015, Quebec, Canada.

Popov AI. 2013. Selected works, and about him. Moscow: Nauchniy Mir; 536(in Russian).

Pumple J, Froese D, Calmels F. 2015. Characterizing permafrost valley fills along the Alaska Highway, southwest Yukon. In Proceedings GeoQuébec 2015–68th Canadian Geotechnical Conference and 7th Canadian Permafrost Conference, 20-23 September 2015, Quebec, Canada.

Raffi R, Stenni B. 2011. Isotopic composition and thermal regime of ice wedges in northern Victoria Land, East Antarctica. *Permafrost and Periglacial Processes* **22**(1): 65–83. DOI:10.1002/ppp.701

Reyes AV, Froese DG, Jensen BJL. 2010. Permafrost response to last interglacial warming: field evidence from nonglaciated Yukon and Alaska. *Quaternary Science Reviews* **29**: 3256–3274. DOI:10.1016/j.quascirev.2010.07.013

Riddle CH, Rooney JW. 2012. Encounters with relict permafrost in the Anchorage, Alaska, area. In *Proceedings of the Tenth International Conference on Permafrost, June 25–29, 2012, Salekhard, Russia*, Hinkel KM (ed), Vol. **1**. International contributions, The Northern Publisher: Salekhard, Russia; 323–328.

Rogov VV. 2009. Fundamentals of Cryogenesis. Novosibirsk: Geo; 203(in Russian).

Schirrmeister L, Kunitsky V, Grosse G, Wetterich S, Meyer H, Schwamborn G, Babiy O, Derevyagin A, Siegert C. 2011. Sedimentary characteristics and origin of the Late Pleistocene Ice Complex on north-east Siberian Arctic coastal lowlands and islands – A review. *Quaternary International* **241**: 3–25. DOI:10.1016/j.quaint.2010.04.004

Schirrmeister L, Froese D, Tumskoy V, Grosse G, Wetterich S. 2013. Yedoma: Late Pleistocene ice-rich syngenetic permafrost of Beringia. In Encyclopedia of Quaternary Science, Second edition, Elias SA, Mock CJ (eds), **2**. Elsevier: Amsterdam; 542–552.

Seppälä M. 2011. Synthesis of studies of palsa formation underlining the importance of local environmental and physical characteristics. *Quaternary Research* **75**: 366–370. DOI:10.1016/j.yqres.2010.09.007

Sharkuu N, Yoshikawa K, Anarmaa S. 2012. Perennial frost mounds in Mongolia. In Proceedings of the Tenth International Conference on Permafrost, June 25-29, 2012, Salekhard, Russia, Hinkel KM (ed), Vol. **1** International contributions. The Northern Publisher: Salekhard, Russia; 371–376.

Shpolyanskaya NA. 2015. Pleistocene-Holocene history of permafrost evolution in the Russian Arctic based on ground-ice studies. Institute of Computer Researches: Moscow-Izhevsk; 344(in Russian).

Shur YL. 1988. The upper horizon of permafrost soils. In *Proceedings of the Fifth International Conference on Permafrost*, Senneset K (ed), Vol. **1**. Tapir Publishers: Trondheim, Norway; 867–871.

Shur YL, Jorgenson MT. 1998. Cryostructure development on the floodplain of the Colville River Delta, northern Alaska. In *Permafrost, Proceedings of the 7th International Conference, Yellowknife, N.W.T, Canada*, Lewkowicz AG, Allard M (eds), Centre d'études Nordiques. Collection Nordicana 57, Université Laval: Quebec; 993–999.

Shur YL, Jorgenson MT, Kanevskiy MZ. 2011. Permafrost. In Encyclopedia of Earth Sciences Series, Encyclopedia of Snow, Ice and Glaciers, Singh VP, Singh P, Haritashya UK (eds). Springer: The Netherlands; 841–848 DOI: 10.1007/978-90-481-2642-2.

Shur YL, Kanevskiy M, Jorgenson T, Dillon M, Stephani E, Bray M. 2012. Permafrost degradation and thaw settlement under lakes in yedoma environment. In Proceedings of the Tenth International Conference on Permafrost, June 25-29, 2012, Salekhard, Russia, Hinkel KM (ed), **1** International contributions. The Northern Publisher: Salekhard, Russia; 383–388.

Skurikhin AN, Gangodagamage C, Rowland JC, Wilson CJ. 2013. Arctic tundra ice-wedge landscape characterization by active contours without edges and structural analysis using high-resolution satellite imagery. *Remote Sensing Letters* **4**: 1077–1086. DOI:10.1080/2150704X.2013.840404

Slagoda EA, Leibman MO, Opokina OL. 2010. Origin of deformations in Holocene-Quaternary deposits with tabular ground ice on Yugorsky peninsula. *Earth Cryosphere XIV* **4**: 30–41(in Russian).

Slagoda EA, Opokina OL, Kurchatova AN, Rogov VV. 2012a. Structure and composition of complex massive ice bodies in Late Pleistocene-Holocene sediments of the Marre-Sale Cape, West Yamal. In Proceedings of the Tenth International Conference on Permafrost, 25–29 June, 2012, Salekhard, Russia, Melnikov VP, Drozdov DD, Romanovsky VE (eds); 415–420.

Slagoda EA, Opokina OL, Rogov VV, Kurchatova AN. 2012b. Structure and genesis of the underground ice in the Neopleistocene-Holocene sediments of Marre-Sale cape, Western Yamal. *Earth Cryosphere XVI* **2**: 9–22(in Russian)..

Sliger M, Fortier D, deGrandpré I, Lapointe-Elmrabti L. 2015. Incidence of pleistocene-holocene climate on the concurrent landscape and permafrost development of the Beaver Creek region, southwest Yukon, Canada. In Proceedings GeoQuébec 2015– 68th Canadian Geotechnical Conference and 7th Canadian Permafrost Conference, 20-23 September 2015, Quebec, Canada.

Solomatin VI. 2013. Physics and geography of underground glaciation. Novosibirsk: Geo; 346(in Russian).

Solomatin VI, Belova NG. 2012. Proof of the glacier origin of tabular massive ice. In Proceedings of the Tenth International Conference on Permafrost, June 25-29, 2012, Salekhard, Russia, Melnikov VP, Drozdov DS, Romanovsky VE (eds), Vol. **2**. Translations of Russian contributions. The Northern Publisher: Salekhard, Russia; 427–432.

Spektor VB, Spektor VV, Bakulina NT. 2008. New data on the Ice Complex of the Lena-Amga rivers plain (Central Yakutia). In Proceedings of the Ninth International Conference on Permafrost, University of Alaska Fairbanks, Fairbanks, **2**; 1681–1684.

Spektor VB, Spektor VV, Bakulina NT. 2011. Buried Snow in the Lena-Amga Plain. *Earth Cryosphere* **15**(4): 16–21(in Russian).

Stephani E, Kanevskiy M, Dillon M, Bray M, Shur Y. 2012. Cryostratigraphy of Yedoma (Ice Complex) in Seward Peninsula, Alaska. In Tenth International Conference on Permafrost, June 25-29, 2012, Salekhard, Russia, Vol. **4**. Extended abstracts. Fort Dialog-Iset: Ekaterinburg, Russia; 569–570.

Stephani E, Fortier D, Shur Y, Fortier R, Doré G. 2014. A geosystems approach to permafrost investigations for engineering applications, an example from a road stabilization experiment, Beaver Creek, Yukon, Canada. *Cold Regions Science and Technology* **100**: 20–35. DOI:10.1016/j.coldregions.2013.12.006

St-Jean M, Lauriol B, Clark ID, Lacelle D, Zdanowicz C. 2011. Investigation of ice-wedge infilling processes using stable oxygen and hydrogen isotopes, crystallography and occluded gases (O_2, N_2, Ar). *Permafrost and Periglacial Processes* **22**: 49–64. DOI:10.1002/ppp.680

Strauss J, Schirrmeister L, Wetterich S, Borchers A, Davydov SP. 2012. Grain-size properties and organic-carbon stock of Yedoma Ice Complex permafrost from the Kolyma lowland, northeastern Siberia.

Global Biogeochemical Cycles **26**: GB3003. DOI:10.1029/2011GB00410410

Strauss J, Schirrmeister L, Grosse G, Wetterich S, Ulrich M, Herzschuh U, Hubberten H-W. 2013. The deep permafrost carbon pool of the Yedoma region in Siberia and Alaska. *Geophysical Research Letters* **40**(23): 6165–6170. DOI:10.1002/2013GL058088

Streletskaya I, Vasiliev A, Meyer H. 2011. Isotopic composition of syngenetic ice wedges and palaeoclimatic reconstruction, western Taymyr, Russian Arctic. *Permafrost and Periglacial Processes* **22**: 101–106. DOI:10.1002/ppp.707

Streletskaya ID, Vasilev AA. 2012. The ice complex of western Taymyr. In Proceedings of the Tenth International Conference on Permafrost, June 25-29, 2012, Salekhard, Russia, Melnikov VP, Drozdov DS, Romanovsky VE (eds), **2** Translations of Russian contributions. The Northern Publisher: Salekhard, Russia; 433–438.

Tumskoy VE. 2012. Peculiarities of cryolithogenesis in Northern Yakutia (middle Neopleistocene to Holocene). *Earth Cryosphere XVI* **1**: 2–21(in Russian).

Ulrich M, Grosse G, Strauss J, Schirrmeister L. 2014. Quantifying Wedge-Ice Volumes in Yedoma and Thermokarst Basin Deposits. *Permafrost and Periglacial Processes* **25**: 151–161. DOI:10.1002/ppp.1810

Vasil'chuk AC, Vasil'chuk YK. 2010. Local pollen spectra as a new criterion for nonglacial origin of massive ice. *Transactions* (*Doclady*) *of Russian Academy of Sciences*. *Earth Sciences* **433**: 985–990. DOI:10.1134/S1028334X10070305

Vasil'chuk AC, Vasil'chuk YK. 2012. Pollen and spores as massive ice origin indicators. In Proceedings of the Tenth International Conference on Permafrost, June 25-29, 2012, Salekhard, Russia, Melnikov VP, Drozdov DD, Romanovsky VE (eds), Vol. **2**. The Northern Publisher: Salekhard, Russia; 487–492.

Vasil'chuk YK. 2009. New approach to estimation of wedge-ice volume. *Inzhenernaya Geologiya (Engineering Geology)* **4**: 40–47(in Russian).

Vasil'chuk YK. 2012. Classification of Massive Ice. In Proceedings of the Tenth International Conference on Permafrost, June 25-29, 2012, Salekhard, Russia, Melnikov VP, Drozdov DD, Romanovsky VE (eds), Vol. **2**. The Northern Publisher: Salekhard, Russia; 493–497.

Vasil'chuk YK. 2013. Syngenetic ice wedges: Cyclical formation, radiocarbon age and stable isotope records by Yurij K. Vasil'chuk, Moscow University Press, Moscow, 2006, 404 pp, ISBN 5-211-05212-9 (Monograph Synopsis). *Permafrost and Periglacial Processes* **24**: 82–93. DOI:10.1002/ppp.1764

Vasil'chuk YK, Vasil'chuk AC, Budantseva NA, Chizhova JN, Papesch W, Podborny YY, Sulerzhitsky LD. 2009. Oxygen Isotope and Deuterium Indication of the Origin and ^{14}C Age of the Massive Ice, Bovanenkovo, Central Yamal Peninsula. *Doklady Earth Sciences* **429**: 1326–1332. DOI:10.1134/S1028334X09080194

Vasil'chuk YK, Budantseva NA, Vasil'chuk AC. 2011. Variations in $\delta^{18}O$, δD, and the concentration of pollen and spores in autochthonic heterogeneous massive ice on the Erkutayaha River in the southern part of the Yamal Peninsula. *Doklady Earth Sciences* **438**: 721–726. DOI:10.1134/S1028334X11050382

Vasil'chuk YK, Vasil'chuk AC, Budantseva NA. 2012. Isotopic and palynological compositions of a massive ice in the Mordyyakha River, Central Yamal Peninsula. *Doklady Earth Sciences* **446**: 1105–1109. DOI:10.1134/S1028334X12090164

Vasil'chuk YK, Budantseva NA, Vasilchuk AC, Yoshikawa K, Podborny YY, Chizhova JN. 2014. Isotope composition of pingo ice core in the Evoyakha river valley, North-West Siberia. *Earth Cryosphere* **XVIII**(4): 47–58(in Russian).

Vasil'chuk YK, Alexeev SV, Arzhannikov SG, Alexeeva LP, Budantseva NA, Chizhova JN, Arzhannikova AV, Vasil'chuk AC. 2015. Lithalsas in the Sentsa River Valley, Eastern Sayan Mountains, Southern Russia. *Permafrost and Periglacial Processes*In press DOI:10.1002/ppp.1876

Vasiliev AA, Streletskaya ID, Melnikov VP, Oblogov GE. 2015. Methane in ground ice and frozen Quaternary deposits of West Yamal. *Doklady Akademii Nauk [Transactions of Academy of Sciences] Earth Sciences* **465**(2): 1289–1292. DOI:10.1134/S1028334X15120168

Wetterich S, Rudaya N, Tumskoy V, Andreev AA, Opel T, Schirrmeister L, Meyer H. 2011. Last Glacial Maximum records in permafrost of the East Siberian Arctic. *Quaternary Science Reviews* **30**: 3139–3151. DOI:10.1016/j.quascirev.2011.07.020

Wetterich S, Tumskoy V, Rudaya N, Andreev AA, Opel T, Meyer H, Schirrmeister L, Hüls M. 2014. Ice Complex formation in arctic East Siberia during the MIS3 Interstadial. *Quaternary Science Reviews* **84**: 39–55. DOI:10.1016/j.quascirev.2013.11.009

Wolfe SA, Stevens CW, Gaanderse AJ, Oldenborger G. 2014. Lithalsa distribution, morphology and landscape associations in the Great Slave Lowland, Northwest Territories, Canada. *Geomorphology* **204**: 302–313. DOI:10.1016/j.geomorph.2013.08.014

Wünnemann B, Reinhardt C, Kotlia BS, Riedel F. 2008. Observations on the relationship between lake formation, permafrost activity and lithalsa development during the last 2000 years in the Tso Kar Basin, Ladakh, India. *Permafrost and Periglacial Processes* **19**: 341–358. DOI:10.1002/ppp.631

Yoshikawa K, Sharkhuu N, Sharkhuu A. 2013. Groundwater hydrology and stable isotope analysis of an open-system pingo in Northwestern Mongolia. *Permafrost and Periglacial Processes* **24**: 175–183. DOI:10.1002/ppp.1773

Paper II

Coring of unconsolidated permafrost deposits: methodological successes and challenges

Graham L. Gilbert
Geology Department, The University Centre in Svalbard, UNIS, Norway & Department of Earth Science, University of Bergen, Norway & Center for Permafrost, Department of Geoscience and Natural Resource Management, University of Copenhagen, Denmark
Hanne H. Christiansen
Geology Department, The University Centre in Svalbard, UNIS, Norway
Ullrich Neumann
Kolibri Geo Services, Risør, Norway

ABSTRACT
This technical note presents three scales of drilling infrastructure for comparison. These three methods include: (1) a small hand-drill designed for retrieving cores down to ca. 5 m depth, (2) the medium-scale UNIS Permafrost Drill Rig (down to ca. 50 m depth), and (3) an industrial drill rig designed for coring to depths of greater than 1 km. All methods vary with respect to maximum drill depth, operational cost, and ease of transport throughout the landscape.

RÉSUMÉ
Cet article compare trois méthodes de forage de tailles différentes. Ces trois méthodes correspondent à: (1) une petite foreuse portative conçue pour récupérer des carottes allant jusqu'à 5 m de profondeur, (2) une foreuse de taille moyenne UNIS Permafrost Drill Rig (jusqu'à environ 50 m de profondeur) et (3) une grosse foreuse industrielle conçue pour forer à des profondeurs de plus d'un km. Les méthodes de forage varient en fonction de la profondeur maximale des forages, des coûts d'exploitation, ainsi que de la facilité de leur transport sur le terrain.

1 INTRODUCTION

Recent field investigation in the Adventdalen Valley (central Spitsbergen, Svalbard) and northeastern Greenland have focused on reconstructing Holocene permafrost and landscape development from frozen sediment cores obtained using three scales of drilling infrastructure. The applied coring techniques range from small, portable hand-drills (**Figure 1A**) to an industrial drill rig, designed for obtaining bedrock cores from depths of greater than one kilometer (**Figure 1B**). In addition, a unique drill rig, designed by Dipl.-Ing. Lutz Kurth Bohr- und Brunnenausrüstungen GmbH in collaboration with Kolibri Geo Services, was acquired in 2011. This drill rig, called the UNIS permafrost drill rig, is intermediate in scale and has obtained core down to a depth of ca. 25 m (**Figure 1C**). The rig can be transported around the landscape by snowmobiles during winter – reducing the environmental impact when retrieving shallow cores from remote Arctic regions. The combination of these three methods has allowed us to assemble knowledge regarding the physical state of permafrost with regards to ground-ice conditions and sediments from different geomorphic settings and sediment types both on Svalbard and in northeast Greenland.

These three scales of infrastructure vary significantly with respect to the quality of retrieved cores, maximum depth of drilling, operational costs, and rig mobility. The objective with all methods is to retrieve cores of sufficient quality to visually classify ground-ice (cryostructures) and sedimentological characteristics. Such cores also permit the calculation of gravimetric moisture content, excess ice content, and sediment grain size distributions. For this reason the retrieval of high-quality, frozen samples is critical. The aim of this paper is todescribe and compare the three drill methods mentioned above.

2 EQUIPMENT AND METHODS

2.1 Hand-drill (**Figure 1A**)

The hand-drill consists of a STIHL^{TM} BT 121 Earth Auger, drilling extensions, and an unflighted (smooth walled) core barrel with diamond cutting teeth. The system has been tested in temperatures as low as -20 °C. The gas-driven power head has a rotation speed of between 0 and 190 RPM, controlled using the throttle. The core barrel, ca. 50 mm in inner diameter, was designed for taking concrete samples and effectively 'melts' through frozen ground using friction generated during rotation. Because of this unfrozen mud accumulates along the core barrel and the system is prone to 'freezing-in' if rotation stops.

During drilling, the equipment is assembled at the ground surface and lowered into the drilled hole. The core barrel and drill extensions are screwed together and tightened by the induced torque during drilling. The power head is connected to the drill string using a wire-lock lynch pin. The series of power head, drill rods, and core barrel must be removed from the hole with each coring attempt. The maximum depth per drilling attempt is ca. 50 cm (the inner length of the core barrel). The core barrel is designed without a core-catching system. We rely on friction, generated between the core and the sidewalls within the barrel, to retrieve the core with each attempt. In order to safely operate the hand drill, an operating team of minimum two is recommended.

Hand drilling is a good, though time consuming, method to retrieve samples from the top 2-5 m of sediments, depending on the sediment type and time available. Typical rates of drilling are between 0.5 and 1.0 m per hour. Since 2012, ca. 30-40 cores from 2 m to 5 m in length have been retrieved from Greenland and Svalbard using this method in both summer and winter.

Figure 1. The different drilling infrastructure. A – Hand Drilling; B – Industrial Drill Rig; C – UNIS Permafrost Drill Rig.

2.2. UNIS Permafrost Drill Rig (**Figure 1C**)

The UNIS permafrost drill rig was acquired in response to the need to evaluate the potential effects of on-going climatic changes on periglacial landforms in permafrost areas throughout Svalbard and Greenland. The rig consists of a hydraulic engine (Honda GX690), two air compressors (CompAir C14), a drill boom, and drill head.

Compressed air is used to cool the drill bit and transport cuttings to the surface. Connected in parallel, the two compressors produce 2.8 m^3 of air per minute at 7 bar. The drill can be equipped with a single core barrel (1 m length), double core barrel (1 m length), or rotary-air hammer drill. Additionally, six drill bits have been designed to meet the challenges posed by drilling in different substrates.

In general, drill bits with impregnated diamonds are used when drilling through rock and gravel, and drill bits with carbide inserts used in fine-grained sediments (**Figure 2**). The rake angle of the carbide bits have been further modified to ease drilling through ice and sediment. For mud and sand, bits with a rake angle of 0° have yielded the best results (**Figure 2A, B, E**). When ice is encountered a bit with a higher rake angle (30°) is used (**Figure 2D**). For bedrock and gravel, impregnated diamond bits are used (**Figure 2C, F**). This combination of drill bits has permitted core recovery from heterolithic substrates. In addition to coring, the drill rig can be equipped with a rotary air hammer drill. This destructive method allows us to make a hole (ca. 55 mm in diameter) and has been used to install casings for monitoring ground temperatures.

During drilling, the core barrel is attached to the drill head (drill motor) by a series of 1 m steel extensions. Following each drill attempt the entire drill string (extensions plus core barrel) must be removed from the hole in order to retrieve the core. The result of this is that the rate of drilling decreases with increasing depth. Over an interval of ca. 20 m the rate of drilling is between 0.5 and 1 m per hour.

The drill rig is mounted on a sledge which can be towed by a snowmobile. The rig has also been used during the snow-free period when it is transported using a fork lift or other transporting devices. The manufacturer states a maximum core retrieval depth of 50 m. However, investigations using coring have not exceeded 25 m to date. Recently, in April 2015, this rig was used to drill a 50 m hole to install temperature sensors for ground thermal monitoring. In this case no core was retrieved. However, this method has been used to recover cores from drill holes totalling 10 m to 25 m in length at ca. 8 sites in Svalbard and on Greenland. An operating crew of three to four is recommended when coring with two responsible for the drill operation, one in charge of core documentation and storage, and potentially one for equipment maintenance.

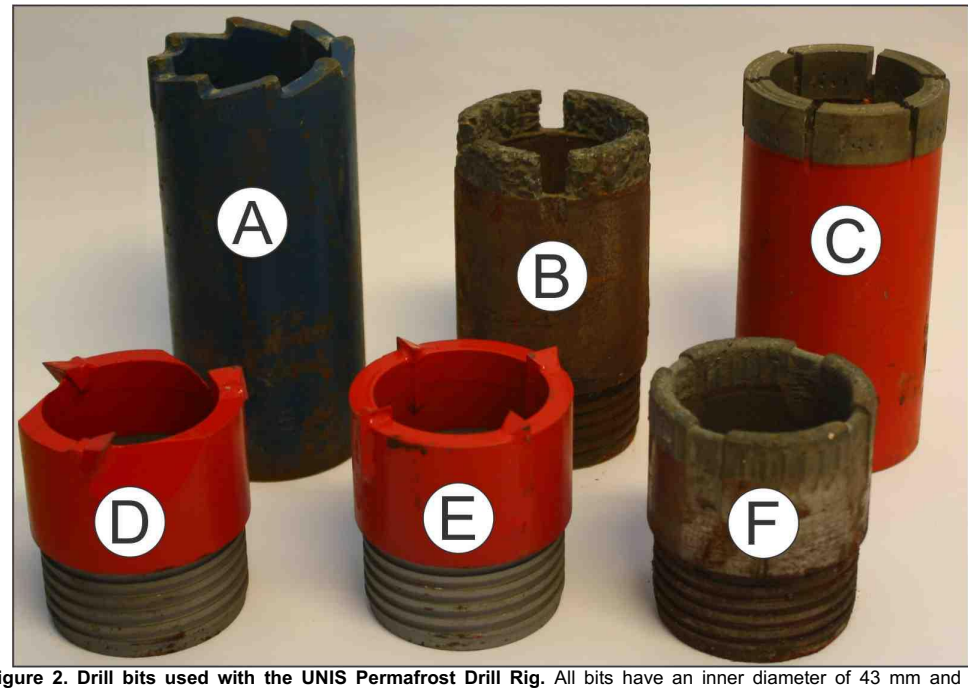

Figure 2. Drill bits used with the UNIS Permafrost Drill Rig. All bits have an inner diameter of 43 mm and are designed to rotate clockwise in a downwards direction. A – Eight hexagonal carbide inserts with rake angle of 0°. B – Impregnated carbide fragments in the crown. C – Impregnated diamond bit. D – Ice bit – three carbide inserts with rake angle of 30°. E – Four carbide inserts with a rake angle of 0°. F – Impregnated diamond bit.

2.2 Industrial Drill Rig (**Figure 1B**)

In September 2012 an industrial rig was used to drill a 60 m well in ice-bonded Quaternary deposits at the UNIS CO_2 Laboratory's well park in the Adventdalen valley bottom (Braathen et al. 2012, Gilbert 2014). This operation utilized a Boart Longyear™ HQ-3 wireline triple core barrel system. This system used water as a cooling and transport fluid. The triple-core barrel system limited the exposure of the core material to the drilling fluid by encasing the sample within a plastic tube during drilling (**Figure 3A**). The inner diameter of the core was 63.5 mm and sections were retrieved in 1.5 m lengths (**Figure 3B**). Drilling was expedited by the wireline system which allowed for core retrieval without removing the drill string. As a result, 60 m was cored in less than 20 hours (ca. 3 m per hour). During operation, the drill was run by two teams of two professional drillers, each working in 12 hour shifts. This process resulted in a retrieval rate of ca. 80 %; 48.1 m of the possible 60 m of sediment was recovered. Unrecovered intervals were distributed across the length of the core, and ranged in thickness from a few centimetres to 1.5 m.

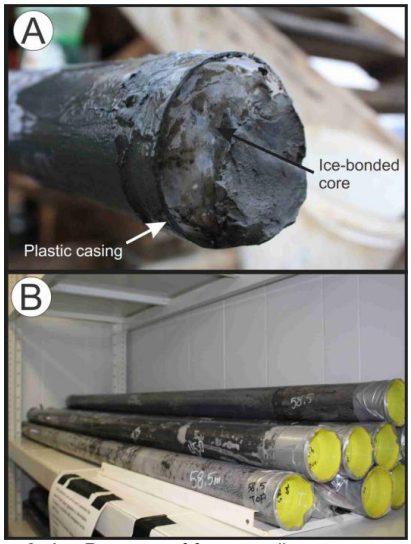

Figure 3. A – Recovery of frozen sediment core encased within the plastic sheathing. B – 1.5 m lengths of frozen cores in storage.

3 TECHNICAL COMMENTS AND CORE QUALITY

A qualitative evaluation of each drilling method in relation to the substrate composition is provided in **Figure 4**. All methods perform well in ice-rich material and fine-grained sediments (i.e. sand and mud). This observation consistent with those reported using other types of drills for permafrost coring (e.g. Brockett and Lawson 1985, Dickinson et al. 1999, Calmels et al. 2005, Saito and Yoshikawa 2009). The effectiveness of coring in these deposits is attributed to the presence of ice and grain size. Ice, acting as cement between individual grains and organic material, prevents core fragmentation during drill operation. Fine-grained sediments are additionally less susceptible to mechanical disintegration than coarser deposits. Both the hand drill and UNIS Permafrost Drill Rig are ineffective when coring in coarser material. This is attributed to the amount of energy generated while cutting through rock fragments, which effectively melts the ice contained in the core resulting in the retrieval of disturbed samples. The distinction between frozen cores from fine-grained deposits and fragmented cores from coarse-grained sediments is illustrated in **Figure 5**.

Unlike the aforementioned methods, the Industrial Drill Rig with the triple-core barrel system was effective across the entire spectrum of deposits encountered in the valley bottom sediments. The Adventdalen deposits range from compact, glacial diamicton (**Figure 6A**) to glaciomarine silts (**Figure 6B**) to sands deposited during delta progradation (**Figure 6C**; Gilbert 2014). The origin of the unretrieved intervals remains is tentatively attributed to two factors. The effects of mechanical abrasion were observed in some core sections, particularly those consisting of relatively well sorted sands and gravel. Here the absence of a mud-rich matrix left sediment grains susceptible to disintegration by the pressurized water, which was used as a drilling fluid. Alternatively, Lecomte et al. (2014) provided evidence for unfrozen pockets (cryopegs) in the valley bottom sediments. Given the influence of marine conditions during deposition the sediment pore water is likely rich in solute. Ground temperature in Adventdalen is on the order of -5 °C (Christiansen et al., 2010), and deposits may contain a significant amount of unfrozen water. However, all retrieved samples appeared well frozen at an ambient laboratory temperature of 6 °C.

4 CONCLUSION

The difficulty with retrieving satisfactory cores from frozen coarse-grained deposits using portable drill rigs remains a limiting factor when attempting to characterize permafrost deposits in mountainous landscapes such as Svalbard and northeast Greenland. The high-operational costs and limited mobility of the Industrial Drill Rig will likely limit the wide-spread use of the triple core barrel system, when coring in permafrost environments. However, the success of this method is in part attributed to the use of water as a drilling fluid. The UNIS Permafrost Drill Rig is also designed to operate with water as a drilling fluid. Future investigations of coarse-grained deposits may have a greater success if this medium is used instead. Hand drilling remains the most reliable and cost-effective method of retrieving short cores from the top 5 m of deposits.

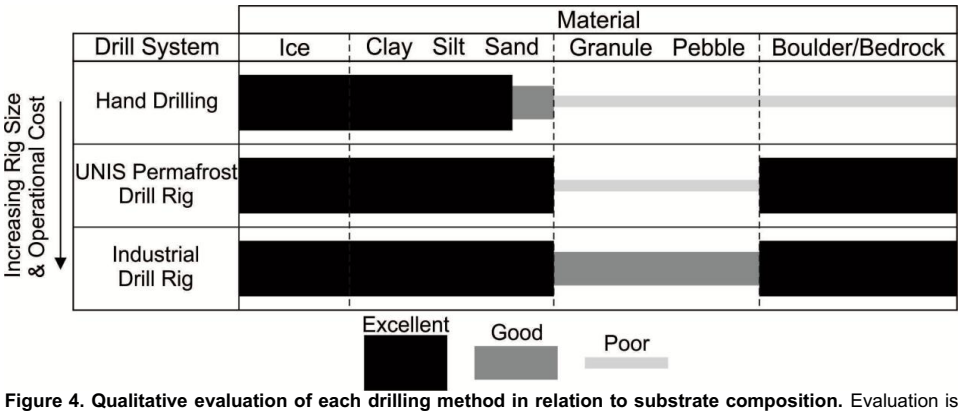

Figure 4. Qualitative evaluation of each drilling method in relation to substrate composition. Evaluation is based on the perceived quality of retrieved cores following laboratory investigation. 'Excellent' – intact cores with little or no evidence of disturbance. 'Good' – mostly intact cores with minimal to moderate disturbance. 'Poor' – complete disturbance with limited retrieval of material (no intact cores with samples thawed during drilling).

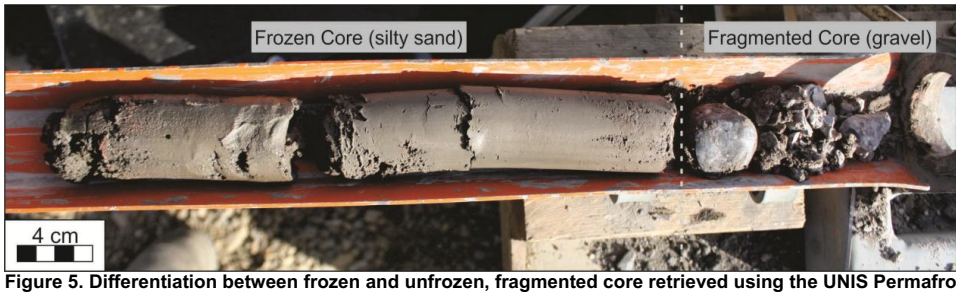

Figure 5. Differentiation between frozen and unfrozen, fragmented core retrieved using the UNIS Permafrost Drill Rig. Upwards direction is towards the left of the image.

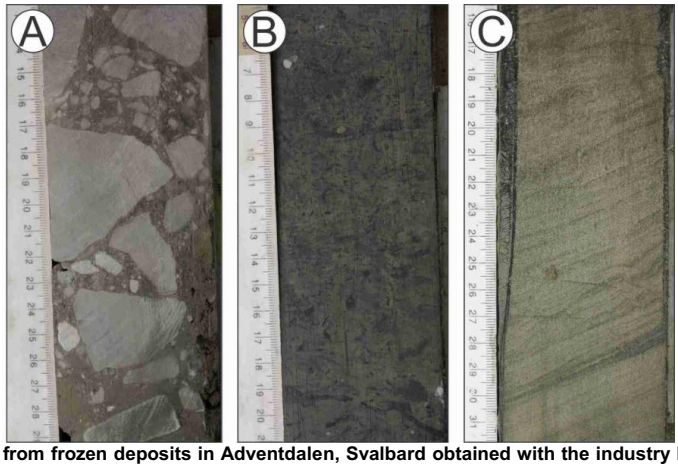

Figure 6. Samples from frozen deposits in Adventdalen, Svalbard obtained with the industry Drill rig. A – glacial diamicton; B – bioturbated marine muds; C – Sand-rich deltaic deposits. Scale in cm.

ACKNOWLEDGEMENTS

Drilling with the Industrial Drill Rig in September 2012 was funded by the UNIS CO_2 Project. Purchase of the UNIS Permafrost Drill Rig was partly financed by the EU 7th framework PAGE 21 Project and by The University Centre in Svalbard.

REFERENCES

Brockett BE, Lawson DE. 1985. Prototype drill for sampling fine-grained perennially frozen ground. CRREL Report 85-1, U.S. Army Engineer Cold Regions Research and Engineering Laboratory, Hanover, NH.

Braathen A, Bælum K, Christiansen HH, Dahl T, Eiken O, Elvebakk H, Hansen F, Hanssen TH, Jochmann M, Johansen TA, Johnsen H, Larsen L, Lie T, Mertes J, Mørk A, Mørk MB, Nemec W, Olaussen S, Oye V, Rød K, Titlestad GO, Tveranger J, Vagle K. 2012. The Longyearbyen CO_2 Lab of Svalbard, Norway – initial assessment of the geological conditions for CO_2 sequestration. *Norwegian Journal of Geology* **92**: 353-376.

Calmels F, Gangnon O, Allard M. 2005. A Portable Earth-drill System for Permafrost Studies. *Permafrost and Periglacial Processes* **16**: 311-315.

Christiansen HH, Etzelmüller B, Isaksen K, Juliussen H, Farbrot H, Humlum O, Johansson M, Ingeman-Nielsen T, Kristensen L, Hjort J, Holmlund P, Sannel ABK, Sigsgaard C, Åkerman HJ, Foged N, Blikra LH, Pernosky MA, Ødegård R. 2010. The Thermal State of Permafrost in the Nordic area during the International Polar Year 2007-2009. *Permafrost and Periglacial Processes* **21:** 156-181.

Dickinson W, Cooper P, Webster B, Ashby J. 1999. A Portable Drilling Rig for Coring Permafrosted Sediments. *Journal of Sedimentary Geology* **69(2)**: 518-527.

Gilbert GL. 2014. Sedimentology and geocryology of an Arctic fjord head delta (Adventdalen, Svalbard). Master's thesis, Department of Geosciences, University of Oslo. 124 p.

Lecomte I, Polom U, Sauvin G, Ruud BO, Christiansen, HH, Gilbert GL. 2014. Shear-wave reflection-seismic pilot study at the UNIS CO_2 Lab site, Longyearbyen, Svalbard. 76th EAGE Conference & Exhibition 2014: Amsterdam, Netherlands.

Saito T, Yoshikawa K. 2009. Portable Drilling for Frozen Coarse-Grained Material. 9th International Conference on Permafrost.

Paper III

The Cryosphere, 11, 1265–1282, 2017
www.the-cryosphere.net/11/1265/2017/
doi:10.5194/tc-11-1265-2017

The Cryosphere Open Access EGU

Cryostratigraphy, sedimentology, and the late Quaternary evolution of the Zackenberg River delta, northeast Greenland

Graham L. Gilbert[1,2], Stefanie Cable[1,3], Christine Thiel[4,5,6], Hanne H. Christiansen[1], and Bo Elberling[3]

[1]Arctic Geology Department, University Centre in Svalbard, PO Box 156, 9170 Longyearbyen, Norway
[2]Department of Earth Science, University of Bergen, Realfagbygget, Allegt. 41, 5007 Bergen, Norway
[3]Center for Permafrost (CENPERM), Department of Geosciences and Natural Resource Management, University of Copenhagen, Øster Voldgade 10, 1350 Copenhagen, Denmark
[4]Nordic Laboratory for Luminescence Dating, Department of Earth Sciences, Aarhus University, Risø Campus, 4000 Roskilde, Denmark
[5]Centre for Nuclear Technologies (Nutech), Technical University of Denmark, Risø Campus, 4000 Roskilde, Denmark
[6]Leibniz Institute for Applied Geophysics, Section S3: Geochronology and Isotope Hydrology, Stilleweg 2, 30655 Hanover, Germany

Correspondence to: Graham L. Gilbert (graham.gilbert@unis.no)

Received: 31 December 2016 – Discussion started: 17 January 2017
Revised: 7 April 2017 – Accepted: 1 May 2017 – Published: 30 May 2017

Abstract. The Zackenberg River delta is located in northeast Greenland (74°30′ N, 20°30′ E) at the outlet of the Zackenberg fjord valley. The fjord-valley fill consists of a series of terraced deltaic deposits (ca. 2 km^2) formed during relative sea-level (RSL) fall. We investigated the deposits using sedimentological and cryostratigraphic techniques together with optically stimulated luminescence (OSL) dating. We identify four facies associations in sections (4 to 22 m in height) exposed along the modern Zackenberg River and coast. Facies associations relate to (I) overriding glaciers, (II) retreating glaciers and quiescent glaciomarine conditions, (III) delta progradation in a fjord valley, and (IV) fluvial activity and niveo-aeolian processes. Pore, layered, and suspended cryofacies are identified in two 20 m deep ice-bonded sediment cores. The cryofacies distribution, together with low overall ground-ice content, indicates that permafrost is predominately epigenetic in these deposits. Fourteen OSL ages constrain the deposition of the cored deposits to between approximately 13 and 11 ka, immediately following deglaciation. The timing of permafrost aggradation was closely related to delta progradation and began following the subaerial exposure of the delta plain (ca. 11 ka). Our results reveal information concerning the interplay between deglaciation, RSL change, sedimentation, permafrost aggradation, and the timing of these events. These findings have implications for the timing and mode of permafrost aggradation in other fjord valleys in northeast Greenland.

1 Introduction

Formerly glaciated valleys and fjords are sedimentary depocentres in which large volumes of sediment have accumulated during the late Weichselian and early Holocene (Aarseth, 1997; Hansen, 2001; Eilertsen et al., 2011). Fjord-valley fills predominantly develop during highstand and relative sea-level (RSL) fall following deglaciation, when sediment yield is high and accommodation space is declining (Ballantyne, 2002; Corner, 2006). The formerly ice-covered areas of coastal Greenland experienced isostatic rebound following deglaciation (Fleming and Lambeck, 2004). This has resulted in uplifting, incision, and erosion of valley-fill deposits by Holocene fluvial and coastal activity. Recent studies have examined the deltaic infill of fjords in high-relief landscapes (Hansen, 2004; Corner, 2006; Eilertsen et al., 2011; Marchand et al., 2013). However, few of these studies were in landscapes with permafrost. Therefore, the relationship between ground ice and the depositional setting in high-relief

landscapes has received less attention. Combining sedimentological observations with the systematic classification of ground ice provides a mechanism to correlate sedimentary facies with cryofacies – resulting in an improved palaeoenvironmental reconstruction.

Cryostratigraphy is the description, interpretation, and correlation of cryofacies and their relationship to the host deposits (French and Shur, 2010; Murton, 2013). Systematic classification of cryofacies permits the differentiation between syngenetic and epigenetic permafrost (Gilbert et al., 2016). In syngenetic settings, permafrost aggrades upwards at a rate proportional to the sedimentation rate at the ground surface. Ground ice in syngenetic permafrost primarily forms as segregated ice at the top of permafrost (Mackay, 1972). Conversely, epigenetic permafrost aggrades downwards after the deposition of the host material. Where moisture and sediment conditions permit, syngenetic permafrost contains a diverse suite of ice-rich cryofacies. Epigenetic permafrost is characteristically ice poor as the moisture source is often restricted to the surrounding sediment (French and Shur, 2010; Murton, 2013). The presence of the pore cryofacies in frost-susceptible material is characteristic of epigenetic permafrost (Stephani et al., 2014). However, ice-rich cryofacies may form in epigenetic permafrost if an external water source is available to recharge the local groundwater system (Pollard, 2000a; Kanevskiy et al., 2014). In addition to the mode of permafrost aggradation, sediment characteristics and the availability of moisture have a controlling influence on the presence and morphology of ground ice (Stephani et al., 2014). The application of cryostratigraphy to palaeo-landscape reconstruction therefore requires consideration of the physical properties of the soil, sediment, or bedrock which host ground ice.

This study reconstructs Holocene permafrost and landscape change in the Zackenberg lowlands using sedimentary and cryofacies. The objectives are (1) to describe sedimentary facies and cryofacies as observed in sections and cores, (2) to relate ground-ice formation in permafrost to sediment properties and depositional environments, and (3) to combine observations to reconstruct landscape change in the Zackenberg lowlands since the Last Glacial Maximum (LGM). This is the first study to investigate cryostratigraphy in northeast Greenland, and sheds new light on the variability of ground ice in high-relief Arctic landscapes.

2 Regional setting

2.1 Glaciation, deglaciation, and relative sea-level change

Zackenberg is located on the Wollaston Forland in northeast Greenland (74°30′ N, 20°30′ E; Fig. 1), 90 km east of the Greenland Ice Sheet margin. This region was glaciated several times during the Quaternary period (Hjort, 1981; Funder et al., 1994; Bennike et al., 2008). The last glaciation culminated in the LGM during the late Weichselian, when the Greenland Ice Sheet extended across the region (Bennike et al., 2008). Sedimentary archives and the geomorphology of the continental shelf and slope indicate that during the LGM, ca. 22 ka, grounded glacier ice extended onto the outer continental shelf (Evans et al., 2002; Ó Cofaigh et al., 2004; Winkelmann et al., 2010). Streamlined subglacial bedforms record the presence of erosive, warm-based ice streams in the major fjords and cross-shelf troughs in NE Greenland during this period. Intervening areas were covered by grounded but non-streaming ice, in some cases preserving pre-existing landforms (Funder et al., 2011). Deglaciation initiated in the coastal areas east of Young Sound between 10.1 and 11.7 ka (Bennike et al., 2008). The inner-fjord areas were ice-free by between 9.5 and 7.5 ka. At Zackenberg, the earliest postglacial radiocarbon date from a marine fossil is 10.1 ka, suggesting the study area was ice-free by this time (Christiansen et al., 2002).

Following deglaciation, the sea inundated low-lying areas of the Zackenberg Valley. Rapid emergence is documented during the early Holocene due to postglacial crustal rebound. Regional RSL curves are reconstructed from the height of raised beach deposits using optically stimulated luminescence (OSL) dating and AMS ^{14}C dating of palaeosurfaces and marine fossils (Bennike and Weidick, 2001; Pedersen et al., 2011). Christiansen et al. (2002) reconstructed RSL changes at Zackenberg using a combination of geomorphological evidence and radiocarbon dates of marine macrofossils and terrestrial plant remains. This curve indicates a late Quaternary marine limit of ca. 40 m a.s.l. During the early Holocene, RSL declined rapidly, reaching present sea level by ca. 5–6 ka (Christiansen et al., 2002).

The erosional competence of ice streams during the LGM, deglaciation history, and subsequent changes in RSL have important implications for both landscape and permafrost development in Zackenberg. Erosive ice streams in the fjords removed much of the sedimentary record from previous glacial–interglacial cycles. At the same time, warm-based glaciers precluded the formation or preservation of permafrost due to frictional heat generated at the base of the sliding glacier and the trapping of geothermal heat under the ice (Humlum, 2005). The age of permafrost in the Zackenberg lowlands is likely linked to the timing of regression, as warm boundary conditions at the sea floor would have prevented permafrost aggradation.

2.2 Climate and permafrost

Mean annual air temperature at Zackenberg between 1996 and 2013 was −9.0 °C. The mean annual precipitation for the same period was 219 mm water equivalent, of which 90 % fell as snow or sleet. Sea ice covers the Young Sound between 9 and 10 months each year from late October (Hansen et al., 2008; Jensen et al., 2014). Hydrology and sediment

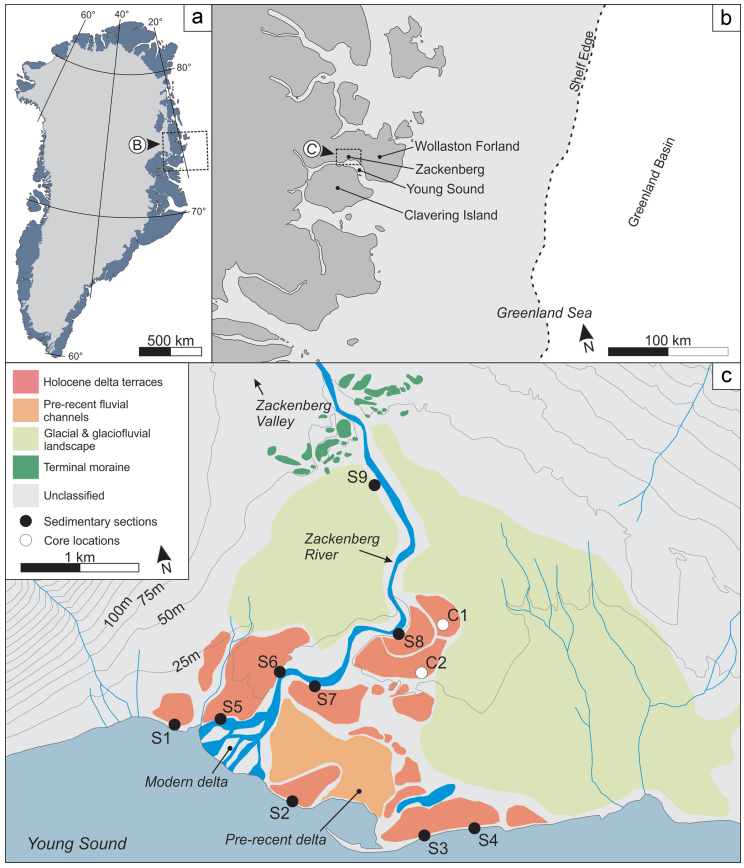

Figure 1. **(a)** Location of the study region in northeast Greenland. **(b)** Regional map of central northeast Greenland showing the location of the study area and key locations mentioned in the text. **(c)** Details of the study area in the Zackenberg lowlands. The glacial and glaciofluvial landscape formed during the late Weichselian, whereas the delta terraces are of late Weichselian to Holocene age. The location of sections (S1–S9) are denoted by black dots. Sediment core locations (C1 and C2) are denoted by white dots.

transport in the Zackenberg River have been summarized by Hasholt et al. (2008). The drainage basin covers an area of 512 km^2, of which 20 % is glaciated. Runoff in the river typically begins in June and continues until September. Sediment transport is dominated by extreme discharge events. In addition to the Zackenberg River, a number of minor rivers and streams drain the hillslopes and lowland area.

Zackenberg is located within the continuous permafrost zone. The permafrost thickness is modelled to be between 200 and 400 m (Christiansen et al., 2008). Ground temperatures are monitored to a depth of 20 m at two locations within the study area (C1 and C2 in Fig. 1c). Temperatures at 20 m depth are ca. −6 °C, with little interannual variation since monitoring began in 2012. Seasonal thaw progression and active-layer thickness has been measured since 1996 (Christiansen et al., 2003). On average, the active-layer thickness varies between 70 and 80 cm – with topography, and its impact on the snow regime and hydrology, being the primary controlling factor (Christiansen et al., 2008).

2.3 Geomorphology and Quaternary geology

The Zackenberg Valley is oriented along a NW-trending fault (Koch and Haller, 1971; Nøhr-Hansen et al., 2011), separating Caledonian gneiss and granite exposed to the west in the Zackenberg Mountain (1303 m a.s.l.) from Cretaceous and Jurassic sedimentary rocks exposed to the east in the Aucellabjerg Mountain (911 m a.s.l.). The valley is ca. 8 km long, expanding from 2 to 7 km in width towards Young Sound (Fig. 1c). The lowlands are defined as the portion

of the landscape below the early Holocene marine limit (40 m a.s.l.). The lowlands are primarily a relict landscape, formed by glacial, fluvial, marine, and periglacial processes during glaciation, deglaciation, and RSL decline. Glacial and glaciofluvial landforms include moraine ridges, ground moraine, meltwater plains, and raised delta terraces (Christiansen and Humlum, 1993; Christiansen et al., 2002). Permafrost landforms include ice-wedge polygons and palsas (Christiansen, 1998a; Christiansen et al., 2008).

The raised palaeo-delta at the mouth of the Zackenberg Valley covers an area of ca. 2 km^2 and consists of a series of terraces. To the west, the spatial extent of the palaeo-delta is restricted by the Zackenberg Mountain. The eastern boundary is less easily defined and grades into glacial and glaciofluvial deposits. Christiansen et al. (2002) determined that the deltaic deposits began to form prior to 9.5 ka.

3 Methods

Data used for this study consists of sedimentological logs from nine river and coastal sections in the delta, geomorphological observations, and cryostratigraphic and sedimentological analysis of two 20 m long, ice-bonded sediment cores. Field data were collected over three summer field campaigns, in 2012, 2013, and 2015.

The natural exposures along the coast and river were examined to determine the sedimentary stratigraphy of the valley deposits (Figs. 1c, 2). Sections, 4 to 22 m high, were photographed, described, and logged in August 2015. It was not possible to describe ground-ice conditions in the sections as the rate of thaw perpendicular to the exposed surface outpaced the rate of backwasting due to erosion.

Two 20 m deep boreholes (C1 and C2) were drilled in September 2012 using a drill rig equipped with a 42 mm core barrel. The sites are located within Holocene delta terraces, ca. 500 m apart (Fig. 1c). Core C1 is located at 38 m a.s.l. At C1, ca. 12 m of undisturbed (frozen) core was retrieved across the 20 m interval. Disturbed (unfrozen) material was concentrated in the unfrozen active layer and in the diamicton encountered below ca. 12 m depth. C2 (28 m a.s.l.) is situated at the base of a small slope, 3 m high. A seasonal snowbank accumulates at this site, which is located in the lee of the dominant northerly wind direction. Sand-rich surface deposits reflect nival-fluvial and aeolian sediment transport. At C2, 14 m of undisturbed core was recovered. Disturbed samples are spread across the length of the core with missing intervals ranging up to 4 m in thickness. Retrieved cores were sealed in sterile plastic bags and stored in a freezer on site. Frozen samples were transported to the University of Copenhagen for laboratory analysis.

In the laboratory, the C1 and C2 were split lengthwise, described, and photographed. Cryostructures were classified using a system adapted from Murton (2013) and French and Shur (2010). Excess ice content and gravimetric ice content were calculated for ca. 180 samples. Samples were selected to account for vertical variations in ground ice and sediment characteristics. Excess ice content (E_i, %), the water content in excess of the pore volume upon thawing, was estimated using the volumes of saturated sediment and supernatant water using (Kokelj and Burn, 2005: Eq. 1)

$$E_i = \frac{(W_v \times 1.09)}{(S_v + (W_v \times 1.09))} \times 100, \quad (1)$$

where W_v and S_v are the volumes of supernatant water and saturated sediment measured in a graduated beaker upon thawing, respectively, and 1.09 is used to estimate the equivalent volume of ice. Gravimetric ice content (G_i, %), the ratio of the mass of water to the mass of dry sample, was estimated using the wet weight and dry weight of each sample using (Murton, 2013: Eq. 1)

$$G_i = \frac{(M_i - M_d)}{M_d} \times 100, \quad (2)$$

where M_i is the mass of the frozen sample and M_d is the mass of the sample following oven drying (90 °C, 24 h).

Reliable OSL dating ages require sufficient exposure to daylight prior to deposition in order to reset (bleach) the sediment at the time of deposition. Incomplete bleaching is potentially a problem in Arctic environments as sediments may have been transported subglacially, over short distances, or during the polar night (Fuchs and Owen, 2008; Rittenour, 2008; Alexanderson and Murray, 2012). If the sediment grains are not completely reset then OSL dating may overestimate the depositional age.

OSL dating was performed on 14 samples from depths of up to 12 m in material from C1 and C2. The ages are based on sand-sized quartz grains, collected and processed under subdued orange light conditions. A single-aliquot regenerative protocol (Murray and Wintle, 2000) with a preheat of 200 °C and a cut heat of 180 °C was applied on the fast-component-dominated fine-sand quartz. To test for incomplete bleaching, infrared-stimulated luminescence (IRSL) doses and ages (IR_{50} and $pIRIR_{225}$) were derived from feldspar samples following the protocol proposed by Buylaert et al. (2009). IR_{50} refers to feldspar luminescence stimulated at 50 °C by infrared light, and $pIRIR_{225}$ refers to feldspar luminescence stimulated at 225 °C by infrared light after stimulation at 50 °C. In nature, the quartz luminescence signal is reset more quickly than the feldspar component. Therefore, if the quartz OSL and feldspar IRSL (in this study IR_{50}) return similar ages (within 10 %), the sediment is determined to be well bleached and the quartz ages are believed to be accurate (Murray et al., 2012). The $pIRIR_{225}$ signal is more difficult to bleach than the IR_{50} signal (Thomsen et al., 2008; Buylaert et al., 2009) and can therefore be used in addition to identify poorly bleached sediments (Buylaert et al., 2011). In this study, the chronology is exclusively based on the quartz OSL ages. Given the distinct bleaching characteristics, the IRSL

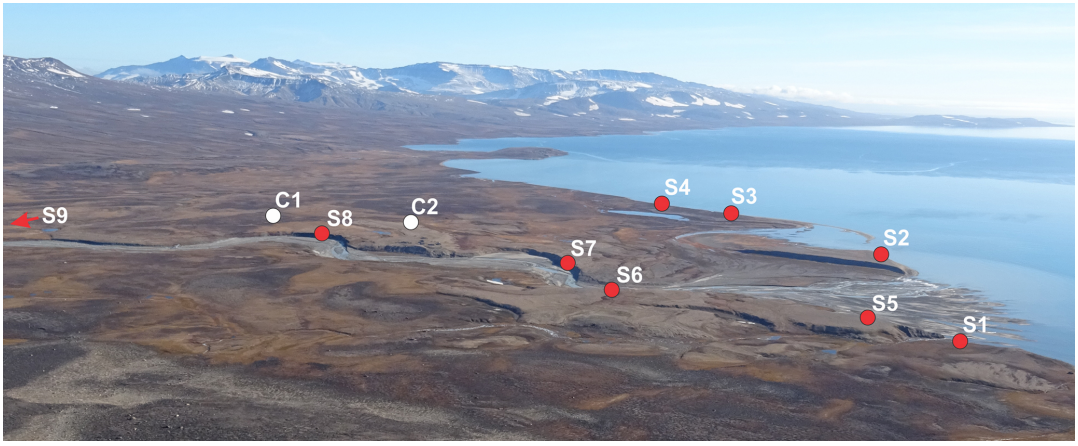

Figure 2. Overview image from the Zackenberg Mountain looking east over the lowlands on 8 September 2016. Site locations are those indicated in Fig. 1. The photo was provided by L. H. Rasmussen.

age was used to evaluate signal resetting. Samples were processed at the Nordic Laboratory for Luminescence Dating, Denmark.

4 Description and interpretation of sedimentary facies and facies associations

Nine sedimentary facies were identified (Table 1). These were defined based on the bulk macroscopic properties of the sediment – texture, structure, and bed boundaries. The facies ranged in lithology from a diamicton (facies 1) to silts, sands, and gravels (facies 2 to 9). Images of each facies are presented in Figs. 3 and 4. The facies were arranged into four facies associations (FA I–FA IV). Each facies association represents a distinct depositional environment. The facies associations are superpositioned in ascending order. FA I – the glacial facies association – occupies the lowermost position where present. The base of FA I was not observed. FA I is overlain by FA II and FA III. Together, FA II (the fjord-basin facies association) and FA III (the delta-slope facies association) form an upwards-coarsening succession. FA IV – the terrace top facies association – is the uppermost unit where present. The distribution of these facies associations is presented in Fig. 5.

4.1 FA I – glacial facies association

FA I was observed at all sites except those bordering the present-day shoreline (S1–S5). Exposures of FA I ranged up to 6 m in thickness and consisted of a compact, sandy, matrix-supported diamicton (facies 1). The diamicton contained angular to subrounded clasts, up to boulder size, of varying provenance. The deposits were overconsolidated when compared to other sedimentary facies. The lower boundary was not observed. The upper boundary to FA II was sharp and decreases in elevation, from ca. 41 m in the upper part of the delta to ca. 12 m towards the modern-day coastline (Fig. 5).

FA I is interpreted as a subglacial till on the basis of its stratigraphic position, compaction, lithology, and lateral extent (Evans and Benn, 2004). The decline in elevation of FA I towards the southeast likely reflects the increasing depth to bedrock. Widespread till deposits have previously been identified in the Zackenberg Valley bottom by Christiansen and Humlum (1993) and Christiansen et al. (2002) and outcrop at the ground surface in the glacial and glaciofluvial lowlands to the east of the delta terraces (Fig. 1). FA I was likely deposited during the last glaciation, when the Zackenberg lowlands were covered by an ice stream.

4.2 FA II – fjord-basin facies association

FA II includes silts (facies 2), interbedded sands and silts (facies 3), and normally graded sands and silts (facies 4). Laminated sands (facies 6) and massive sands (facies 7) are recorded in the lower portion of FA II at S6 and S7. FA II outcrops at all locations with the exception of S3, S4, and S9 (Fig. 5). Individual beds appear horizontal. The thickness of this unit ranged between 2 and 10 m. The upper boundary is transitional when overlain by FA III and sharp and erosional when overlain by FA IV. At S6, C1, and C2, FA II initially fines upwards before an upwards coarsening into FA III (Fig. 5). At these sites, coarse-grained facies (facies 6 and 7) were observed at the base of FA II. In other sections, FA II generally fines upwards. Bioturbation was uncommon and restricted to facies 2. Macrofossils consisted of bivalve shells and shell fragments. Isolated outsized clasts were observed.

Table 1. Sedimentary facies descriptions and interpretations.

Facies	Facies description	Bed contacts and thickness	Interpretation
1. Diamicton (Fig. 3)	Sandy, matrix-supported diamicton with clast-supported portions. Overconsolidated compared to other units.	Lower contact is not observed, upper contact is sharp. Thickness of 2–6 m in sections and cores.	Basal till – based on compaction, clast contact, position, and extent (Christiansen and Humlum, 1993; Benn and Evans, 2010).
2. Silts (Fig. 4)	Weakly laminated silts with variable degrees of bioturbation.	Sharp or transitional contacts. Up to 1 m thick.	Fallout from suspended sediment plumes and deposition by mud-rich turbidity currents (Hansen, 2004).
3. Interlaminated sands and silts (Fig. 4)	Fine sands and silts with occasional outsized clasts. Individual lamina range from 2 to 20 mm in thickness and may be either graded or ungraded.	Lower boundary is commonly diffuse, while upper contact may be sharp. Beds up to 50 cm thick.	Deposition by low-density turbidity currents and suspended sediment fallout (Reading, 2009).
4. Normally graded sands and silts (Fig. 4)	Normally graded beds of sand and silt. Some beds fine upwards into planar-parallel lamination or ripple cross-laminated sands or silts.	Lower boundary is sharp and may contain evidence of loading, scour, or water escape. Upper boundary is gradational or sharp. Beds are 1 to 25 cm thick.	Deposition by surge-like turbidity currents (Plink-Björklund and Ronnert, 1999).
5. Cross-stratified sands (Fig. 3)	Fine to coarse-grained sand with planar cross stratification.	Sharp, erosive base. Sharp upper contact. Beds are 10 to 40 cm thick.	Deposition by unidirectional, tractional currents. Cross-strata record the migration of dunes (Winsemann et al., 2007).
6. Laminated sands (Fig. 4)	Laminated very fine to coarse sands.	Sharp lower contact. Sharp or gradational upper contact. Beds up to 20 cm thick.	Deposition from sustained hyperpycnal currents subject to waxing and waning (Hansen, 2004). Alternatively, upper-flow regime planar-parallel stratification (Reading, 2009).
7. Massive pebbly sands (Fig. 3)	Matrix-supported pebbly sands. Massive or weak inverse grading. Clasts are granule to pebble sized.	Sharp upper and lower contacts. Beds are 5 to 50 cm thick.	Deposition from sandy debris flows (Nemec, 1990), either as Gilbert-type delta foresets or fluvial channel deposits.
8. Stratified pebbly sands and gravels (Fig. 3)	Clast-supported gravels and pebbly sands, high-angle cross bedding (up to ca. 20°).	Sharp, flat upper and lower contacts. Beds are 10 to 50 cm thick.	Foreset beds deposited from grain flows or noncohesive debris flows (Plink-Björklund and Ronnert, 1999; Hansen, 2004).
9. Gravels (Fig. 3)	Clast-supported massive or stratified gravels, with evidence of imbrication.	Sharp, flat, occasionally erosive contacts. Beds are 30 to 120 cm thick.	Deposited by tractional currents (Miall, 2010). Likely bedload transport in a braided-river system.

FA II is polygenetic and was deposited into a fjord environment during RSL highstand during and following deglaciation. The deposits consist of parallel-bedded fine sands and silts and reflect deposition by suspension fallout from hyperpycnal plumes and low-density turbidity currents (Table 1). The upwards fining and thinning observed at S6 and in C1 and C2 records the withdrawal of the sediment source as the ice front retreated north during deglaciation towards its grounding line at the mouth of the Zackenberg Valley (Ó Cofaigh et al., 1999). The upper portion of FA II is characterized by an upwards coarsening and thickening. This unit is interpreted as the prodelta environment. The high sand content of deposits from suspension is typical of steep, shallow-water deltas, where sand is carried beyond

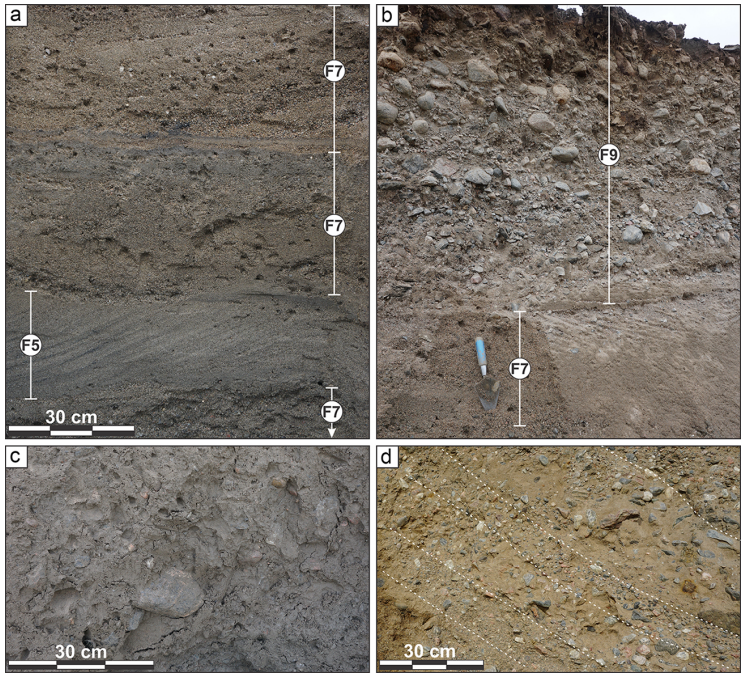

Figure 3. Coarse-grained sedimentary facies. **(a)** Cross-stratified sands (facies 5) and massive pebbly sands (facies 7). Image from S3 at 6 m a.s.l. **(b)** Massive gravels (facies 9) and massive pebbly sands (facies 7) at S9 (41 m a.s.l.). Note trowel is 30 cm in length. **(c)** Diamicton (facies 1) – the lowermost exposed unit at S7 (ca. 14 m a.sl.). **(d)** Cross-stratified gravels and pebbly sands (facies 8) at S6 (ca. 27 m a.s.l.). Individual strata are separated by dashed lines.

the delta slope by hypopycnal plumes (Corner, 2006). Turbidites record instabilities on the surrounding slopes, periods of high-river discharge, variations in glacier front position, or collapsing sediment plumes (Gilbert, 1983; Hansen, 2004). The relative absence of bioturbation and limited number of trace-making organisms indicates a stressed environment with turbid water conditions and relatively high sedimentation rates (Netto et al., 2012). Overall, the vertical changes in the relative dominance of the facies records an approaching delta front.

4.3 FA III – delta-slope facies association

FA III consists of interbedded sands and silts (facies 3), graded sands and silts (facies 4), laminated sands (facies 6), massive pebbly sands (facies 7), and stratified pebbly sands and gravels (facies 8). FA III is exposed at S2–S6 and in both C1 and C2. Exposures range in thickness from 2 to 10 m (Fig. 5). The relative influence of facies 3 and facies 4 decreases upwards as the unit coarsens and beds increase in thickness. Evidence for soft-sediment deformation is occasionally observed in association with dewatering structures. At sites S2–S6, beds dip 5–25° southeast, towards Young Sound (Fig. 4a). Dip angles increase upwards as the beds coarsen and thicken towards the top of the exposures.

The inclined, planar beds of FA III are interpreted as foresets deposited during the progradation of a Gilbert-type delta. The overall decline in the elevation towards Young Sound indicates that this facies association was deposited during RSL fall. Variations in gain size and facies composition reflect differences in their proximity to fluvial channels, variations in discharge, and sediment transport processes. The deposits reflect suspension settling, turbidity currents, debris flows, and grain flows associated with slope failure on the delta front. Facies 7 and 8 were deposited by gravitational avalanches and debris flows following accumulation on the upper delta slope (Nemec, 1990; Plink-Björklund and Ronnert, 1999; Hansen, 2004). Facies 3, 4, and 6 record the activity of turbidity currents either due to underflow of sediment-laden river water or flow transformation (Kneller and Buckee, 2000; Winsemann et al., 2007). The presence of soft-sediment deformation structures and absence of bioturbation suggest a rapid sedimentation rate for FA III.

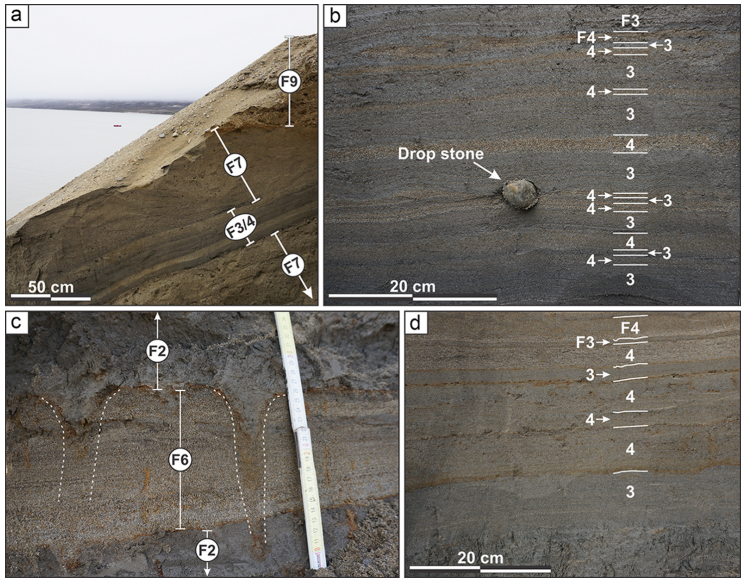

Figure 4. Fine-grained sedimentary facies. **(a)** Massive gravels (facies 9) truncating massive pebbly sand (facies 7), interbedded sands and silts (facies 3), and graded sands (facies 4) at S2 at 11 m a.s.l. **(b)** Alternating facies 3 and facies 4 at S5 (9 m a.s.l.). Note the presence of an outsized clast. **(c)** Bioturbated silts (facies 2) and laminated sands (facies 6) at S5 (6 m a.s.l.). Note vertically oriented burrows outlined with white dashed lines. **(d)** Alternating facies 3 and facies 4 at S2 (5 m a.s.l.).

4.4 FA IV – terrace-top facies association

FA IV consists of cross-stratified sands (facies 5), laminated sands (facies 6), massive pebbly sands (facies 7), and gravels (facies 9). The facies association ranges between 0.5 and 3.0 m in thickness and is exposed at elevations between 5 and 45 m a.s.l. The elevation of FA IV declines towards Young Sound both to the south and east (Fig. 5). Facies 9 increases in dominance with distance inland. FA IV has a sharp, erosive contact with the underlying unit.

FA IV is polygenetic and the component facies are related to a range of depositional processes and environments. Deposits are interpreted to primarily reflect fluvial activity associated with a deltaic distributary plain or braided-river system. Diffusely stratified gravels with imbrication (facies 9) and planar-parallel laminated sands (facies 6) indicate bedload transport by unidirectional currents of varying strength (Miall, 2010). Cross-stratified sand beds record the migration of dunes in braided-river channels or distributary systems (Miall, 2006; Winsemann et al., 2007). Massive pebbly sands (facies 7) are deposits of pseudoplastic debris flows (Miall, 2010). Secondary processes include winnowing by wind, marine reworking during RSL fall, and redistribution of sediment by snowmelt (Christiansen and Humlum, 1993; Christiansen, 1998b; Christiansen et al., 2002). FA IV developed at successively lower levels during RSL fall and fluvial incision and channel migration.

5 Cryofacies

Three cryofacies are visually identified in C1 and C2 based on the bulk macroscopic characteristics of ground ice – namely the morphological expression of ice and the proportion of ice to sediment. These cryofacies are (1) pore cryofacies (Po), (2) layered cryofacies (La), and (3) suspended cryofacies (Su). An example of each cryofacies is given in Fig. 6. In addition, disturbed sections were identified where samples were thawed during the drilling process. In these cases, ice present within the samples melted and the cryofacies were destroyed. The vertical distributions of the cryofacies and disturbed intervals are given in Figs. 7 and 8.

Po dominates at both C1 and C2. Po develops due to the in situ freezing of pore water in the spaces between mineral grains, cementing individual grains. The interstitial ice is not visible to the unaided eye. La occurs in various lithologies in both C1 and C2. Ice layers are less than 5 cm in thickness and may contain sediment grains or aggregates. La is observed in FA II and FA III in C1 as well as in FA III in C2. Su develops where sediment grains or aggregates are suspended in ice. The visible ice content of Su exceeds 50 %. Su is ob-

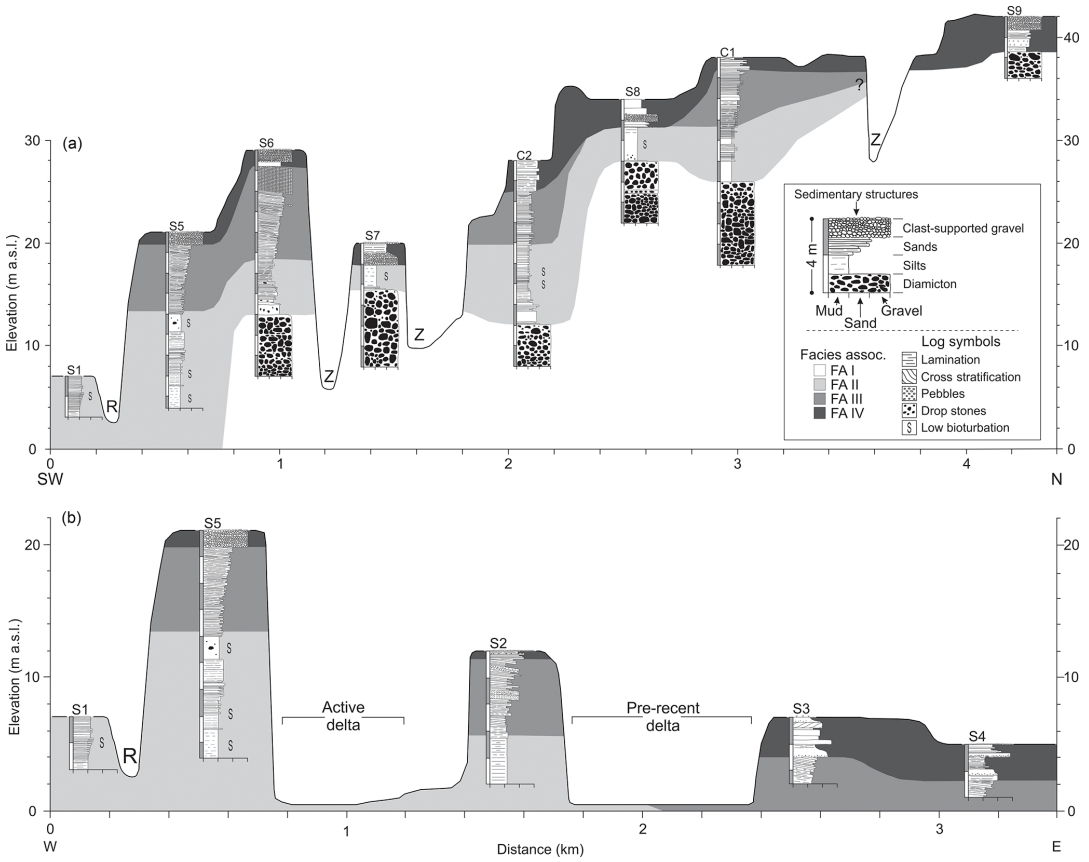

Figure 5. Correlation panel of sedimentary logs and facies associations from **(a)** the sections along the Zackenberg River (S1 and S5–S9) and cores (C1 and C2) and **(b)** coastal section (S1–S5). The site identities, above each log, correspond to those in Fig. 1. Z and R indicate the location of the Zackenberg River and minor streams, respectively.

served in FA II at C1. The variation between La and Su likely reflects differences in the freezing rate and availability of water during permafrost aggradation (Calmels et al., 2012). It is hypothesized that both La and Su form from the injection of pressurized water in sediment during epigenetic permafrost formation (Murton, 2013).

Ground-ice content varies with cryofacies. Gravimetric moisture content and excess ice content were highest in intervals with either La or Su. Sections with Po were devoid of excess ice and were typified by low gravimetric moisture contents. At C1, the gravimetric moisture content of core samples with Po ranged from 20 to 48 %, with no clear variation in depth. Samples from intervals with La and Su ranged from 56 to 274 % (Fig. 7). Where present, excess ice content ranged from 2 to 52 %. At C2, gravimetric moisture content in samples with Po was uniformly low and ranged between 11 and 48 % – no excess ice was observed in these samples (Fig. 8). One La sample containing excess ice (5 %) was obtained from 3 m depth (24 m a.s.l.) in C2. Analysis of disturbed sections was not conducted as the natural moisture content was altered during drilling.

6 Geochronology

Six OSL samples were analysed from C1 (Table 2). There are discrepancies between the OSL and IR_{50} ages and between the IR_{50} and $pIRIR_{225}$ ages for most samples. It is therefore not possible to entirely exclude incomplete bleaching at this site. Sample 131 548 (32.8 m a.s.l.) is an exception to this as the OSL and IR_{50} ages are in close agreement (± 10 %). Nevertheless, the entire core sequence reflects a short time span, ranging from 11.9 ± 0.7 ka (sample 131 543; 37.3 m a.s.l.) to

Table 2. Summary of core samples for luminescence dating, depths, quartz OSL, and feldspar IRSL equivalent doses (De) and ages. The feldspar doses and ages are based on the measurements of three aliquots per sample and are only used to check for incomplete signal resetting. The quartz ages are the basis for the chronologies of the sediment cores. *n* is the number of aliquots. SE is the standard error. IR_{50} is the feldspar luminescence stimulated at 50 °C by infrared light. $pIRIR_{225}$ is the feldspar luminescence stimulated at 225 °C after stimulation at 50 °C.

Site	Laboratory ID	Depth (m a.s.l.)	FA	Quartz OSL			Feldspar IRSL			
				n	De ± SE (Gy)	Age ± SE (ka)	IR_{50} De ± SE (Gy)	$pIRIR_{225}$ De ± SE (Gy)	IR_{50} age ± SE (ka)	$pIRIR_{225}$ age ± SE (ka)
C1	131 543	37.3	IV	20	29.8 ± 1.1	11.9 ± 0.7	46 ± 5	103 ± 9	15 ± 2	34 ± 3
	131 544	36.3	III	18	32.1 ± 0.7	11.9 ± 1.2	58 ± 2	156 ± 9	18 ± 2	48 ± 5
	131 547	33.4	III	18	35 ± 2	12.6 ± 0.8	55.8 ± 0.8	145 ± 6	16.6 ± 0.7	43 ± 3
	131 548	32.8	III	18	45 ± 2	12.4 ± 0.7	56 ± 4	155 ± 8	13.4 ± 1.1	37 ± 3
	131 550	31.0	II	20	47 ± 4	12.9 ± 1.3	80 ± 9	205 ± 32	19 ± 2	49 ± 8
	131 552	29.7	II	20	38 ± 4	13 ± 2	67 ± 4	175 ± 12	19 ± 2	50 ± 6
C2	131 554	27.1	IV	18	4.3 ± 0.2	1.6 ± 0.1	3.7 ± 0.2	8.6 ± 0.1	1.2 ± 0.1	2.7 ± 0.1
	131 555	26.9	IV	18	14.9 ± 1.1	7.4 ± 0.7	14.8 ± 0.3	22 ± 4	5.8 ± 0.3	9 ± 2
	131 556	26.3	IV	18	23.9 ± 0.7	9.7 ± 0.5	20 ± 2	41 ± 7	6.5 ± 0.6	14 ± 2
	131 557	26.1	IV	18	25.8 ± 1.0	10.3 ± 0.6	20.4 ± 0.8	41 ± 2	6.7 ± 0.4	13.4 ± 0.9
	131 558	25.3	IV	18	26.6 ± 1.3	11.8 ± 0.8	28.9 ± 0.6	85 ± 8	10.3 ± 0.5	30 ± 3
	131 560	23.7	III	18	31.7 ± 1.0	11.7 ± 0.6	38 ± 2	115 ± 7	11.6 ± 0.7	36 ± 3
	131 561	18.7	II	18	25.9 ± 1.0	10.6 ± 0.6	34 ± 3	107 ± 9	11.4 ± 1.0	36 ± 3
	131 562	16.5	II	18	39.2 ± 1.0	12.0 ± 0.7	39.0 ± 0.9	126 ± 6	10.3 ± 0.5	33 ± 2

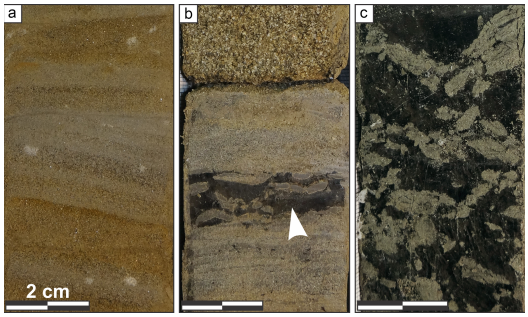

Figure 6. Cryofacies. **(a)** Pore (Po) cryofacies. **(b)** Layered (La) cryofacies indicated by the white arrow. **(c)** Suspended (Su) cryofacies. Note the ice appears black in the images.

13 ± 2 ka (sample 131 552; 29.7 m a.s.l.). The ages are similar and within the error margins, indicating that the sampled interval at C1 was likely deposited between ca. 13 and 12 ka (Fig. 7).

In comparison with C1, the eight samples taken from C2 show a clearer age trend with depth (Fig. 8). The lowermost six samples at C2 (below 26 m a.s.l.) indicate that the sediments were deposited between 12 and 10 ka. However, the two uppermost samples are considerably younger – suggesting that the site continued to aggrade during the Holocene. Continued deposition likely relates to localized nival-aeolian processes (Christiansen, 1998b). In general, the OSL and IR_{50} ages at C2 are in good agreement, while the $pIRIR_{225}$ ages provide an age overestimate. This indicates that the bleaching time was long enough to reset the OSL and IR_{50} signals but not the $pIRIR_{225}$ signal (Murray et al., 2012). The overestimate of the $pIRIR_{225}$ signal may also originate from the larger residual found in any post-IR IRSL signal (Buylaert et al., 2011). The agreement of the OSL and IR_{50} ages indicates that there is little or no incomplete bleaching at C2 and that the OSL ages are accurate.

The OSL results of the 14 samples from C1 and C2 indicate a late Weichselian to early Holocene depositional age of the sediment in FA II, FA III, and FA IV. These results suggest that the majority of the sedimentation in the valley bottom took place in a narrow time interval following deglaciation (between 13 and 11 ka). The OSL ages are supported by Christiansen et al. (2002), who presented ^{14}C AMS dating results for samples from S5 that suggest the fjord-basin deposits were aggrading at approximately 10.1 ka.

7 Discussion

7.1 Permafrost aggradation

Few studies have examined the relationship between ground-ice characteristics and postglacial landscape development in Greenland (Gilbert et al., 2016). Pollard and Bell (1998), however, presented a model for ground-ice aggradation

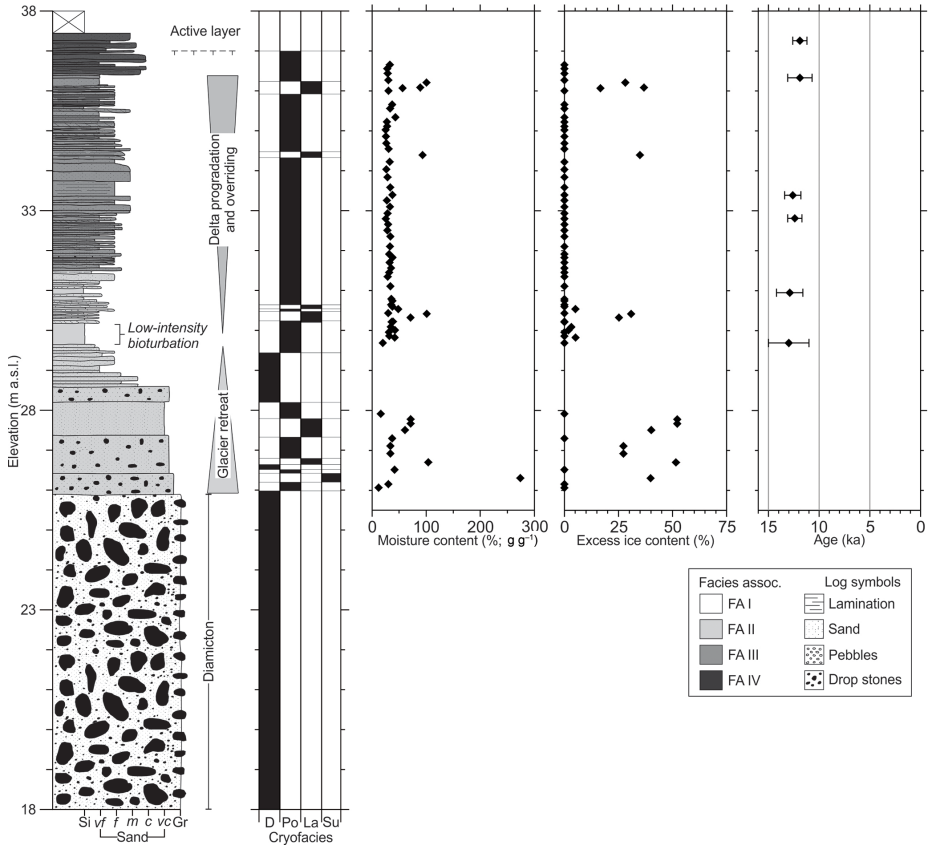

Figure 7. Log for C1 illustrating vertical variations in sediment grain size, facies associations, ground-ice characteristics and OSL ages. D, Po, La, and Su denote disturbed sections, pore, layered, and suspended cryofacies, respectively.

within epigenetic permafrost below the Holocene marine limit in the Eureka Sound lowlands on the Fosheim Peninsula in high-Arctic Canada. Here, the nature and distribution of ground ice was related to RSL change, sediment grain size, and epigenetic permafrost aggradation. On the Fosheim Peninsula, massive intrasedimental ice bodies are observed at the contact between marine silts and underlying gravels and sands, deposited during transgression. Low hydraulic conductivities in the overlying fine-grained sediments did not permit sufficient water migration resulting in the formation of reticulate, layered, lenticular, and pore cryofacies (Pollard, 2000a). Massive ice bodies and cryofacies were interpreted to have formed during and following deglaciation, when glacier meltwater and brackish sea water were available to recharge local groundwater systems (Pollard, 2000b).

C1 and C2 are generally ice poor and the majority of the cores are characterized by the pore cryofacies. Cryofacies with visible ice (La and Su) are restricted to the fjord-basin and delta-slope facies associations. A similar pattern is observed in gravimetric moisture content and excess ice content (Figs. 7, 8). The distribution of ground ice in the Zackenberg River delta is similar to that described by Pollard (2000a, b). The presence of the layered cryofacies in epigenetic permafrost has also been described by Kanevskiy et al. (2014) in lacustrine sediments in interior Alaska. The suspended cryofacies is likely a more developed form of the layered cryofacies, forming during increased moisture availability or slower rates of freezing. The absence of appreciable ground ice in the remainder of the core indicates that permafrost in the Zackenberg lowlands is primarily epigenetic and formed following sea-level fall during the early Holocene. The differences in ice content and cryofacies between C1 and C2 likely relate to either variations in site-specific moisture availabil-

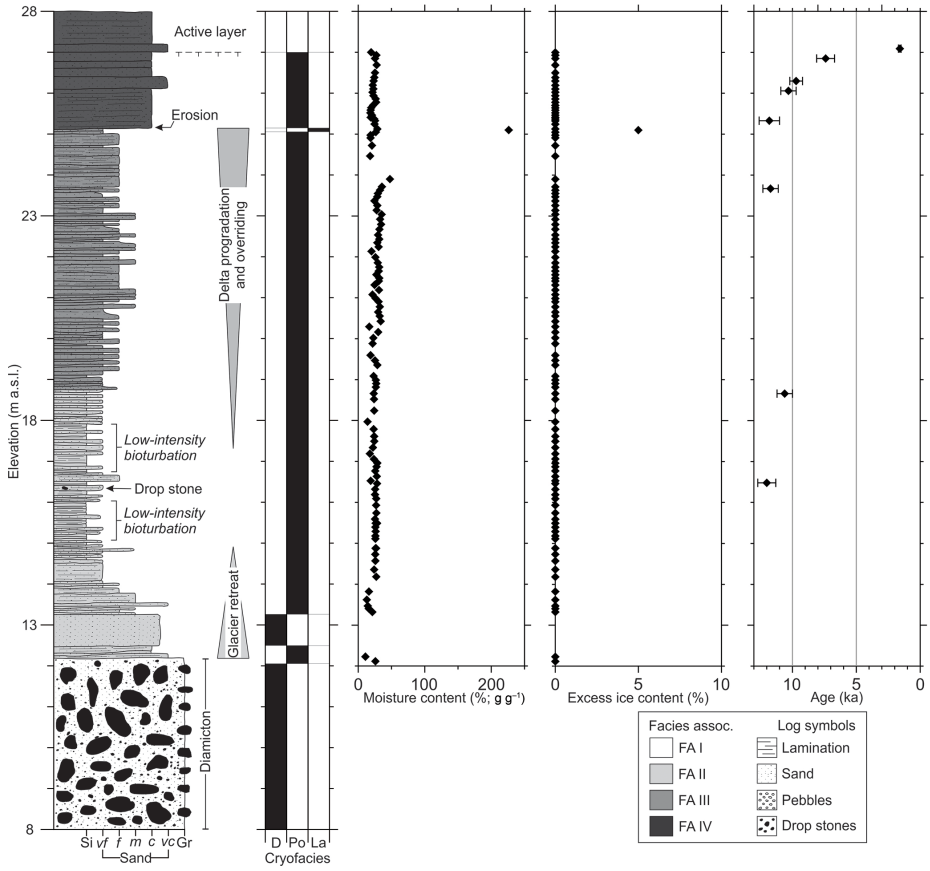

Figure 8. Log for C2 illustrating vertical variations in sediment grain size, facies associations, ground-ice characteristics, and OSL ages. D, Po, and La denote disturbed sections, pore, and layered cryofacies, respectively. Note the difference in axis range compared with Fig. 7.

ity during permafrost aggradation or lateral variations in sediment characteristics that are unresolvable at the core scale.

The presence of syngenetic permafrost is inferred using a combination of sedimentology and the dating results in the top of C2 – which record continued sedimentation following subaerial exposure. Here, the development of syngenetic permafrost is related to localized accumulation of niveo-aeolian sediments and organic material (Christiansen, 1998b; Christiansen et al., 2002). The uppermost syngenetic component in FA IV is almost 3 m in thickness. Despite continuous sedimentation and sufficient moisture availability, syngenetic permafrost at C2 consists of pore cryofacies. This is attributed to the coarse-grained sediment and the absence of frost-susceptible silts. Syngenetic permafrost is thus of local occurrence on the palaeo-delta surface and relates to periglacial, nival, fluvial, and aeolian activity during the Holocene.

7.2 Valley-fill history and delta progradation

During the past 13 ka, the Zackenberg lowlands have undergone major environmental changes through periods of glacial, marine, fluvial, and periglacial dominance. Sedimentological, cryostratigraphic, and geomorphological observations are combined with the OSL dating results to produce a model for the landscape and permafrost development of the Zackenberg lowlands. This model is condensed into three stages – illustrating the major changes in sediment supply, sea level, and sedimentary processes following glaciation (Fig. 9). The model provides a framework in which to discuss changes in the sedimentary facies and cryostratigraphy and improves our understanding of the amount of ground ice

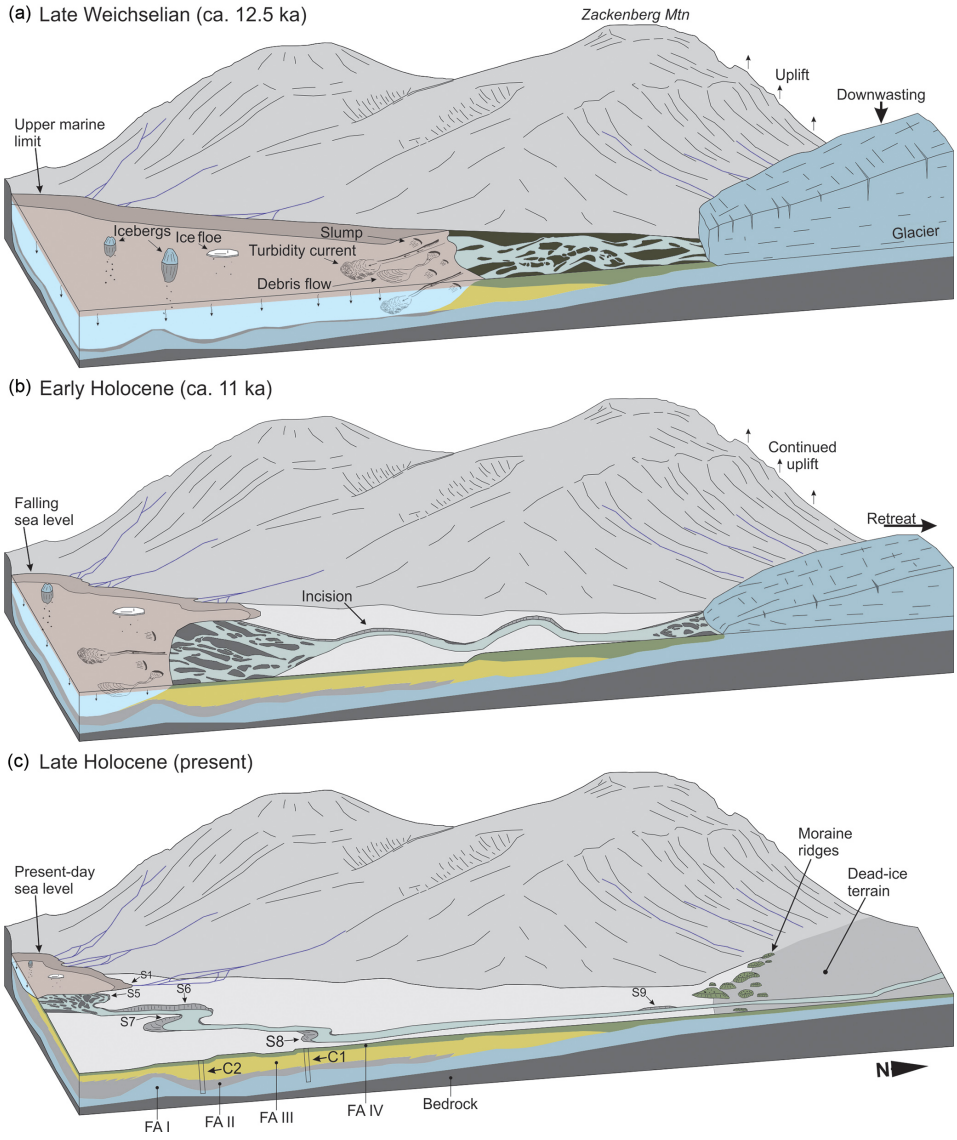

Figure 9. Schematic model of the three main stages of landscape development of the Zackenberg River delta and adjacent lowlands. The model illustrates the essential processes and sediment sources which contributed to the development of the valley-fill deposits. **(a)** Late Weichselian deglaciation and inundation. Sediment was supplied by a proximal glacier and by mobilization of glacial deposits by contemporary fluvial networks. **(b)** Early Holocene sea-level fall and areal deglaciation. High sedimentation rates and rapid delta progradation during sea-level fall. Sediment supplied primarily through the reworking of deposits by glaciofluvial erosion and incision during isostatic uplift. The landscape is slowly dissected by a meandering braided-river system resulting in the terracing observed in the landscape today. Locally, permafrost began to aggrade in the lowlands following subaerial exposure. **(c)** Modern landscape with select sections and coring locations. Sediment supplied by the fluvial reworking of raised deposits. Permafrost is continuous under stable, exposed land surfaces.

in Arctic valleys. This is important as the amount of ground ice determines the potential landscape response due to climate change.

A stratigraphic model for fjord-valley infilling in Norway has been presented by Corner (2006). This tripartite model consists of a deglacial transgressive systems tract (DTST), a deglacial highstand systems tract (DHST), and a postglacial forced-regressive systems tract (PRST). The DTST is deposited during deglaciation by retrogradational stacking of proglacial sediments. Sedimentation is concurrent with marine inundation and the early stages of sea-level fall during isostatic rebound. The DHST is characterized by the rapid progradation of glaciofluvial deltas and concurrent deposition of glaciomarine deposits on the basin floor. Lastly, the PRST forms following areal deglaciation and is characterized by fluvial delta progradation, fluvial incision, and terracing during RSL fall. A similar model was developed for the Scoresby Sound region, ca. 750 km south of the Zackenberg area, by Hansen (2004). Though the details of the stratigraphy vary between locations, the underlying controls identified in these models – sediment supply, accommodation space, and RSL change – remain the same.

7.2.1 Deglaciation and sea-level highstand

The regional glaciation during the LGM is recorded by a presence of a basal till in FA I (Christiansen and Humlum, 1993; Christiansen et al., 2008). Though earlier studies have suggested a deglaciation age of 11.7 to 10.1 ka (Bennike and Weidick, 2001; Bennike et al., 2008), the results of this investigation indicate that the Zackenberg lowlands may have been ice-free as early as 13 to 11 ka (Table 2; Figs. 7 and 8). This discrepancy may be because previous studies have relied on radiocarbon dating of marine macrofossils. Environmental restrictions on the organisms which produce these shells such as brackish water, high sedimentation rates, and suspended sediment concentrations may have restricted their presence during deglaciation (Netto et al., 2012). However, given the errors associated with OSL ages, it is not possible to conclude this with certainty. Ice retreated initially to a grounding line in the Zackenberg Valley, depositing an end-moraine complex (Figs. 1c, 9a).

Following deglaciation of the Young Sound, the Zackenberg lowlands were inundated by the sea. The maximum flooding surface corresponds with the transition from glacial (FA I) to glaciomarine (FA II) deposits. This stratigraphic boundary marks the maximum landward incursion of marine-influenced deposits following deglaciation (Hansen, 2004). At Zackenberg, the transition from the DTST to DHST is only observed at three locations (S6, C1, and C2) and is marked at the transition from upwards fining to upwards coarsening in FA II (Fig. 5). Marchand et al. (2013) observed a similar transition in the deposits of the Matane River valley (Québec, Canada), noting a reduction in ice-rafted debris in the non-glacially influenced facies. The scarcity of drop stones in most of FA II and FA III suggests that areal deglaciation started shortly after the transition to FA II. The OSL dates from C1 and C2 suggest that this transition was 13–11 ka.

During the DHST, the basin received sediment from suspension plumes and low-density turbidity currents contributing to the aggradation of FA II. A shallow-water highstand delta likely developed in front of a proglacial meltwater plain during this period. Deltaic deposits were not observed north of C1. Permafrost was likely absent in the lowlands during the DTST and DHST as thermal boundary conditions in the marine environment and beneath the unstable braided-river channels were too warm to permit permafrost aggradation.

7.2.2 Delta progradation and relative sea-level fall

RSL fell during the Holocene and reached its present-day limit ca. 4.5 ka (Bennike et al., 2008; Pedersen et al., 2011). The topography of the glacial and glaciofluvial landscape deposited during the DTST and DHST controlled the delta location. To the east, the adjacent lowlands (ca. 30–40 m a.s.l.) are higher in elevation than the pre-delta terrain surface. The delta was thus deposited in the lowest part of the landscape. During sea-level recession, river networks were directed to the west of the glacial and glaciofuvial deposits, where the deltaic deposits are located today (Figs. 1c, 9b). The OSL ages from the upper part of the delta in C1 and C2 constrain the timing of initial delta deposition to between 13 and 11 ka (Table 2). Christiansen et al. (2002) presented dating results indicating that the delta was active at S5, ca. 10.1 ka.

Most of the sediments comprising FA II, FA III, and FA IV were deposited during the PRST. During this period, RSL was in decline, resulting in a reduction in accommodation space in the basin. Areal deglaciation reduced fluvial discharge and the available sediment to that which could be mobilized and reworked by the palaeo-river system (Christiansen and Humlum, 1993). Progradation of the delta continued during the PRST, but the rate of progradation was probably slower than during the DHST due to the factors mentioned above (Corner, 2006; Eilertsen et al., 2006). Despite the declining accommodation space, the sedimentary facies of FA III at the fjord-proximal sites (S1–S6) reflect deeper water conditions, as the delta prograded into the basin (Eilertsen et al., 2011).

The rapid incision of the Zackenberg River during Holocene sea-level decline limited the erosion of the underlying facies, forming the terraces and exposures documented in this study. FA IV records variable hydraulic conditions in the palaeo-Zackenberg River. At S9, FA IV was deposited at part of a large glaciofluvial outwash plain, where sediment was primarily transported as bedload. The river switched to a single-channel system with mixed sediment transport once incision began ca. 9.5 ka. This could be explained by the exhaustion of the sediment source once the glacier retreated (Marchand et al., 2013).

Permafrost began to aggrade in the lowlands following sea-level decline and delta progradation in the late Weichselian or early Holocene. This is reflected in the assemblage of cryofacies, indicating epigenetic permafrost formation. The formation of the La and Su cryofacies in FA II and FA III was likely facilitated by glacier meltwater or seawater incursion that provided a moisture source for excess ice development. Permafrost landforms, such as ice-wedge polygons, and podsols also began to form during this time (Christiansen et al., 2002, 2008).

7.2.3 Present delta system

The final stage of delta formation encompasses the period of relatively stable sea level after 4.5 ka. Landscape changes after this time were minor compared to those during sea-level fall. The raised terraces reflect shifting zones of erosion and deposition during the PRST and Holocene emergence. The progradation rate of the delta declined as availability was restricted and the delta approached the edge of the Young Sound. Sediments in the drainage basin consist of mainly periglacial and glaciofluvial deposits. Late Weichselian glacial deposits have primarily been reworked (Fig. 9c). Deep incision during RSL fall limited erosion, preserving the terrace morphology.

Ice-wedge polygons formed and periglacial nivation processes have been active in the delta since its exposure as permafrost probably established quickly in this high-Arctic setting (Christiansen et al., 2002). Additionally, palsas developed in the low-lying areas since emergence. In addition, niveo-fluvial and niveo-aeolian sediment transport continues to modify the landscape downslope of snow patches (Christiansen, 1998b; Christiansen et al., 2002). At present, permafrost exists under all terrestrial surfaces.

7.3 Application to other fjord valleys

Recent studies have presented models for infilling of formerly glaciated fjord valleys from Greenland (Hansen, 2001, 2004), Norway (Nemec et al., 1999; Corner, 2006; Eilertsen et al., 2006; Hansen et al., 2009; Eilertsen et al., 2011), Canada (Marchand et al., 2013), Sweden (Plink-Björklund and Ronnert, 1999), and Germany (Winsemann et al., 2007). These investigations demonstrate that fjord valleys are primarily infilled during deglaciation and RSL fall, resulting in a complex stratigraphy, which can vary substantially between locations. However, recent studies also indicate that the underlying depositional regime controls are the same (Eilertsen et al., 2011). With the exception of the investigations in Greenland, these studies are restricted to non-permafrost environments. No previous studies have investigated ground ice or cryofacies in valley-fill deposits.

Previous studies have identified similar infilling patterns of valleys following regional deglaciation. Given similarities in sedimentary facies and landscape development, it is reasonable to expect that the aggradational history of permafrost is similar as well. This suggests that permafrost below the upper marine limit of large tributaries valleys throughout northeast Greenland is likely a Holocene phenomenon, with the exact age corresponding to the timing of subaerial exposure following marine transgression. These coarse-grained deposits contain an assemblage of cryofacies characteristics of ice-poor epigenetic permafrost.

8 Summary and conclusions

The valley-fill deposits in the Zackenberg lowlands formed during highstand and RSL fall following deglaciation, ca. 13 to 11 ka. The majority of the sedimentary deposits accumulated by the early Holocene, ca. 10 ka. During this period, the reduction in accommodation space during RSL fall and high glacial and paraglacial sediment yield resulted in rapid sedimentation and progradation of the delta. Permafrost began to aggrade in subaerial land surfaces following exposure, ca. 11 ka. In the Zackenberg lowlands, permafrost history is closely tied with delta progradation.

The following conclusions are drawn from this study:

- Following deglaciation, three distinct phases of delta formation are recognized in the sedimentary facies and cryofacies. The majority of the delta accumulated during the late Weichselian and early Holocene. Rapid sedimentation and delta progradation are attributed to high sediment yield from glaciers and glaciofluvial erosion and transport and the decline in accommodation space during sea-level fall.

- Permafrost in the Zackenberg lowlands is a Holocene phenomenon. The vertical distribution of cryofacies and absence of appreciable ground ice in frost-susceptible sediments indicates permafrost in the Zackenberg River delta deposits post-dates deglaciation. The onset of conditions conducive to permafrost aggradation is concurrent with subaerial exposure following RSL decline or delta progradation. The resultant epigenetic permafrost is ice poor, overall. The results of this investigation may have applications for other formerly glaciated fjord valleys in permafrost regions.

Data availability. The ground ice and stratigraphic data used in this paper can be obtained by contacting the corresponding author.

Competing interests. The authors declare that they have no conflict of interest.

Acknowledgements. This investigation was financed by the PAGE21 (Changing permafrost in the Arctic and its Global Effects in the 21st Century) project – grant agreement number 292700

under the EU Seventh Framework Programme. Additional funding was provided by the Centre for Permafrost (CENPERM) at the University of Copenhagen, funded by the Danish National Research Foundation (CENPERM DNRF1000) and by the Nordic Centre of Excellence, DEFROST (Impacts of a changing cryosphere – depicting ecosystem–climate feedbacks from permafrost, snow, and ice). Christine Thiel received funding from the German Research Foundation (DFG grant TH1651/1-1). We thank Andrew Murray and Jan-Pieter Buylaert (Nordic Laboratory for Luminescence Dating) for their assistance with luminescence dating and in the preparation of this paper. We gratefully acknowledge the hospitality and assistance of the staff at the Zackenberg Ecological Research station. Special thanks to Ulrich Neumann (Kolibri Geoservices) and Jordan Mertes for their assistance during drilling in summer 2012. This paper has benefited from constructive comments from Michael Fritz and two anonymous reviewers. We would also like to thank the handling editor, Scott Lamoureux.

Edited by: S. Lamoureux
Reviewed by: M. Fritz and two anonymous referees

References

Aarseth, I.: Western Norwegian fjord sediments: age, volume, stratigraphy, and role as temporary depository during glacial cycles, Mar. Geol., 143, 39–53, doi:10.1016/S0025-3227(97)00089-3, 1997.

Alexanderson, H. and Murray, A. S.: Luminescence signals from modern sediments in a glaciated bay, NW Svalbard, Quat. Geochronol., 10, 250–256, doi:10.1016/j.quageo.2012.01.001, 2012.

Ballantyne, C. K.: Paraglacial geomorphology, Quaternary Sci. Rev., 21, 1935–2017, doi:10.1016/S0277-3791(02)00005-7, 2002.

Benn, D. I. and Evans, D. J. A.: Glaciers and Glaciation, 2 ed., Routledge, 816 pp., 2010.

Bennike, O. and Weidick, A.: Late Quaternary history around Nioghalvfjerdsfjorden and Jokelbugten, North-East Greenland, Boreas, 30, 205–227, 2001.

Bennike, O., Sorensen, M., Fredskild, B., Jacobsen, B. H., Bocher, J., Amsinck, S. L., Jeppesen, E., Andreasen, C., Christiansen, H. H., and Humlum, O.: Late quaternary environmental and cultural changes in the Wollaston Forland region, Northeast Greenland, Adv. Ecol. Res., 40, 45–79, doi:10.1016/S0065-2504(07)00003-7, 2008.

Buylaert, J. P., Murray, A. S., Thomsen, K. J., and Jain, M.: Testing the potential of an elevated temperature IRSL signal from K-feldspar, Radiat. Meas., 44, 560–565, doi:10.1016/j.radmeas.2009.02.007, 2009.

Buylaert, J.-P., Thiel, C., Murray, A. S., Vandenberghe, D. A. G., Yi, S., and Lu, H.: IRSL and post-IR IRSL residual doses recorded in modern dust samples from the Chinese Loess Plateau, Geochronometria, 38, 432, doi:10.2478/s13386-011-0047-0, 2011.

Calmels, F., Froese, D. G., and Clavano, W. R.: Cryostratigraphic record of permafrost degradation and recovery following historic (1898–1992) surface disturbances in the Klondike region, central Yukon Territory, Can. J. Earth Sci., 49, 938–952, doi:10.1139/e2012-023, 2012.

Christiansen, H. H.: "Little Ice Age" nivation activity in northeast Greenland, Holocene, 8, 719–728, doi:10.1191/095968398666994797, 1998a.

Christiansen, H. H.: Nivation forms and processes in unconsolidated sediments, NE Greenland, Earth Surf. Proc. Land., 23, 751–760, 1998b.

Christiansen, H. H. and Humlum, O.: Glacial history and periglacial landforms of the Zackenberg area, Northeast Greenland: preliminary results, Geogr. Tidsskr., 93, 19–29, 1993.

Christiansen, H. H., Bennike, O., Bocher, J., Elberling, B., Humlum, O., and Jakobsen, B. H.: Holocene environmental reconstruction from deltaic deposits in northeast Greenland, J. Quaternary Sci., 17, 145–160, doi:10.1002/jqs.665, 2002.

Christiansen, H. H., Åkerman, J. H., and Repelewska-Pekalowa, J.: Active layer dynamics in Greenland, Svalbard and Sweden, Extended abstract for the 8th International Permafrost Conference, 21–25 July 2003, Zurich, Switzerland, 2003.

Christiansen, H. H., Sigsgaard, C., Humlum, O., Rasch, M., and Hansen, B. U.: Permafrost and periglacial geomorphology at Zackenberg, Adv. Ecol. Res., 40, 151–174, doi:10.1016/S0065-2504(07)00007-4, 2008.

Corner, G. D.: A transgressive-regressive model of fjord-valley fill: stratigraphy, facies and depositional controls, in: Incised Valleys in Time and Space, edited by: Dalrymple, R. W., Leckie, D. A., and Tillman, R. W., Society of Sediment. Geol. (SEPM), 161–178, 2006.

Eilertsen, R. S., Corner, G. D., Aasheim, O., Andreassen, K., Kristoffersen, Y., and Ystborg, H.: Valley-fill stratigraphy and evolution of the Målselv fjord valley, northern Norway, in: Incised-Valleys in Time and Space, edited by: Dalrymple, R. W., Leekie, D., and Tilman, R., 179–195, 2006.

Eilertsen, R. S., Corner, G. D., Aasheim, O. D. D., and Hansen, L.: Facies characteristics and architecture related to palaeodepth of Holocene fjord–delta sediments, Sedimentology, 58, 1784–1809, doi:10.1111/j.1365-3091.2011.01239.x, 2011.

Evans, D. J. A. and Benn, D. I.: A Practical Guide to the Study of Glacial Sediments, Routledge, London, United Kingdom, 280 pp., 2004.

Evans, D. J. A., Dowdeswell, J. A., Grobe, H., Niessen, F., Stein, R., Hubberten, H. W., and Whittington, R. J.: Late Quaternary sedimentation in Kejser Franz Joseph Fjord and the continental margin of East Greenland, in: Glacier-Influenced Sedimentation on High-Latitude Continental Margins, edited by: Dowdeswell, J. A. and O Cofaigh, C., The Geological Society of London, London, United Kingdom, 149–179, 2002.

Fleming, K. and Lambeck, K.: Constraints on the Greenland Ice Sheet since the Last Glacial Maximum from sea-level observations and glacial-rebound models, Quaternary Sci. Rev., 23, 1053–1077, doi:10.1016/j.quascirev.2003.11.001, 2004.

French, H. and Shur, Y.: The principles of cryostratigraphy, Earth-Sci. Rev., 101, 190–206, doi:10.1016/j.earscirev.2010.04.002, 2010.

Fuchs, M. and Owen, L. A.: Luminescence dating of glacial and associated sediments: review, recommendations and future directions, Boreas, 37, 636–659, doi:10.1111/j.1502-3885.2008.00052.x, 2008.

Funder, S., Hjort, C., and Landvik, J. Y.: The Last Glacial Cycles in East Greenland, an Overview, Boreas, 23, 283–293, doi:10.1111/j.1502-3885.1994.tb00601.x, 1994.

Funder, S., Kjeldsen, K. K., Kjær, K. H., and Ó Cofaigh, C.: The Greenland Ice Sheet During the Past 300,000 Years: A Review, in: Developments in Quaternary Science, edited by: Ehlers, J., Gibbard, P. L., and Hughes, P. D., Elsevier, Amsterdam, the Netherlands, 699–713, 2011.

Gilbert, G. L., Kanevskiy, M., and Murton, J. B.: Recent Advances (2008–2015) in the Study of Ground Ice and Cryostratigraphy, Permafrost Periglac, 27, 377–389, doi:10.1002/ppp.1912, 2016.

Gilbert, R.: Sedimentary processes of Canadian Arctic fjords, Sediment. Geol., 36, 147–175, doi:10.1016/0037-0738(83)90007-6, 1983.

Hansen, B. U., Sigsgaard, C., Rasmussen, L., Cappelen, J., Hinkler, J., Mernild, S. H., Petersen, D., Tamstorf, M. P., Rasch, M., and Hasholt, B.: Present-Day Climate at Zackenberg, in: Advances in Ecological Research, edited by: Meltofte, H., Christensen, T. R., Elberling, B., Forchhammer, M. C., and Rasch, M., Academic Press, Oxford, UK, 111–149, 2008.

Hansen, L.: Landscape and Coast Development of a Lowland Fjord Margin following Deglaciation, East Greenland, Geogr. Ann. A, 83, 131–144, 2001.

Hansen, L.: Deltaic Infill of a Deglaciated Arctic Fjord, East Greenland: Sedimentary Facies and Sequence Stratigraphy, J. Sediment. Res., 74, 422–437, doi:10.1306/102703740422, 2004.

Hansen, L., Beylich, A., Burki, V., Eilertsen, R. S., Fredin, O. L. A., Larsen, E., Lyså, A., Nesje, A., Stalsberg, K., and Tønnesen, J. F.: Stratigraphic architecture and infill history of a deglaciated bedrock valley based on georadar, seismic profiling and drilling, Sedimentology, 56, 1751–1773, doi:10.1111/j.1365-3091.2009.01056.x, 2009.

Hasholt, B., Mernild, S. H., Sigsgaard, C., Elberling, B., Petersen, D., Jakobsen, B. H., Hansen, B. U., Hinkler, J., and Søgaard, H.: Hydrology and Transport of Sediment and Solutes at Zackenberg, in: Advances in Ecological Research, edited by: Meltofte, H., Christensen, T. R., Elberling, B., Forchhammer, M. C., and Rasch, M., Academic Press, Oxford, UK, 197–221, 2008.

Hjort, C.: A Glacial Chronology for Northern East Greenland, Boreas, 10, 259–274, doi:10.1111/j.1502-3885.1981.tb00487.x, 1981.

Humlum, O.: Holocene permafrost aggradation in Svalbard, in: Cryospheric Systems: Glaciers and Permafrost, edited by: Harris, C. and Murton, J. B., The Geological Society of London, London, United Kingdom, 119–129, 2005.

Jensen, L. M., Christiansen, T. R., and Schmidt, N. M.: Zackenberg Ecological Research Operations: 19th Annual Report 2013, DCE – Danish Centre for Environment and Energy, Aarhus University, Denmark, 130, 2014.

Kanevskiy, M., Jorgenson, T., Shur, Y., O'Donnell, J. A., Harden, J. W., Zhuang, Q., and Fortier, D.: Cryostratigraphy and Permafrost Evolution in the Lacustrine Lowlands of West-Central Alaska, Permafrost Periglac, 25, 14–34, doi:10.1002/ppp.1800, 2014.

Kneller, B. and Buckee, C.: The structure and fluid mechanics of turbidity currents: a review of some recent studies and their geological implications, Sedimentology, 47, 62–94, doi:10.1046/j.1365-3091.2000.047s1062.x, 2000.

Koch, L. and Haller, J.: Geological map of East Greenland 72–76 N.Lat. (1 : 250,000), in: Meddeleser om Grønland 3rd ed., 1–26, 1971.

Kokelj, S. V. and Burn, C. R.: Near-surface ground ice in sediments of the Mackenzie Delta, Northwest Territories, Canada, Permafrost Periglac, 16, 291–303, doi:10.1002/ppp.537, 2005.

Mackay, J. R.: The world of underground ice, Annals of the Association of American Geographers, 62, 1–22, doi:10.1111/j.1467-8306.1972.tb00839.x, 1972.

Marchand, J.-P., Buffin-Bélanger, T., Hétu, B., and St-Onge, G.: Stratigraphy and infill history of the glacially eroded Matane River Valley, eastern Quebec, Canada, Can. J. Earth Sci., 51, 105–124, doi:10.1139/cjes-2013-0054, 2013.

Miall, A.: The geology of fluvial deposits: sedimentary facies, basin analysis, and petroleum geology, Springer, 581 pp., 2006.

Miall, A. D.: Alluvial deposits, in: Facies models 4, edited by: James, N. P. and Dalrymple, R. W., Geological Association of Canada, St. John's, Canada, 105–138, 2010.

Murray, A. S. and Wintle, A. G.: Luminescence dating of quartz using an improved single-aliquot regenerative-dose protocol, Radiat. Meas., 32, 57–73, doi:10.1016/S1350-4487(99)00253-X, 2000.

Murray, A. S., Thomsen, K. J., Masuda, N., Buylaert, J. P., and Jain, M.: Identifying well-bleached quartz using the different bleaching rates of quartz and feldspar luminescence signals, Radiat. Meas., 47, 688–695, doi:10.1016/j.radmeas.2012.05.006, 2012.

Murton, J. B.: Ground Ice and Cryostratigraphy, in: Treatise on Geomorphology: Glacial and Periglacial Geomorphology, edited by: Giardino, R. and Harbor, J., Academic Press, San Diego, USA, 173–201, 2013.

Nemec, W.: Aspects of sediment movement on steep delta slopes, Coarse-grained deltas, 10, 29–73, 1990.

Nemec, W., Lønne, I. D. A., and Blikra, L. H.: The Kregnes moraine in Gauldalen, west-central Norway: anatomy of a Younger Dryas proglacial delta in a palaeofjord basin, Boreas, 28, 454–476, doi:10.1111/j.1502-3885.1999.tb00234.x, 1999.

Netto, R. G., Benner, J. S., Buatois, L. A., Uchman, A., Mangano, M. G., Ridge, J. C., Kazakauskas, V., and Gaigalas, A.: Glacial Environments, in: Trace Fossils as Indicators of Sedimentary Environments, edited by: Knaust, D. and Bromley, R. G., Elsevier, Amsterdam, the Netherlands, 299–327, 2012.

Nøhr-Hansen, H., Nielsen, L. H., Sheldon, E., Hovikoski, J., and Alsen, P.: Palaeogene deposits in North-East Greenland, Geol. Surv. Den. Greenl., 23, 61–64, 2011.

Ó Cofaigh, C., Lemmen, D. S., Evans, D. J. A., and Bednarski, J.: Glacial landform-sediment assemblages in the Canadian High Arctic and their implications for late Quaternary glaciation, Ann. Glaciol., 28, 195–201, doi:10.3189/172756499781821760, 1999.

Ó Cofaigh, C., Dowdeswell, J. A., Evans, D. J. A., Kenyon, N. H., Taylor, J., Mienert, A., and Wilken, M.: Timing and significance of glacially influenced mass-wasting in the submarine channels of the Greenland Basin, Mar. Geol., 207, 39–54, doi:10.1016/j.margeo.2004.02.009, 2004.

Pedersen, J. B. T., Kroon, A., and Jakobsen, B. H.: Holocene sea-level reconstruction in the Young Sound region, Northeast Greenland, J. Quaternary Sci., 26, 219–226, doi:10.1002/jqs.1449, 2011.

Plink-Björklund, P. and Ronnert, L.: Depositional processes and internal architecture of Late Weichselian ice-margin submarine fan and delta settings, Swedish west coast, Sedimentology, 46, 215–234, doi:10.1111/j.1365-3091.1999.sed195.x, 1999.

Pollard, W. H.: Distribution and characterization of ground ice on Fosheim Peninsula, Ellesmere Island, Nunavut, in: Environmental Response to Climate Change in the Canadian High Arctic, edited by: Garneau, M. and Alt, B. T., Geological Survey of Canada, Ottawa, Ontario, Canada, 207–233, 2000a.

Pollard, W. H.: Ground ice aggradation on Fosheim Peninsula, Ellesmere Island, Nunavut, in: Environmental Response to Climate Change in the Canadian High Arctic, edited by: Garneau, M. and Alt, B. T., Geological Survey of Canada, Ottawa, Ontario, Canada, 325–333, 2000b.

Pollard, W. H. and Bell, T.: Massive ice formation in the Eureka Sound Lowlands: a landscape model, Seventh International Conference on Permafrost, Yellowknife, Canada, 1998.

Reading, H. G.: Sedimentary environments: processes, facies and stratigraphy, Blackwell Science, Oxford, UK, 2009.

Rittenour, T. M.: Luminescence dating of fluvial deposits: applications to geomorphic, palaeoseismic and archaeological research, Boreas, 37, 613–635, doi:10.1111/j.1502-3885.2008.00056.x, 2008.

Stephani, E., Fortier, D., Shur, Y., Fortier, R., and Doré, G.: A geosystems approach to permafrost investigations for engineering applications, an example from a road stabilization experiment, Beaver Creek, Yukon, Canada, Cold Reg. Sci. Technol., 100, 20–35, doi:10.1016/j.coldregions.2013.12.006, 2014.

Thomsen, K. J., Murray, A. S., Jain, M., and Bøtter-Jensen, L.: Laboratory fading rates of various luminescence signals from feldspar-rich sediment extracts, Radiation Measurements, 43, 1474–1486, doi:10.1016/j.radmeas.2008.06.002, 2008.

Winkelmann, D., Jokat, W., Jensen, L., and Schenke, H. W.: Submarine end moraines on the continental shelf off NE Greenland – Implications for Lateglacial dynamics, Quaternary Sci. Rev., 29, 1069–1077, doi:10.1016/j.quascirev.2010.02.002, 2010.

Winsemann, J., Asprion, U., Meyer, T., and Schramm, C.: Facies characteristics of Middle Pleistocene (Saalian) ice-margin subaqueous fan and delta deposits, glacial Lake Leine, NW Germany, Sediment. Geol., 193, 105–129, doi:10.1016/j.sedgeo.2005.11.027, 2007.

Paper IV